NASA Technical Memorandum 100746

The GEM-T2 Gravitational Model

J.G. Marsh, F. J. Lerch, B.H. Putney,
T.L. Felsentreger, B.V. Sanchez,
S.M. Klosko, G.B. Patel, J.W. Robbins,
R.G. Williamson, T.E. Engelis, W.F. Eddy,
N.L. Chandler, D.S. Chinn, S. Kapoor,
K.E. Rachlin, L.E. Braatz, and E.C. Pavlis

October 1989

NASA

NASA Technical Memorandum 100746

The GEM-T2 Gravitational Model

J.G. Marsh, F.J. Lerch, B.H. Putney,
T.L. Felsentreger, B.V. Sanchez
Goddard Space Flight Center
Greenbelt, Maryland

S.M. Klosko, G.B. Patel, J.W. Robbins,
R.G. Williamson, T.E. Engelis, W.F. Eddy,
N.L. Chandler, D.S. Chinn, S. Kapoor,
K.E. Rachlin, L.E. Braatz
ST Systems Corporation
Lanham, Maryland

E. C. Pavlis
University of Maryland
College Park, Maryland

NASA
National Aeronautics and
Space Administration

Goddard Space Flight Center
Greenbelt, MD

1989

ABSTRACT

GEM-T2 is the latest in a series of Goddard Earth Models of the terrestrial gravitational field. It was designed to bring modeling capabilities one step closer towards ultimately determining the TOPEX/Poseidon satellite's radial position to an accuracy of 10-cm RMS. It also improves our models of the long wavelength geoid to support many oceanographic and geophysical applications. GEM-T2 extends the static portion of the field's determination to include more than 600 coefficients above degree 36 (which was the limit for its predecessor, GEM-T1) and provides a dynamically determined model of the major tidal lines which contains 90 terms. Like GEM-T1, it was produced entirely from satellite tracking data, but it now uses nearly twice as many satellites (31 vs. 17), contains four times the number of observations (2.4 million), and has twice the number of data arcs (1132). GEM-T2 utilizes laser tracking from 11 satellites, Doppler data from four satellites, two- and three-way range-rate data from Landsat-1, satellite-to-satellite tracking data between the geosynchronous ATS-6 and the GEOS-3 satellites, and optical observations on 20 different orbits. This observation set nearly exhausts the inclination distribution available for gravitational field development from our historical database.

Extension of GEM-T2 to even higher degree and order was made possible through the application of a constrained least squares technique which uses the known spectrum of the Earth's gravity field as apriori information. The error calibration of the model is now performed concurrently with the model's generation through the use of an optimal weighting procedure which tests the model against solution subsets. This procedure is used herein for the first time. It iteratively determines the optimal weight for each constituent data set by testing the complete model against a test solution which omits each of the data sets individually. The differences in the solutions isolate the contribution of a given data set and tests the consistency of the magnitude of these differences against their expected values from the respective solution covariances. The process yields optimal data weights and assures a model which is self-consistent and well calibrated. It is also objective and eliminates heuristic approaches which lack its rigor. GEM-T2 has benefitted by its application as demonstrated through tests using independent altimeter derived gravity anomalies.

Results for the GEM-T2 error calibration indicate significant improvement over previous satellite-only GEM models. The accuracy assessment of the lower degree and order coefficients indicate that GEM-T2 has reduced their uncertainty by 20% as compared to GEM-T1. The error of commission in determining the geoid has been reduced from 155 cm in GEM-T1 to 105 cm for GEM-T2 for the 36 x 36 portion of the field, and 141 cm for the entire model. The orbital accuracies achieved using GEM-T2 are likewise improved. This is especially true for the Starlette and GEOS-3 orbits where higher order resonance terms are now well-represented in GEM-T2 whereas they were not present in GEM-T1 (e.g., terms where m=42,43).

Finally, the projected radial error on the TOPEX satellite orbit indicates 9.4-cm RMS for GEM-T2, compared to 24.1-cm for GEM-T1. This improvement in orbit prediction extends across all orbit inclinations. This confirms our conclusion that GEM-T2 is a genuine advance in the state of knowledge of the Earth's gravity field.

SECTION 1. INTRODUCTION

Goddard Earth Model (GEM) -T2 is the latest in a series of improved gravitational models developed at NASA/Goddard Space Flight Center using supercomputer capabilities, modern geodetic constants and reference parameters, and a new optimum data weighting and error calibration technique (Lerch, 1989) for its determination. GSFC has undertaken an effort, requiring both pre- and post-launch activities, to develop force models capable of supporting the orbital positioning and geoid accuracy required for the TOPEX/Poseidon mission. GEM-T2, like its predecessor GEM-T1 (Marsh et al., 1987, 1988), has been determined solely from satellite tracking data. The solution for the Earth's geopotential field, both static and tidally induced, has been extended to higher degree and order in GEM-T2. The static geopotential is complete for many orders to degree 50 to better accommodate zonal, low-order and satellite orbital resonance effects. The gravitational model has increased in size by more than 600 coefficients beyond the 36 x 36 solution of GEM-T1. The GEM-T2 tidal model includes adjustment for 90 harmonics (as compared to 66 coefficients in GEM-T1) distributed over 12 major tides which are solved in the presence of a comprehensive ocean tidal model containing long wavelength information for 32 major and minor constituents. This ocean tidal model contains over 600 coefficients and was developed to provide a much more complete description of the long wavelength ocean tides to improve the separation of static and temporally varying gravitational effects. Such a model is needed as described in Christodoulidis et al., (1988).

In accordance with the plans described in Marsh et al., (1987), Goddard Space Flight Center has been approaching the gravity modeling problem in progressive stages. Each of the available satellite tracking, surface gravimetric and altimeter observation subsets is being evaluated and qualified for its inclusion within the GEM models. As a prelude to combination models which contain mixed and subtly incompatible types of observations (i.e. mixing large numbers of satellite tracking observations with those provided by surface gravimetry and satellite altimetry which have a different bandwidth of field sensitivity), we find it desirable to develop preliminary models which are largely free of these concerns. These "satellite-only" models, like GEM-T1 and now GEM-T2, are then thoroughly evaluated, optimized and calibrated (Lerch et al., 1988) to better understand their accuracies and limitations. Much of the error calibration for GEM-T2 is built into the solution through our application of an iterative optimal data weighting technique. By design, this method yields a well calibrated result.

Satellite tracking data provides the most unambiguous available measure of the long wavelength geopotential. A large historical database spanning all of the major tracking technologies has been developed at GSFC. Altimetry and surface gravimetry are known to have modeling inaccuracies and inadequacies when describing the long wavelength geoid, and these two surface data types are not strictly compatible with the attenuated gravitational signal seen from an evaluation of perturbed orbital behavior within tracking data. Therefore, in our approach, larger comprehensive models using surface gravimetry and altimetry are based on these "satellite-only" fields. A 50 x 50 combination model called GEM-T3 is under development with a preliminary version, PGS-3337 now available (Marsh et al, 1989a). Altimetry and surface gravimetry will be contained within GEM-T3 and will provide an excellent resource for directly mapping the short wavelength geopotential over regions where these data are available. Furthermore, by progressively developing more complete and complex fields in a systematic way based upon well-calibrated base models, field optimization is more readily attained, data incompatibilities are more easily located and reliable assessments of the solution's uncertainties are obtained.

When beginning our most recent GEM modeling activities in 1984, an improved set of Earth constants and reference frame parameters were incorporated. The solutions are based on the state-of-the-art in satellite geodesy in the 1984-5 timeframe. The constants described for use in the MERIT Campaign (Melbourne et al., 1983) provided the starting point for this assessment. The adoption of these values (which will be reviewed in Section 2.) and their uniform application across all tracking technologies, laid the foundation in achieving the higher accuracy found in our most recent GEM-T1 and -T2 solutions. Of equal or greater

importance was the development of the optimal data weighting algorithms, improved solution calibration/testing methods, and the overall extension of the models to higher degree and order.

Extending the model to high degree and order has been a very important development in our latest models. This reduces the errors resulting from spectral leakage coming from the omitted portion of the gravitational field beyond the limits of the recovered model. By necessity, all omitted terms are implicitly assumed to have zero values. The GEM-T2 model has been solved to as high a degree and order as necessary to exhaust the attenuated gravitational signal contained in the tracking data. A constrained least squares solution (Lerch et al., 1979) is used to stabilize the behavior of the solution at high degree and order where correlation and small data sensitivities are a problem. The availability of the Cyber-205 supercomputer greatly increased our capabilities for extending the field size and developing solution optimization techniques.

The major advancements of GEM-T2 over its predecessor, GEM-T1, include:

(a) the near-doubling of the number of distinct orbits sampled to form the model. GEM-T1 used tracking data from 17 satellites. GEM-T2 contains contributions from 31. The major new observation subsets include TRANET Doppler data acquired on the polar NOVA-1 satellite, Unified S-Band average range-rate tracking on Landsat-1, laser data on the Japanese Ajisai satellite, satellite-to-satellite range-rate data taken from the geosynchronous ATS-6 to GEOS-3, nine additional optical satellites and TRANET Doppler data taken on GEOSAT.

(b) the data set for GEM-T2 has also more than doubled. GEM-T1 was determined using 793,900 observations contained within 581 individual orbital arcs whereas GEM-T2 contains 2,386,000 observations from 1130 arcs.

(c) there has been a significant improvement in the laser data set utilized within GEM-T2. Third-generation laser data from the 1980 and 1981 time periods has been included from both GEOS-1 and GEOS-3. This represents a substantial upgrading of the information available from these satellites as compared to the 1975 to 1977 data utilized in GEM-T1. These satellites are similar in inclination to that nominally proposed for TOPEX/Poseidon and will strengthen the model when determining precise TOPEX/Poseidon ephemerides. LAGEOS ranging has been extended by nearly 3 years to include the global data taken during 1984, 1985, 1986 and the first 2 months of 1987. Likewise, ranging on Starlette has been extended to include data taken during 1984 and 1986, and the 1500-km orbit of Ajisai is also included.

(d) there has been a major advance in our solution technique through the introduction of an optimal data weighting and automatic error calibration approach. These products are now an integral part of the estimation procedure.

(e) GEM-T2 is a significant improvement over GEM-T1 both in terms of its geoid representational accuracy and in its satellite orbit modeling uncertainties. This is especially true in terms of its predicted performance on TOPEX/Poseidon's radial accuracy using covariance propagations.

All of these issues, including in particular, a thorough error assessment of GEM-T2, will be described in detail within this report.

SECTION 2. REFERENCE PARAMETERS

A terrestrial gravity field solution must be defined within a well understood reference system. The dynamic satellite orbit computations are connected to ground-based observers through these definitions. The orbital trajectories are integrated in the Conventional Inertial Reference System (CIRS) which needs to be connected in time to the Conventional Terrestrial Reference System (CTRS) which is realized by the global network of Earth-fixed tracking stations. Application of terrestrial gravitational accelerations along the orbit are made using these same transformations.

Since 1979, the tracking data themselves have been sufficiently robust to allow a direct adjustment of the geocentric station locations, the Earth's polar motion and the change in the length of day (using 5-day averaging intervals) which provides a satellite-based definition of the CTRS. This system is dominated or exclusively based on the satellite laser ranging acquired on the high-altitude LAGEOS satellite. Within GEM-T1 and GEM-T2, we have adjusted the Earth orientation parameters as part of the solution. This was desirable since we have moved our definition of the CTRS to a new terrestrial origin (i.e., we are using a "zero-mean" definition for polar motion based on LAGEOS and have transformed the historical Bureau International de l'Heure (BIH) series which is referred to CIO into this new system; see Marsh et al., 1987, 1988). There is a near-singularity when simultaneously defining the satellite's right ascension of the ascending node and UT1 using laser data given the weak sensitivity of the orbit to short wavelength longitudinal gravity signals. The orbit can be rotated in longitude by 30-100m with little change in field performance. A change in UT1 of the same magnitude has the same effect. Thereby, the BIH definition of UT1 is adopted at the epoch of each 30-day LAGEOS orbit. The laser data then yields a well resolved measure of the change in length of day based on this BIH origin. The adopted tidal variations in the Earth rotation (UT1) series are those of Yoder et al., (1981).

The laser station coordinates which are utilized are from the GSFC LAGEOS SL6 (Christodoulidis et al., 1986) and SL7.1 (Smith et al., 1989 in press) solutions. The laser coordinate network is rotated through a fixed angle (defined by the offset of CIO with respect to our new terrestrial origin) yielding a consistent definition of geodetic latitude for the sites within our new CTRS. We have tied non-laser tracking systems into this definition of CTRS using a series of transformations and analyses as described in Marsh et al., (1987; Chapter 6).

The J2000 Reference System with its associated DE200/LE200 planetary ephemeris forms the basis for our CIRS definition. This connects the CTRS series in time using the nutation series of the IAU 1980 provided by Wahr (1979) and the IAU 1976 precession series developed by Lieske (1976)

As the accuracy of tracking instruments has evolved, the requirements for accurate reference frame definitions and consistent constants have become much more stringent. Physical models of increasing complexity are required to both exploit and explain these very precise satellite measurements. The advance of satellite geodesy has been oriented towards amplifying the science yield from increasingly more accurate data, and in parallel, developing newer tracking systems which permit more complex natural phenomena to be modelled. For the problem of determining a gravitational model, the solution output is a mathematical model of a physical phenomenon whose empirical coefficients taken individually are not directly observed. Thereby, complex geophysical interpretations of the GEM gravitational models are difficult unless strict attention is paid to these fundamental definitions. Errors in these models or neglected effects cause problems in the definition and interpretation of these fields. For example, this is important in advanced analyses like those in physical oceanography where the GEM geoid is used to isolate non-gravitational signals exhibited by the ocean topography. For this reason we have taken great care in selecting the reference frame definition and constants for the recent GEM solutions.

The following table lists the values adopted for the constants that enter into the models used to create GEM-T2. Only the most important ones have been included. We have also avoided repeating numbers which are implicitly embedded in well-known standard models which are referenced and adopted in the whole (e.g., the constants describing the Wahr nutation model or Lieske's expressions for the precessional matrix).

2.1 Astronomical Constants

Speed of Light	299792458 m/s
Equatorial radius of the Earth	6378137 m
Flattening of the Earth	1/298.257
Mean spin rate of Earth	0.00007292115 rad/s
Geocentric Gravitational Constant	398600.436 km^3/s^2
Moon-Earth mass ratio	0.012300034
Astronomical unit	149597870660 m
Sun-Earth mass ratio	332946.038

2.2 Dynamical Models

Static Geopotential	Adjusting, GEM-T1 apriori
Solid Earth Tides	Wahr (1979)
Ocean Tides	GEM-T1 apriori with 90 adjusting coefficients
Radiation pressure at 1 AU	0.0000045783 $kg/m/s^2$
o radiation pressure coefficient	adjusted
Atmospheric Drag	Jacchia (1971) with daily values of F10.7 and Kp flux
o atmospheric drag coefficient	adjusted; nominally once/day

2.3 Measurement Models

2.3.1 Optical Data

parallactic refraction	Hotter (1968)
annual abberation	"
diurnal abberation	"
precession/nutation of images	Wahr/Lieske
proper motions	Hotter (1968)
satellite clock corrections for active satellites	APL provided values

2.3.2 TRANET Doppler Data

Time tag correction from WWV	O'Toole (1976)
Tropospheric refraction	Modified Hopfield Model of Goad (Martin et al., 1987)
Ionospheric refraction	First-order correction obtained from difference of 150- and 400-MHz freq.
Frequency bias correction	pass-by-pass bias adjustment

2.3.3 Laser Range Data

Pre- and post-pass range calibrations	Figgatte and Polesco (1982)
Tropospheric refraction	Marini and Murray (1973)

2.3.4 S-band Average Range-rate Data

Tropospheric refraction	Modified Hopfield Model of Goad (Martin et al., 1987)
Ionospheric refraction	none
Antenna axis offset correction for non-az/el mounts	Gross (1968)/Martin et al., (1987)

2.4 Reference System

CIRS	J2000.0
Planetary Ephemeris	JPL DE200
Terrestrial time scale	UTC (USNO)
Precession	IAU 1976 (Lieske, 1976)
Nutation	IAU 1980 (Wahr, 1979)
CTRS	Lageos global solution SL6 rotated to "zero-mean" system

SECTION 3. THE GEM-T2 OBSERVATIONS

The tracking observations available for gravitational modeling span 30-years of technology change. These data contain a wide range of data precision and sophistication. The earliest observations were taken at moments of opportunity when satellites or their rocket body fragments were illuminated by the sun, yet visible to a pre-dawn or after-dusk shrouded Earth observer. The satellite was photographed against the star background and positioned within a celestial system yielding a satellite right ascension and declination in the reference system of the FK4 star catalogue. These images were capable of locating the satellite's direction vis-a-vis the observer to a precision of one to two topocentric seconds of arc which for most satellite altitudes translated into positioning of approximately 10-meters.

Today's tracking technologies have advanced enormously, with active laser ranging systems tracking passive orbiting targets during day or night with single shot precision, which for the best systems, have sub-centimeter noise levels.

However, even for the extensive laser network now deployed to support the NASA/Crustal Dynamics Program and the European Wegener/Medlas activities, the fact remains that these data are obtained primarily for precision orbit determination. They are used for force modeling improvements as they become available and are not part of a cohesive program designed to optimize gravity field recovery. Absent a dedicated gravitational mission, these observations will not significantly improve in global coverage. Furthermore, these tracking data will remain limited in their ability to sense the terrestrial gravity model at shorter wavenumbers. Surface gravity observations and satellite altimetry help this situation in certain regions, but there remain large, geographically dependent gaps in data availability; there is also another problem with surface gravimetry due to the large variation in the global quality of these observations themselves.

Therefore, even the most modern tracking technologies provide insufficient global coverage and adequate sensitivity for resolving the geoid at intermediate and short frequencies. Furthermore, all contemporary geopotential modeling solutions must still rely on older, less precise observation subsets to provide the orbital coverage needed to resolve the fields, even at their present dimensions. Only a dedicated gravitational mission will likely have significant impact on this situation for the foreseeable future.

While the foregoing limitations will be dramatically improved when future missions planned for the 1990s (e.g. Aristoteles) reach orbit, significant progress has been made in exploiting the historical observations to improve our knowledge of the long wavelength geopotential field. GEM-T1 and GEM-T2 heavily rely on the precise range measurements acquired by a global network of satellite laser ranging systems. Many more laser observations are now included in GEM-T2 than were used in GEM-T1.

Table 3.1 gives the orbital characteristics of the satellites which provided tracking data within the GEM-T2 model. Figure 3.1 graphically displays these orbits and presents a comparison of the inclination and altitude distribution of the satellites for both GEM-T1 and GEM-T2. Many of the satellites selected for GEM-T2, especially the additional optical satellites, were used to improve the distribution of orbital inclinations within the model, giving improved resolution of especially the zonal harmonics.

Table 3.2 compares the number of orbital arcs in GEM-T1 with the data set which is now used in GEM-T2. There have been major new observation sets added to the gravitational field models with GEM-T2. Nearly all of the satellites previously used in models like GEM-9 (Lerch et al., 1979) and GEM-L2 (Lerch et al., 1982b) are now included within this most recent model. This section will briefly review these additional observation subsets. Marsh et al., (1987) contains a detailed discussion of the GEM-T1 observations and the data reduction process. Herein, we

Table 3.1

Satellite Orbital Characteristics for GEM-T2
Ordered by Inclination

Satellite Name	Semi-major Axis (Km)	Eccentricity	Inclination (Degrees)	Data* Type
ATS-6	41867.	.001	0.9	SST
Peole	7006.	.016	15.0	L,O
Courier 1B	7469.	.016	28.3	O
Vanguard 2	8298.	.164	32.9	O
Vanguard 2RB	8496.	.183	32.9	O
D1-D	7622.	.085	39.5	L,O
D1-C	7341.	.053	40.0	L,O
BE-C	7507.	.026	41.2	L,O
Telestar-1	9669.	.243	44.8	O
Echo-1RB	7966.	.012	47.2	O
Starlette	7331.	.020	49.8	L
Ajisai	7870.	.001	50.0	L
Anna-1B	7501.	.008	50.1	O
GEOS-1	8075.	.072	59.4	L,O
Transit-4A	7322.	.008	66.8	O
Injun-1	7316.	.008	66.8	O
Secor-5	8151.	.079	69.2	O
BE-B	7354.	.014	79.7	O
OGO-2	7341.	.075	87.4	O
OSCAR-7	7440.	.002	89.2	O
OSCAR-14	7448.	.004	89.2	D
5BN-2	7462.	.006	90.0	O
NOVA	7559.	.001	90.0	D
Midas-4	9995.	.011	95.8	O
Landsat-1	7286.	.001	99.1	S
GEOS-2	7711.	.033	105.8	L,O
Seasat	7171.	.001	108.0	L,D
Geosat	7169.	.001	108.0	D
Lageos	12273.	.001	109.9	L
GEOS-3	7226.	.001	114.9	L
OV1-2	8317.	.018	144.3	O

* SST - Satellite-to-Satellite Tracking Range Rate
L - Laser
O - Optical
D - TRANET/OPNET Doppler
S - S-Band Average Range Rate

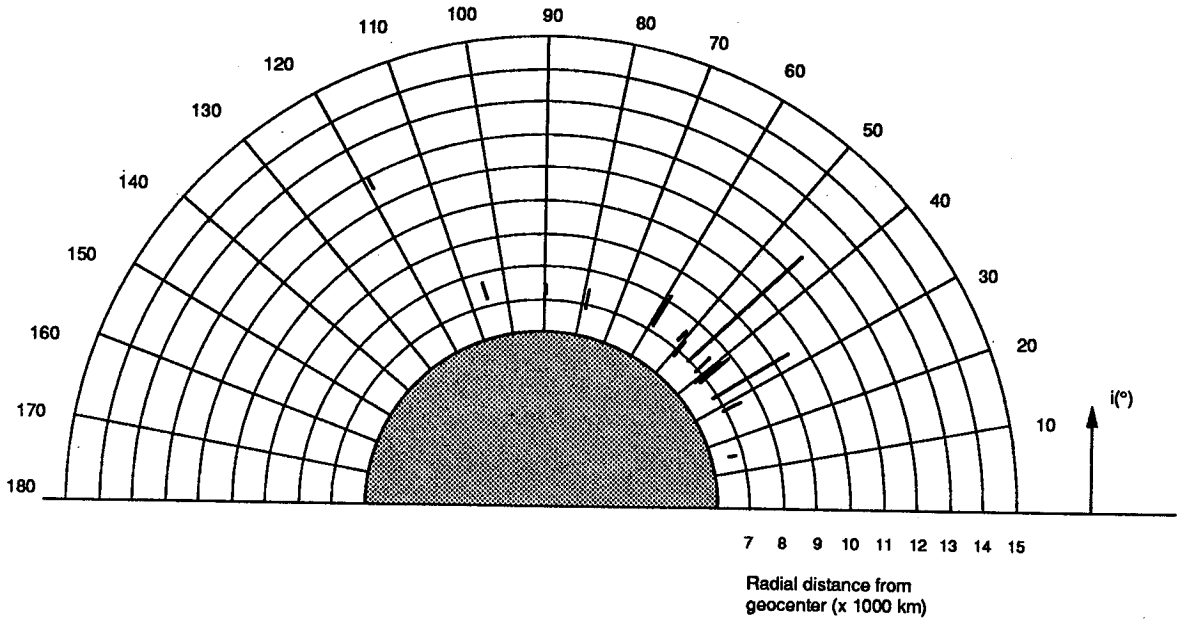

Figure 3.1a Orbital Characteristics of the Satellites Used in Determining the GEM-T1 Gravity Model

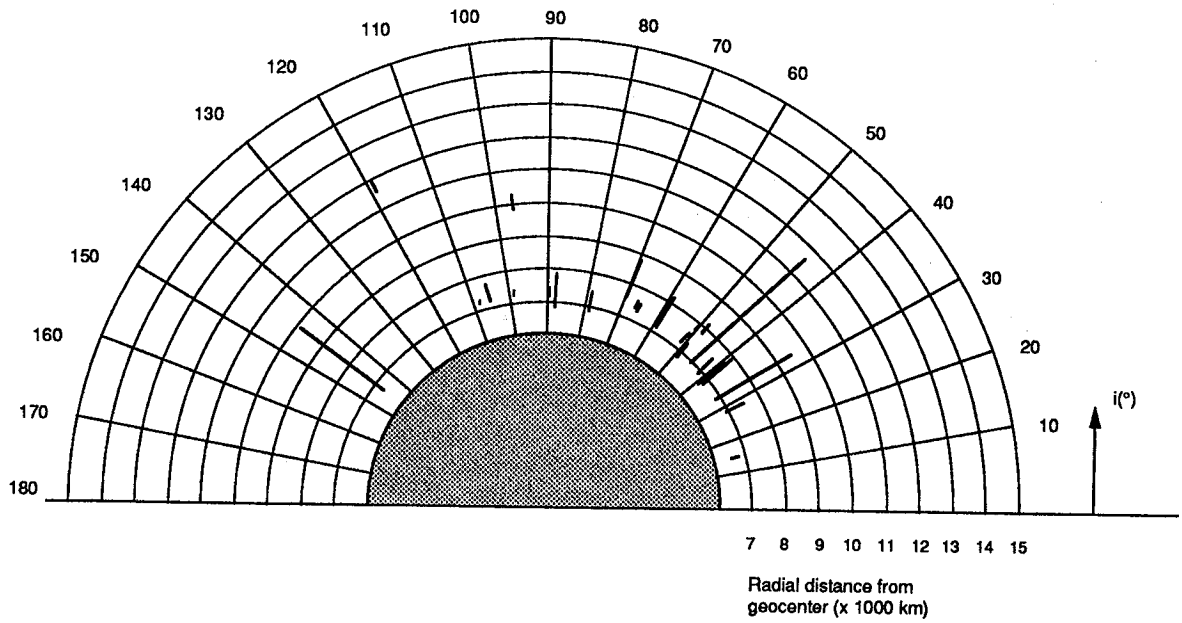

Figure 3.1b Orbital Characteristics of the Satellites Used in Determining the GEM-T2 Gravity Model

wish to augment this overview with the GEM-T2 complement of additional observations.

3.1 Laser Observations Added to GEM-T2

The major laser observation subsets which were added to GEM-T1 in forming GEM-T2 include:

O Lageos monthly arcs from the end of the MERIT Campaign in September of 1984 through February of 1987. This is a major addition to the Lageos data complement providing improved global coverage.

O Starlette 5-day arcs for 1984 and 1986 were reduced, nearly quadrupling the number of Starlette arcs being used. Again, these data benefitted from improved global coverage.

O 30 5-day arcs of GEOS-1 laser data acquired during 1980 were added to the solution. These data were of a much higher quality than the data previously used from the 1977 to 1978 timeframe. These earlier data were dominantly acquired by high noise Smithsonian Astrophysical Observatory (SAO) laser systems. The SAO systems were upgraded in 1979 with the installation of a pulse chopper and improved optical sensitivity. These improvements brought these systems from the 50-cm to the 10-cm level of tracking precision. Additionally, the NASA mobile systems operating at the few-cm level were first deployed in the fall of 1979. These new data were very important for improving the prediction of the GEM-T2 model at these middle inclinations in support of TOPEX/Poseidon.

O 50 5-day arcs of GEOS-3 laser observations acquired during 1980 were also added to the solution. Like GEOS-3 discussed above, these data were found to be much improved over earlier GEOS-3 subsets for the same reason. These GEOS-3 data provided the single most important contribution when assessing GEM-T2's improvement over GEM-T1 for predicting TOPEX/Poseidon radial orbit performance. GEOS-3 is very close to the nominal inclination proposed for TOPEX/Poseidon.

O The Japanese launched the Ajisai satellite in the summer of 1986 to support geodynamics using both laser and optical systems. The satellite was quite large (approximately 1-m radius), permitting both laser and optical tracking. However, the satellite was placed into a high 1500-km orbit, so atmospheric drag effects were small. An excellent laser ranging data set has been acquired on Ajisai, and 36 5-day arcs have been utilized in GEM-T2. This satellite is important since it orbits at an altitude similar to that proposed for TOPEX/Poseidon. Table 3.3 summarizes these Ajisai orbital arcs.

3.2 Doppler Data in GEM-T2

There have been two additional TRANET data sets used in GEM-T2 which were unavailable for use with GEM-T1. The first was an extensive set of GEOSAT TRANET observations. These data provide a complement to the unfortunately short SEASAT data set in an essentially comparable orbit. The U.S. Navy's GEOSAT satellite was launched on March 12, 1985. GEOSAT is equipped with a radar altimeter and its orbit is tracked exclusively by the TRANET dual frequency Doppler systems which have data precision at the 0.4- to 0.6-cm/s levels. On November 8, 1986, the satellite completed its maneuvers placing it into a 17-day Exact Repeat Mission (ERM) where its groundtrack repeated that of SEASAT when it was deployed in a similar groundtrack repeat interval. GEOSAT's groundtracks overfly those of SEASAT within 1 km at the equator. GEOSAT is supplying altimeter data in a later time period and these data far surpass those which were taken on SEASAT. SEASAT suffered a critical power failure 3 months into its mission, whereas the ERM data on GEOSAT have now been obtained for nearly 20 months as of

Table 3.2

GEM-T2 TRACKING DATA SUMMARY

SAT. NAME	INCLINATION (DEG)	DATA TYPE *	ARCS GEM-T1	ARCS GEM-T2
ATS-6/GEOS-3	0/115.0	SST	-	26
PEOLE	15.0	L,O	6	6
COURIER-1B	28.3	O	10	10
VANGUARD-2	32.9	O	10	10
VANGUARD-2RB	32.9	O	10	10
D1-D	39.5	L,O	15	15
D1-C	40.0	L,O	14	14
BEC	41.2	L,O	89	89
TELESTAR-1	44.8	O	30	30
ECHO-1RB	47.2	O	-	32
STARLETTE	49.8	L	46	157
AJISAI	50.0	L	-	36
ANNA-1B	50.1	O	30	30
GEOS-1	59.3	L,O	91	121
TRANSIT-4A	66.8	O	-	50
INJUN-1	66.8	O	-	44
SECOR-5	69.2	O	-	13
BE-B	79.7	O	20	20
OGO-2	87.4	O	-	16
OSCAR	89.2	D	13	13
OSCAR-7	89.7	O	-	4
SBN-2	90.0	O	-	17
NOVA	90.0	D	-	16
MIDAS-4	95.8	O	-	50
LANDSAT-1	98.5	S-BAND	-	10
GEOS-2	105.8	L,O	74	74
SEASAT	108.0	D,L	29	29
GEOSAT	108.0	D	-	13
LAGEOS	109.9	L	58	85
GEOS-3	114.9	L	36	86
OVI-2	144.3	O	-	4
TOTAL			581	1130

* SST Satellite-to-Satellite Tracking

L Laser ranging

O Optical

D Doppler

S-Band Unified S-Band average range-rate

this writing. Altimeter data from GEOS-3, SEASAT and GEOSAT will be included in future combination gravity models with GEOSAT playing a dominant role in the contributions from this type of data.

In total, we received 80 days worth of data from a global tracking network of 45 sites. These data were reduced in the same approach as described in Marsh et al., (1987) for the SEASAT TRANET data (also see Anderle, 1983). Orbit computations for the GEOSAT ERM data were performed using the GEM-T1 gravity and tide models. Overall, 13 6-day arcs of GEOSAT TRANET data encompassing the time period of November 8, 1986 to January 25, 1987 were included in GEM-T2. Because of orbital maneuvers which were needed to maintain the rigid repeating groundtrack geometry, some arcs which were analyzed departed slightly from the nominal 6-day length.

An overall average RMS of fit obtained apriori from these data was 1.28 cm/s. Our assessment of data noise was 0.98 cm/s. This somewhat degraded result is attributable to other effects in the data like third-order ionospheric refraction errors which caused the performance of these systems to degrade, especially at times of high solar activity. However, these data are quite dense when 45 stations supported the GEOSAT Mission, so these data remain quite useful for gravitational modeling attempts. Within a 6-day time span, we found from 460 to nearly 900 passes of data to be available after editing low elevation passes.

The second source of TRANET data was provided by the NOVA-1 satellite. This U.S. Navy navigation satellite was placed in a circular polar orbit at 1180 km altitude. In addition, NOVA-1 was equipped with a DISCOS single-axis drag compensation system which serves to correct the satellite trajectory along track for non-conservative force model effects such as atmospheric drag and solar radiation pressure. This satellite was unique in this aspect, for it had much smaller drag perturbations than a typical satellite passively orbiting at the same altitude. On NOVA, one along-track acceleration parameter per day was adjusted to accommodate the along-track radiation pressure from our radiative pressure model and any systematic bias in the drag compensation system. However, for a non-drag compensated satellite at this altitude, the drag effects would be much larger. Non-conservative force model parameters are empirically adjusted along with the orbital state within GEM-T2 and can be confused with gravity coefficients having long period orbital effects like satellite resonance terms when they are adjusted within a given arc. NOVA observations provide a good sensing of the gravitational field and by being polar in inclination, the entire Earth was mapped by these data. Our NOVA data analysis efforts benefitted substantially from the work on the same satellite by Tepper (1987).

The NOVA-1 data used in our analysis was taken as part of the MERIT Campaign in a Doppler supported effort called MERITDOC. The data spanned 95 days from March 30 to July 2, 1984. Sixteen globally distributed stations contributed tracking data to this campaign although data was not available from each for the entire campaign interval. In total, 16 6-day NOVA-1 arcs were orbitally reduced and included in the GEM-T2 solution. These orbital arcs are summarized in Table 3.4.

3.3 Satellite-to-Satellite Tracking Range-Rate Measurements

A satellite-to-satellite tracking experiment was conducted to enhance the normal tracking data sensitivity associated with localized geopotential mapping. This technique entailed the inter-satellite Doppler measurement between a high orbiting geosynchronous spacecraft ATS-6 and the lower orbiting GEOS-3. An earlier experiment, where a manned Apollo spacecraft served as the lower satellite, yielded very localized gravity anomaly recovery (see Kahn et al., 1982). This Satellite-to-Satellite Tracking (SST) geometry is often referred to as the high/low configuration. The enhancement in sensitivity to geopotential signal is a result of the availability of a spaceborne Doppler system having high precision levels (.03 cm/s and .01 cm/s for the destruct and non-destruct data respectively) and an inter-satellite visibility of over one-half of the lower satellite's revolution.

As elaborated upon in VonBun et al., (1980) the basic SST range-rate measurement is constructed from the link between a ground station, a geosynchronous satellite and a near-Earth

Table 3.4
NOVA-1 Orbital Arc Summary
(6-day arcs)

Epoch YYMMDD	No. Obs.	RMS (cm/s)
840330	2854	0.459
840405	4218	0.438
840411	4528	0.456
840417	5402	0.437
840423	5528	0.453
840429	6036	0.459
840505	6240	0.484
840511	6402	0.517
840517	5178	0.515
840523	5030	0.485
840529	3930	0.488
840604	3909	0.515
840610	3317	0.476
840616	4239	0.504
840622	4069	0.464
840628	2359	0.477
TOTALS	73239	0.469

Table 3.3
Ajisai Orbital Arc Summary

Epoch (YYMMDD)	No. Obs.	RMS (cm)	No. Stations
860818	5859	31.2	10
823	3416	29.4	12
828	2197	18.8	10
901	5305	34.4	12
906	3803	22.8	12
911	3281	22.6	12
860916	3471	21.2	11
921	3663	27.7	9
926	3003	24.9	9
1001	3053	26.2	9
1006	5480	21.6	10
1011	3543	21.6	10
861016	3503	29.7	13
1021	3514	23.5	10
1026	3039	24.4	10
1101	3280	26.4	11
1106	3584	22.4	11
1111	4306	21.0	12
861116	2538	18.7	11
1121	4319	22.4	11
1126	5425	23.1	11
1201	5605	25.5	11
1206	2854	24.0	9
1211	1678	21.8	6
861216	2876	24.4	8
1221	1208	23.9	7
1226	898	13.8	5
870106	6495	20.8	7
111	7059	18.2	7
116	4743	10.4	7
870121	4831	20.0	9
126	9173	23.5	11
201	7522	18.7	7
206	6414	15.5	10
211	2705	10.4	8
216	12558	17.8	9

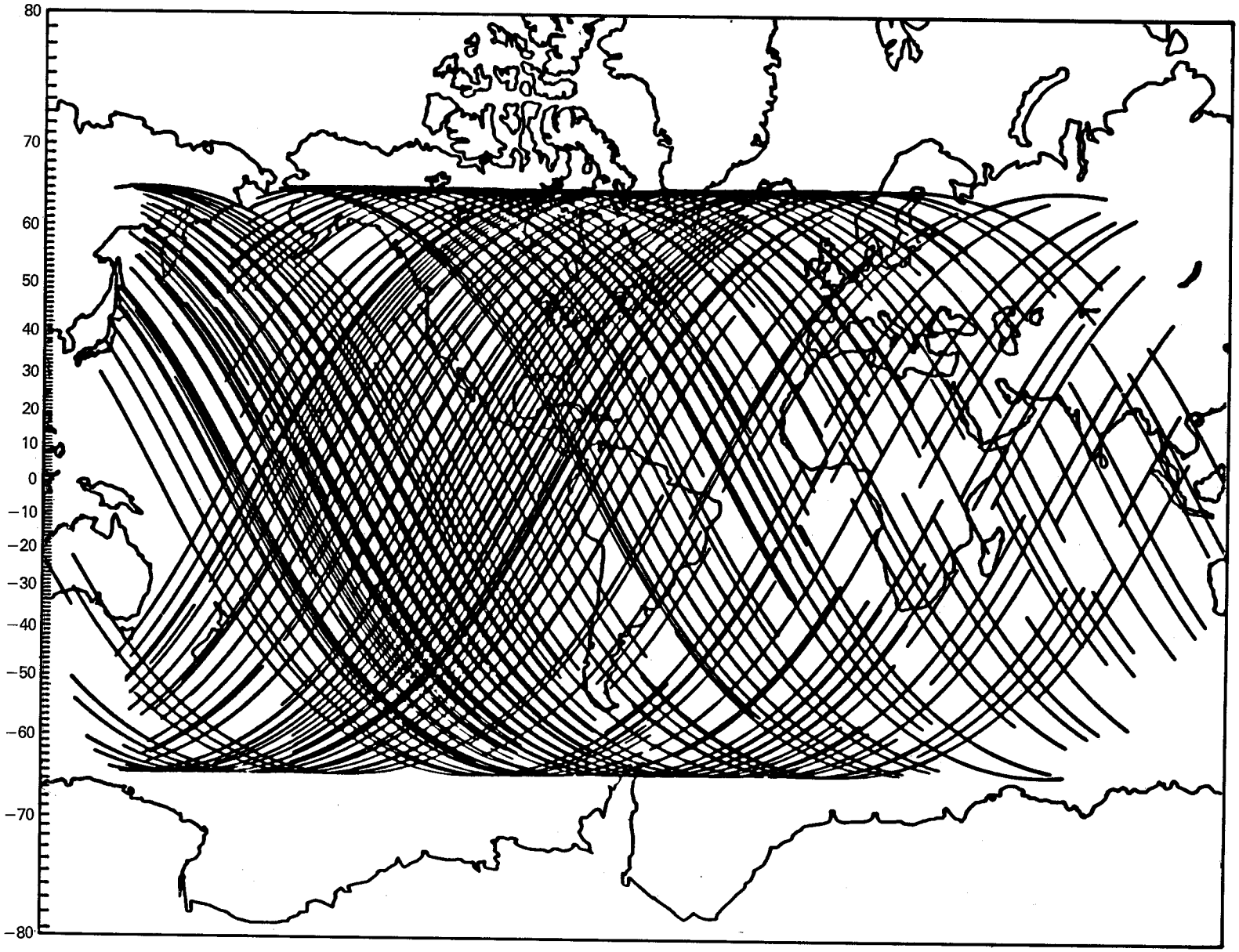

Figure 3.2 ATS—6/GEOS—3 Ground Tracks 1975-1978

Table 3.5
GEOS-3/ATS-6 ORBITAL ARC SUMMARY

ARC TIME START YYMMDDHHMMSS	ARC TIME STOP YYMMDDHHMMSS	NO. PASSES SST	NO. PASSES Laser	SST Rng-Rate RMS (cm/s)	SST Rng-Rate NOBS	Laser Range RMS (m)	Laser Range NOBS
750425000000	750430000000	14	13	0.140	3007	0.441	445
750507000000	750508112320	3	5	0.134	590	0.228	129
750510000000	750514000000	9	13	0.104	1612	0.545	261
750518000000	750520194010	8	9	0.108	1549	0.727	298
750522000000	750526182500	16	10	0.202	3069	0.311	219
750527000000	750531153850	15	13	0.174	3078	0.312	431
750617000000	750621000000	13	13	0.233	2116	0.452	444
761219000000	761224033934	10	18	0.251	2579	0.354	519
761226000000	761229164804	6	8	0.151	1474	0.420	363
770626000000	770630000000	2	19	0.073	223	0.644	772
770712000000	770716000000	2	8	0.077	173	0.423	378
770727000000	770731000000	5	17	0.177	568	0.658	795
770803000000	770807000000	6	18	0.116	534	0.961	783
770808000000	770812000000	5	25	0.137	691	0.745	1122
770813000000	770817000000	3	19	0.106	397	0.557	688
770818000000	770821000000	2	6	0.057	311	0.231	194
780921000000	780925000000	2	14	0.092	399	0.602	540
780926000000	781001170654	4	28	0.211	803	0.688	1287
781004000000	781008170424	4	21	0.168	882	0.660	802
781010000000	781014185044	2	37	0.050	382	0.700	1446
781018000000	781022000000	2	23	0.061	370	0.603	936
781025000000	781029215134	4	20	0.157	757	0.799	805
781107000000	781112214700	4	22	0.200	734	0.696	732
790109000000	790116000000	2	23	0.049	409	1.551	955
790117000000	790121181500	3	18	0.047	353	1.626	863
790212000000	790216183454	2	17	0.050	338	0.650	820

satellite. The dominant portion of the range-rate signal is the inter-satellite range-rate between the geosynchronous satellite and the low orbiting satellite. The-ground-to-ATS-6 link in the measurement is made at S-Band frequencies while the inter-satellite link is made at C-Band. Fortunately, this later link takes place above the atmosphere and only at the extremes involving horizon tracking, does the inter-satellite signal penetrate the ionosphere. In such circumstances (i.e., if the inter-satellite vector passes within 300 km of the Earth's surface) these data were edited.

The SST data available from GEOS-3/ATS-6 is presented in Figure 3.2. ATS-6 was at 140°W longitude for most of the observations taken over the Pacific Ocean. The satellite was moved to a position over Africa for the acquisition of the eastern hemisphere data. While ATS-6 was in its drift phase between these locations, passes over South America and the Atlantic Ocean were observed. Nearly two-thirds of these data -- 148 out of a possible 226 passes -- were used (the others lacked suitable ground tracking support) for the 26 5-day arcs of SST utilized in GEM-T2. This is the first time any of these data have been utilized within the GEM model development. Table 3.5 summarizes these arcs and the initial observation statistics obtained in forming the normal equations. GEM-T1 was used as the apriori model for these computations.

3.4 Landsat-1 S-Band Radar Two-way and Three-way Average Range-Rate Observations

Landsat-1 is an Earth imaging satellite placed into a circular sun-synchronous orbit at an altitude of approximately 900 km. Being Earth imaging, Landsat required active attitude maintenance throughout its entire mission. However, when the satellite was deactivated in 1974, two months of thrust-free data were acquired on this satellite to support geodetic modeling efforts. Landsat-1 observations are very important for geopotential field recovery for many satellites are placed into orbit at this inclination for sun-synchronous mission requirements. SPOT-2, EOS and ERS-1 are future missions requiring precise orbits, and which are to be placed into orbits having very similar characteristics. Landsat-1 is also very interesting from a satellite geodesy standpoint given its very large, shallow resonance perturbations with the 14th, 28th and 42nd order terms in the gravity spherical harmonic expansion. These resonance effects are given in Table 3.6 and represent some of the largest such effects seen within GEM-T2.

The Landsat data were acquired by the Unified S-Band Tracking Network which was the operational network supporting NASA missions throughout the 1970's. Two-way (i.e., station to satellite to station) average range-rate data were acquired by sites located at GSFC, Madrid (Spain), Guam, Goldstone (California), Ascension Island, Bermuda and Hawaii. Three-way data were also acquired between several antennas located at GSFC and Goldstone where one station transmitted while two widely separated stations received the satellite return signal. Unfortunately, these data lacked any correction for ionospheric refraction effects which for daytime passes during high solar activity could produce measurement errors of 1 to 2 cm/s which is at the level of fit we find for these observations. However, the data residuals were scrutinized and an elevation angle cutoff of 10 degrees was used (whereas these systems typically tracked to the horizon) to reduce problems resulting from this error source.

3.5 New Optical Data in GEM-T2

Table 3.7 summarizes the additional optical satellites which were added to GEM-T1 in forming GEM-T2. Briefly stated therein is the reason these data were selected for the GEM-T2 solution. Figure 3.3 shows the SAO Baker-Nunn camera locations which provided the tracking for these satellites whereas Table 3.8 shows the number of observations from each station included in the field. The geographic distribution of the stations is good and all sites acquired significant numbers of observations. Table 3.9 summarizes the number of 7-day arcs and the number of observations utilized in GEM-T2. It also compares the current processing of these observations for inclusion in GEM-T2 versus that for GEM-7 in 1976 which was the last time these data were reduced to form normal equations. Improved processing and apriori information is evident. In total, 9 new optical data sets were added to GEM-T1 giving more than twice the number of these observations within the GEM-T2. Surprisingly, these data are important for the definition of the field, especially in the determination of the zonal and resonance orders in the gravity model.

Table 3.6
Landsat-1 Satellite Resonance Perturbations

m	Beat Period (Days)	Along-Track Perturbation (meters)
	MAIN RESONANCES	
14th Order	18.17	6400
28th Order	9.09	76
42nd Order	4.51	10
	SIDEBAND RESONANCES	
13th Order	1.06	11
15th Order	0.94	24
16th Order	0.48	7
17th Order	0.33	3

Table 3.7

NEW OPTICAL DATA FOR GEM-T2

No.	SATELLITE	INCLINATION DEGREE	MEAN MOTION REV/DAY	REASON FOR SELECTION
1	OVI-2	144.27	11.45	Fill in inclination gap.
2	ECHO-1RB	47.21	12.21	Fill in inclination gap.
3	SECOR-5	69.22	11.79	Inclination near TOPEX.
4	INJUN	66.82	11.79	Inclination near TOPEX.
5	TRANSIT-4A	66.82	13.85	Inclination near TOPEX.
6	5BN-2	89.95	13.46	Resonance close to TOPEX.
7	OGO-2	87.37	13.79	Resonance close to TOPEX.
8	OSCAR-7	89.70	13.60	Resonance close to TOPEX.
9	MIDAS-4	95.83	8.69	Unique resonance and inclination.

Table 3.8

DISTRIBUTION OF OBSERVATIONS FROM BAKER-NUNN STATIONS

SATELLITE	SAO BAKER-NUNN STATIONS											
	9001	9002	9003	9004	9005	9006	9007	9008	9009	9010	9011	9012
OVI-2	114	71	138	70	30	134	90	112	48	96	4	66
ECHO-1RB	428	558	686	404	226		224	362	162	489	549	394
SECOR-5	48	123	165	32	6	42	34	32	36	30	134	44
INJUN-1	499	427	522	120	262	108	167	104	186	169	322	428
TRANSIT-4A	595	546	787	246	267	54	134	116	146	196	310	435
5BN-2	150	74	58	44	16	104	20	62	54	76	58	104
OGO-2	135	154	115	98	36	87	102	54	32	81	86	156
OSCAR-7	63	118	246	80		380	194	102	94	34	186	365
MIDAS-4	4056	843	766	2722	1306	2929	2550	2658	3146	2174	2243	2839
TOTAL	6088	2914	3483	3816	2149	3838	3515	3602	3904	3345	3892	4831

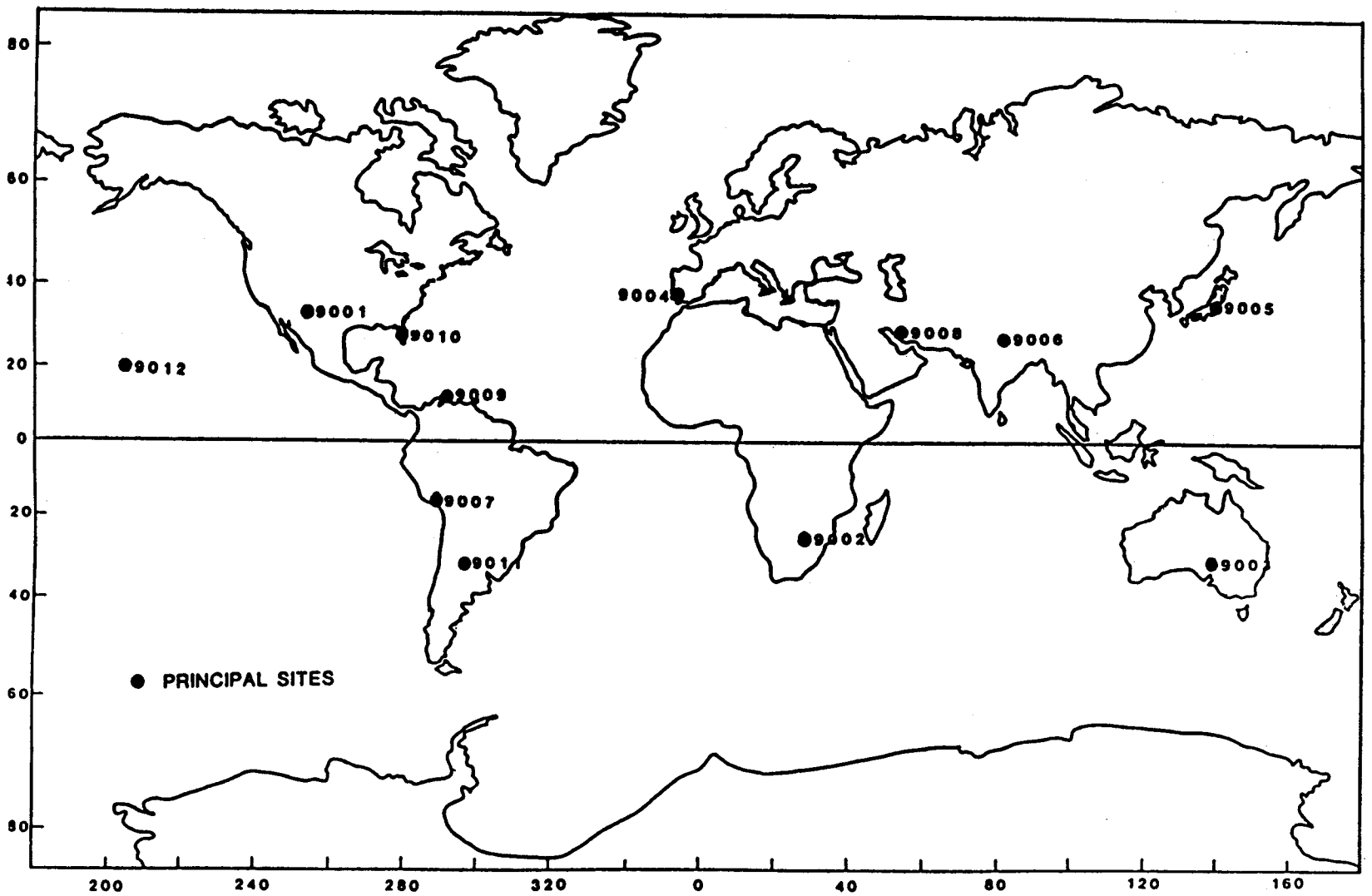

Figure 3.3 SAO BAKER-NUNN Camera Stations

Table 3.9

NEW OPTICAL DATA FOR GEM-T2

SUMMARY

	DATA IN	GEM-L2	GEM-T2	GEM-L2	GEM-T2	GEM-L2	GEM-T2
No.	SATELLITE	ARCS		OBS.		AVG. RMS in ARCSEC/2 with	
						GEM4	GEM10B
1	OVI-2	4	4*	910	973	1.953	1.552
2	ECHO-1RB	18	32	2420	4482	1.552	1.219
3	SECOR-5	4	13*	290	726	1.319	1.224
4	INJUN-1	9	44	768	3310	1.409	1.386
5	TRANSIT-4A	14	50	1316	3832	1.280	1.309
6	5BN-2	5	17*	355	820	3.428	1.235
7	OGO-2	7	16	461	1207	3.640	2.353
8	OSCAR-7	4	4*	1780	1862	1.465	1.069
9	MIDAS-4	20	50	14879	31779	0.969	0.905
	TOTAL	85	230	23179	48991	1.890	1.363

** maximum data available*

SECTION 4. SOLUTION DESIGN: ESTIMATION WITH OPTIMUM DATA WEIGHTING

Our general method of weighted least squares with apriori signal constraints was implemented for the estimation of the Goddard Earth Models in the late 1970's (Lerch et al., 1979). This method has been modified in GEM-T2 to include a new optimum data weighting technique which automatically calibrates the errors for the estimated gravity field (Lerch, 1989). Some review is made herein of our general solution methodology. Our constrained least squares method is analogous to least squares collocation (Moritz,1980) and has permitted us to extend the size of the adjusting model. The extension of the size of the solution to higher degree and order allows us to more thoroughly exhaust the gravitational signal sensed by ever more precise tracking technologies. Stable solutions extending beyond 16x16 were possible using this method whereas correlation among high degree coefficients caused unreliable coefficient adjustments when models were made lacking these constraints. As computer capabilities improved, satellite-only models were extended to degree and order 36 (as in GEM-T1) and increased significantly to the present size of GEM-T2. This earlier method (which now has been extended to provide optimal data weighting) is discussed in detail within Marsh et al., (1988) where it was shown to be analogous to the work of Moritz (1980).

In our general estimation process of the GEM solutions the new weighting technique has been integrated into the solution design. The method determines the weights for the data subsets across the different satellite tracking systems on different orbits in order to automatically obtain an optimum least squares solution and an error calibration of the adjusted parameters. The weighting system is designed to produce realistic error estimates. The data receive optimal weight in the solution according to their contribution to the model's accuracy. The method employs data subset solutions in comparison with the complete solution and uses an algorithm to adjust the data weights by requiring that the differences of the parameters between solutions agree with their corresponding error estimates. With the adjusted weights, the process provides for an automatic calibration of the solution's error estimates. The data weights which are obtained are generally much smaller than the weights associated with the accuracies of the observations (noise-only) themselves.

This algorithm is now an integral part of our general estimation technique. The weighting algorithm has been applied to the least squares process of minimizing the weighted observation residuals with apriori constraints on the size of the signal obtained from the known power spectrum of the terrestrial gravity field. The main purpose of the apriori signal constraints is to provide stability for the high degree terms, allowing the signal to be exhausted by the model.

The data weighting previously used in GEM-T1 and other earlier GEM models was based on a series of tests using selected arcs of tracking data, independent gravity anomaly data, and orbital deep resonance predictions to test the characteristics, performance and sensitivity of candidate fields. Models which were found to give better performance on these tests were studied, and data weights were further refined until an optimal model was developed based upon these criteria. The new weighting system is an outgrowth of the process undertaken to evaluate in great detail, the accuracy of GEM-T1 (Lerch et al., 1989) and the overall means for calibrating model uncertainties. The data weights selected for GEM-T1 have been specifically confirmed in these studies. However, when the complete data set for GEM-T2 is assembled, even the weights for GEM-T1's original data show some variation because of the increased data coverage in GEM-T2.

There are two major concerns in the proper weighting of least squares normal equations:

(a) weighting the individual observations corresponding to the expected accuracy of the observations within an aposteriori context. Ideally, these are the so-called "noise-only" statistics; and

(b) accounting for the effects of unmodelled biases and forces on the solution by reweighting the normal equations to balance the solution for the non-uniform presence of these effects.

The normal least squares solution accounts for (a) but not for the effects of (b) without some special analysis and selection of an optimal data weighting algorithm.

Within a least squares solution in the ideal case, the observation residuals approximate their noise-only distribution so that:

$$((\Sigma r^2/\sigma^2)/\text{num}) \approx 1 \qquad (4.1)$$

where r is the observation residual, num is the number of observations and σ corresponds to its noise-only observational uncertainty. This behavior is common in theory where observations are unbiased, uncorrelated and where data noise is the dominant error source. However, the observations available for gravitational field recovery and the ancillary force and measurement models which are required to isolate this gravitational signal depart markedly from this ideal case. Our solution suffers from a great many sources of systematic error, imperfect environmental and measurement models, neglected small force modeling effects and a host of other problems which need to be addressed if an optimal gravitational modeling solution is to result. Our understanding of these problems is presently limited to approximate estimates of the error magnitudes in our models, and we unfortunately lack the observations and the resources to improve everything which is part of our solution environment. The net result is that our solution aposteriori can only fit our most precise data sets, such as the observations provided by advanced laser systems, to a factor of 3 to 10 worse than their noise-only expectation of system performance. These problems cause optimization of data weighting and field calibration to be major undertakings if an improved solution with well understood and reliable error estimates is to result. Unfortunately, data noise has only a modest impact on the final data weights which are obtained.

Satellite orbital characteristics, area-to-mass ratios and the number/deployment of components comprising the satellite bus etc. are highly variable, which causes some satellites to experience much larger and more difficult to model non-conservative force model effects. Atmospheric drag for lower altitude satellites presents a serious modeling problem with present state-of-the-art atmospheric density models yielding errors of 20 to 30% for satellites at geodetically useful orbits of 800 to 1200 km altitude (Hedin, 1988). Adjustment of empirical coefficients scales the effective atmospheric density given by the drag models through a scaling of the drag acceleration over some temporal interval in an averaged sense. However, these coefficients do little to ameliorate problems associated with the nature and detailed structure of the fluctuations in density which exist but are presently unmodeled by contemporary density models within these averaging intervals. Drag is by no means unique in its imperfect representation.

The aposteriori RMS of fit to the observations gives some measure for determining the effective data weights by reflecting, in a relative sense, these force model difficulties especially when common tracking systems are used to acquire data on different orbits. Obviously, this relative comparison cannot be applied uniformly since few satellites are tracked by more than one tracking technology, and the tracking systems evolve over time. Nevertheless, the relative RMS of fit achieved from the solution is still used. However, assessment made across data sets can only be approximated and is based on some broad characterization of system noise-only characteristics when determining relative data weights.

However, when these systematic errors are present, they do not manifest themselves as random data residuals. This non-randomness (strongly seen within a pass of observation residuals) must also be accommodated through data reweighting. Furthermore, this requires taking into account the number of points in a typical pass of data so affected. This reweighting W_j, must be optimized across all data subsets j, which are used in combination to form the

combined solution normal-equations whose inversion yields the gravitational solution. W_j as derived in Lerch, (1989) can be shown to approximate:

$$W_j = 1 / \hat{\sigma}_j^2$$

$$\approx \frac{1}{(Nobs_j)(RMS_j)^2} \qquad (4.2)$$

where: (Since the assigned apriori data noise uncertainty should represent the true noise in the data although this is seldom the case, an additional adjustment to the data weights is commonly needed.) RMS_j is the aposteriori rms of fit to the observation subset j, and $Nobs_j$ is a value corresponding to a typical number of points in a pass of tracking data. In practice, the RMS_j is scaled by a factor which changes with differing tracking technologies. Hence $\hat{\sigma}_j$ indicates the error showing the true value of a single observation of type j on the solution (see Tables 4.1 and 4.2).

The method for the solution requires the minimization of the sum Q which is a combination of signal and noise as follows:

$$Q = \Sigma \frac{C^2_{l,m} + S^2_{l,m}}{\sigma^2_l} + \Sigma W_j r_j^2 \qquad (4.3)$$

where the signal is given by

$C_{l,m}$ and $S_{l,m}$: which are the spherical harmonics composing the solution coefficients; and

σ_l : is a modified version of Kaula's rule which is the known power of the terrestrial gravitational field.

The noise is given by:

r_j : which are the observation residuals of the respective tracking system; and

W_j : which is the optimal weighting factor which compensates for unmodeled error effects (which should ideally equal the reciprocal variance of the noise of the respective tracking system).

When minimizing Q using the least squares method, the normal metric equation and error covariance is obtained as follows:

$W_j N_j x = W_j R_j$ are the original normal equations for the jth data subset (see Lerch, 1989).

The solution is formed after summing each of the satellite data normal matrices N_j over the entire range of data subsets giving a combined normal matrix for the solution by:

$$N = K^{-1} + \Sigma W_j N_j \qquad (4.4)$$

The:

$$K = \Sigma \frac{C^2_{lm} + S^2_{lm}}{\sigma^2_l} \qquad (4.5)$$

matrix is the diagonal signal matrix which is introduced to achieve improved stability for the gravitational model adjustment. This modified least squares method stabilizes the solution through the minimization of the size of the adjusting gravitational terms above a certain degree cutoff.

Letting j=0 denote the least squares subset normals for the apriori signal constraints for the coefficients, K (as in 4.5), then the complete normals for minimizing Q in (4.3) is given by:

$$N x = R \qquad (4.6)$$

where

$$N = \sum_{j=0} W_j N_j$$

$$R = \sum_{j=0} W_j R_j$$

and

$V_{xx} = N^{-1}$ is the approximate form for the error covariance matrix which should yield reliable parameter uncertainties if proper weighting factors (W_j) are used.

The weight W_0 signifies the scale for the apriori signal constraints on the static gravity parameters. It is held fixed at unity since the power spectrum of the gravity field is well known. On the other hand, the optimal weights W_j for the satellite tracking data are quite variable as shown in Tables 4.1 and 4.2, and can depart from the nominal noise-only values by up to two orders of magnitude. Clearly, it is these weights which must be determined and optimized. We view the automation of this process as a considerable advancement.

4.1 The Optimal Weighting Algorithm

The automatic data weighting algorithm as developed by Lerch (1989) is given by the following procedure:

Let the normals for data set t be defined as (w ≡ W):

$$w_t N_t = w_t R_t \qquad (4.7)$$

where N is the normal matrix for data set t, R is the normal matrix of observation residuals, and w_t is the weight in the iterative solution. The complete solution containing all data sets is given as:

$$x = (\sum_j w_j N_j)^{-1} (\sum w_j R_j) \tag{4.8}$$

A subset solution which lacks data set t is given as:

$$x_t = (\sum_{j \neq t} w_j N_j)^{-1} (\sum_{j \neq t} w_j R_j) \tag{4.9}$$

The covariances for solution x and x_t are respectively:

$$V(x) = (\sum_j w_j N_j)^{-1} \quad \text{and} \quad V(x_t) = (\sum_{j \neq t} w_j N_j)^{-1} \tag{4.10}$$

The normal residuals for these solutions are:

$$R(x) = (\sum_j w_j R_j) \quad \text{and} \quad R(x_t) = (\sum_{j \neq t} w_j R_j) \tag{4.11}$$

The difference between the subset and full solutions can be predicted by their respective covariances. This is the principle behind this calibration and determination of optimal data weighting technique. The difference between the two fields reflects the unmodeled errors in data set t, since the error effects to first order, subtract out for the data sets common to both solutions. The difference is simply:

$$x_t - x = V(x_t)\, R(x_t) - V(x)\, R(x) \tag{4.12}$$

If E is used to express the expected value, then the differences in these models are predicted by the error covariances of the solution differences given by:

$$E(x_t - x)(x_t - x)^T = V(x_t) - V(x)$$
$$= V(x_t - x) \tag{4.13}$$

We can now introduce the calibration factor k_t for the t data subset which is being computed. If the trace of a matrix is denoted as TR and we restrict the analysis to only the gravity coefficients, then k_t is given as:

$$(x_t - x)^T (x_t - x) = k_t \, TR \, [V(x_t - x)] \tag{4.14}$$

and the adjusted weight as:

$$w_t^* = w_t/k_t \tag{4.15}$$

Since the subset and complete solution alike change when the weight on a subset data set is altered, these weights require iteration. Several successive solutions are produced using improved weights until the calibration factor, k_t, equals 1 for each data subset. Quite remarkably, the weights converge in only a few iterations, as shown later in Table 6.1. Moreover, these calibrated weights largely follow the estimate based on the aposteriori RMS of fit and number of points in a typical pass as shown in equation (4.2).

Tables 4.1a and 4.1b present the major data subsets comprising GEM-T2. Also shown is the aposteriori RMS of fit (approximate) of the observations and the final weights computed. The computation of the weights and the automatic error calibration which results is discussed thoroughly in Section 6.

Table 4.1a

SATELLITE DATA IN GEM-T1

SATELLITE	SEMI MAJOR AXIS (km.)	ECC	INCL DEG	DATA TYPE	# OF ARCS	# OF OBS	RMS RESID. σ_t	SIGMA* WEIGHTS $\hat{\sigma}_t$
1 LAGEOS	12273.	.0038	109.85	LASER	57	144527	10cm.	112cm.
2 STARLETTE	7331.	.0204	49.80	LASER	46	57356	20cm.	224cm.
3 GEOS-3	7226.	.0008	114.98	LASER	36	42407	70cm.	816cm.
4 PEOLE	7006.	.0164	15.01	LASER	6	4113	90cm.	816cm.
5 BE-C	7507.	.0257	41.19	LASER	39	64240	50cm.	577cm.
				CAMERA	50	7501	2 arcsec	5.6 arcsec
6 GEOS-1	8075.	.0719	59.39	LASER	48	71287	70cm.	667cm.
				CAMERA	43	60750	1 arcsec	8.9 arcsec
7 GEOS-2	7711.	.0330	105.79	LASER	28	26613	80cm.	816cm.
				CAMERA	46	61403	1 arcsec	8.9 arcsec
8 DI-C	7341.	.0532	39.97	LASER	4	7455	150cm.	816cm.
				CAMERA	10	2712	2 arcsec	7.3 arcsec
9 DI-D	7622.	.0848	39.46	LASER	6	11487	100cm.	816cm.
				CAMERA	9	6111	2 arcsec	8.9 arcsec
10 SEASAT	7170.	.0021	108.02	LASER	14	14923	70cm.	707cm.
				DOPPLER	14	138042	.5cm/sec	7cm/sec
11 OSCAR-14	7440.	.0029	89.27	DOPPLER	13	63098	1cm/sec	8cm/sec
12 ANNA-1B	7501.	.0082	50.12	CAMERA	30	4463	2 arcsec	4.5 arcsec
13 BE-B	7354.	.0135	79.69	CAMERA	20	1739	2 arcsec	4.5 arcsec
14 COURIER-1B	7469.	.0161	28.31	CAMERA	10	2476	2 arcsec	4.5 arcsec
15 TELSTAR-1	9669.	.2429	44.79	CAMERA	30	3962	2 arcsec	4.5 arcsec
16 VANGUARD-2RB	8496.	.1832	32.92	CAMERA	10	686	2 arcsec	4.5 arcsec
17 VANGUARD-2	8298.	.1641	32.89	CAMERA	10	1299	2 arcsec	4.5 arcsec

* $SIGMA\ (\hat{\sigma}) = \left(\frac{1}{w}\right)^{\frac{1}{2}}$

Table 4.1B

NEW SATELLITE DATA IN GEM-T2 IN ADDITION TO GEM-T1

SATELLITE	SEMI MAJOR AXIS (km.)	ECC	INCL DEG.	DATA TYPE	# OF ARCS	# OF OBS.	RMS RESID. σ_t	SIGMA WEIGHTS $\hat{\sigma}_t$
LAGEOS '84,'85,'86,'87	12273	.0038	109.85	LASER	29	134093	10cm.	112cm.
STARLETTE '83,'84	7331	.024	49.80	LASER	38	40041	20cm.	224cm.
STARLETTE '86				LASER	73	411102	20cm.	500cm
AJISAI	7870	.0006	50.0	LASER	36	156021	16cm.	316cm.
GEOS-1 '80	8075	.0719	59.39	LASER	30	54129	32cm.	258cm.
GEOS-3 '80	7226	.0008	114.98	LASER	50	54526	25cm.	224cm.
GEOS-3				LASER	26	17027	70cm.	816cm.
GEOS-3:ATS '75,'76	41867	.001	0.9	SST	9	19074	.4cm/sec	7.1cm/sec
GEOS-3:ATS '77,'78,'79				SST	17	8326	.2cm/sec	3.2cm/sec
NOVA	7559	.0011	89.96	DOPPLER	16	73238	.4cm/sec	2.6cm/sec
LANDSAT-1	7286	.0012	99.12	DOPPLER	10	26426	1.5cm/sec	10.5cm/sec
GEOSAT	7169	.0008	108.0	DOPPLER	13	549141	1.3cm/sec	4.5cm/sec
OVI-2	8317	.0184	144.27	CAMERA	4	973	2 arcsec	5.8 arcsec
ECHO-1RB	7966	.0118	47.21	CAMERA	32	4482	2 arcsec	8.2 arcsec
SECOR-5	8151	.0793	69.22	CAMERA	13	726	2 arcsec	5.8 arcsec
INJUN-1	7316	.0079	66.82	CAMERA	44	3310	2 arcsec	8.2 arcsec
TRANSIT-4A	7322	.0076	66.82	CAMERA	50	3832	2 arcsec	8.2 arcsec
5BN-2	7462	.0058	89.95	CAMERA	17	820	2 arcsec	8.2 arcsec
OGO-2	7341	.0752	87.37	CAMERA	16	1207	2 arcsec	8.2 arcsec
OSCAR-7	7411	.0224	89.70	CAMERA	4	1862	2 arcsec	5.8 arcsec
MIDAS-4	9995	.0112	95.83	CAMERA	50	31779	2 arcsec	8.2 arcsec

SECTION 5. THE GEM-T2 GRAVITATIONAL MODELING SOLUTION RESULTS

This section discusses the major products of the GEM-T2 solution which include:

- O the static gravitational model,
- O an expanded model for selected long wavelength ocean tidal terms,
- O station coordinates for the 45 TRANET sites tracking GEOSAT, and
- O the Earth polar motion and orientation series.

Where applicable, these models and their uncertainty estimates will be compared with other solutions to provide a qualitative understanding of the accuracy of these results.

5.1 The GEM-T2 Gravitational Solution

Table 5.1 presents the normalized spherical harmonic coefficients for GEM-T2. These coefficients describe the static geopotential in classical spherical harmonic form given by:

$$U = \frac{GM}{r} \left\{ 1 + \sum_{l=2}^{lmax} \sum_{m=0}^{l} (a_e/r)^l \; P_{l,m} (\sin \phi) \cdot \left(C_{l,m} \cos m\lambda + S_{l,m} \sin m\lambda \right) \right\} \qquad (5.1)$$

where:

G	is the gravitational constant,
M	is the mass of the Earth,
ϕ	is the satellite geocentric latitude,
λ	is the satellite east longitude,
P_{lm}	is the normalized associated Legendre function of the first kind; and
C_{lm},S_{lm}	are the normalized geopotential coefficients.

The geopotential forces are computed as the gradient of the potential U. The calibration of the model uncertainties are discussed in Section 6.

5.2 The GEM-T2 Ocean Tidal Solution

The GEM-T2 solution solves for temporal changes in the external gravitational attraction of the Earth sensed by near-Earth orbiting objects at the major astronomical frequencies. These tidal terms are not exactly equivalent with those measured on the ocean surface although they can be similar in magnitude and of a comparable physical origin. Even when tides themselves are being sensed, a satellite experiences an attenuated signal from the solid Earth/oceans/atmosphere which is a combined effect. An artificial satellite senses the mass redistribution associated with the tides, but the tracking data taken on these objects has no way of discriminating between the tidal effects caused by deformation within the solid Earth apart from the oceans. We choose to solve for terms in the space of ocean tides using a classical spherical harmonic representation as described in Christodoulidis et al., (1988), but this is merely a matter of convenience and not one of necessity. This approach is chosen since we believe that contemporary models of the frequency-dependent solid Earth tidal response (Wahr, 1981) are better known at the

Table 5.1

GEM-T2 NORMALIZED COEFFICIENTS

UNITS OF 10^{-6}

ZONALS

INDEX N	INDEX M	VALUE	INDEX N	INDEX M	VALUE	INDEX N	INDEX M	VALUE	INDEX N	INDEX M	VALUE	INDEX N	INDEX M	VALUE
2	0	-484.1652998	3	0	0.9570331	4	0	0.5399078	5	0	0.0686883	6	0	-0.1496092
7	0	0.0900847	8	0	0.0483835	9	0	0.0284403	10	0	0.0549673	11	0	-0.0519374
12	0	0.0340918	13	0	0.0429873	14	0	-0.0208746	15	0	0.0008078	16	0	-0.0069674
17	0	0.0211398	18	0	0.0086686	19	0	-0.0048120	20	0	0.0199685	21	0	0.0095754
22	0	-0.0101581	23	0	-0.0241859	24	0	0.0010847	25	0	0.0069648	26	0	0.0009484
27	0	0.0027591	28	0	-0.0064182	29	0	-0.0008836	30	0	-0.0009634	31	0	0.0076193
32	0	-0.0027771	33	0	0.0051093	34	0	-0.0057588	35	0	0.0078141	36	0	-0.0047918
37	0	0.0022441	38	0	0.0013147	39	0	-0.0010497	40	0	0.0020610	41	0	0.0011051
42	0	0.0013010	43	0	0.0021499	44	0	0.0002269	45	0	0.0020158	46	0	-0.0008216
47	0	0.0008891	48	0	-0.0002987	49	0	0.0000776	50	0	0.0002472			

SECTORIALS AND TESSERALS

INDEX N	INDEX M	VALUE C	VALUE S	INDEX N	INDEX M	VALUE C	VALUE S	INDEX N	INDEX M	VALUE C	VALUE S
2	2	2.4390067	-1.4000870								
3	1	2.0307524	0.2496027	3	2	0.9035391	-0.6189858	3	3	0.7215073	1.4137252
4	1	-0.5352557	-0.4741332	4	2	0.3482596	0.6640236	4	3	0.9913108	-0.2014288
4	4	-0.1893677	0.3089680								
5	1	-0.0607595	-0.0950258	5	2	0.6560800	-0.3241298	5	3	-0.4518505	-0.2170711
5	4	-0.2950497	0.0513561	5	5	0.1719075	-0.6690593				
6	1	-0.0771405	0.0253197	6	2	0.0524466	-0.3752434	6	3	0.0584154	0.0068782
6	4	-0.0888267	-0.4711255	6	5	-0.2660832	-0.5368830	6	6	0.0096978	-0.2369657
7	1	0.2818503	0.0962266	7	2	0.3209757	0.0956941	7	3	0.2523951	-0.2095998
7	4	-0.2742482	-0.1241968	7	5	-0.0001020	0.0196942	7	6	-0.3585523	0.1515878
7	7	-0.0014862	0.0252823								

Table 5.1

GEM-T2 NORMALIZED COEFFICIENTS (continued)

UNITS OF 10^{-6}

SECTORIALS AND TESSERALS

INDEX N	INDEX M	VALUE C	VALUE S	INDEX N	INDEX M	VALUE C	VALUE S	INDEX N	INDEX M	VALUE C	VALUE S
8	1	0.0245721	0.0584482	8	2	0.0695068	0.0672988	8	3	-0.0165651	-0.0870735
8	4	-0.2431044	0.0670171	8	5	-0.0236439	0.0871455	8	6	-0.0648602	0.3101548
8	7	0.0689064	0.0747229	8	8	-0.1214399	0.1206619				
9	1	0.1421125	0.0253655	9	2	0.0284926	-0.0349829	9	3	-0.1613077	-0.0856736
9	4	-0.0121815	0.0258612	9	5	-0.0240867	-0.0575285	9	6	0.0667472	0.2233634
9	7	-0.1229254	-0.0951409	9	8	0.1881954	-0.0037058	9	9	-0.0613486	0.0970425
10	1	0.0831559	-0.1356199	10	2	-0.0819359	-0.0501065	10	3	-0.0040960	-0.1604117
10	4	-0.0939427	-0.0688070	10	5	-0.0489204	-0.0458035	10	6	-0.0344837	-0.0783753
10	7	0.0090179	-0.0022192	10	8	0.0421606	-0.0928536	10	9	0.1243856	-0.0389412
10	10	0.0966394	-0.0189409								
11	1	0.0187900	-0.0302389	11	2	0.0125806	-0.0919944	11	3	-0.0310305	-0.1317779
11	4	-0.0363188	-0.0702274	11	5	0.0404925	0.0583781	11	6	-0.0022096	0.0280076
11	7	0.0032535	-0.0874471	11	8	-0.0059489	0.0237541	11	9	-0.0401308	0.0432696
11	10	-0.0529919	-0.0213622	11	11	0.0455060	-0.0645895				
12	1	-0.0542526	-0.0442035	12	2	0.0067317	0.0318030	12	3	0.0403968	0.0175864
12	4	-0.0632924	-0.0045521	12	5	0.0372697	0.0044109	12	6	-0.0021614	0.0427936
12	7	-0.0159953	0.0348520	12	8	-0.0233721	0.0148369	12	9	0.0421812	0.0236585
12	10	-0.0084006	0.0319901	12	11	0.0097894	-0.0084029	12	12	-0.0051825	-0.0111076
13	1	-0.0578349	0.0450475	13	2	0.0531545	-0.0631397	13	3	-0.0168961	0.0833743
13	4	-0.0089251	-0.0017503	13	5	0.0486179	0.0541729	13	6	-0.0231957	0.0010616
13	7	-0.0031866	-0.0056732	13	8	-0.0101581	-0.0099146	13	9	0.0182999	0.0462252
13	10	0.0400341	-0.0414749	13	11	-0.0430363	-0.0000298	13	12	-0.0310323	0.0840309
13	13	-0.0625300	0.0680460								
14	1	-0.0165468	0.0271254	14	2	-0.0384924	-0.0000438	14	3	0.0391644	0.0203106
14	4	-0.0079895	-0.0005932	14	5	0.0245675	-0.0148326	14	6	-0.0095223	0.0072857
14	7	0.0366711	-0.0026792	14	8	-0.0345926	-0.0190955	14	9	0.0345501	0.0290567
14	10	0.0364787	-0.0031316	14	11	0.0138047	-0.0404306	14	12	0.0078664	-0.0320212
14	13	0.0320213	0.0454383	14	14	-0.0512674	-0.0050594				

Table 5.1

GEM-T2 NORMALIZED COEFFICIENTS (continued)

UNITS OF 10^{-6}

SECTORIALS AND TESSERALS

INDEX N	INDEX M	VALUE C	VALUE S	INDEX N	INDEX M	VALUE C	VALUE S	INDEX N	INDEX M	VALUE C	VALUE S
15	1	0.0122177	0.0111280	15	2	-0.0251562	-0.0288124	15	3	0.0401686	0.0262597
15	4	-0.0435169	0.0075971	15	5	0.0100013	0.0175705	15	6	0.0256916	-0.0515399
15	7	0.0607753	0.0152877	15	8	-0.0331076	0.0235607	15	9	0.0113370	0.0445301
15	10	0.0090273	0.0113802	15	11	0.0021578	0.0233866	15	12	-0.0321733	0.0087246
15	13	-0.0290699	-0.0041930	15	14	0.0067593	-0.0247259	15	15	-0.0189824	-0.0057180
16	1	0.0297624	0.0240565	16	2	-0.0140907	0.0248689	16	3	-0.0326144	-0.0439916
16	4	0.0396039	0.0473846	16	5	-0.0067956	0.0018428	16	6	0.0063436	-0.0284975
16	7	-0.0009530	-0.0126372	16	8	-0.0182064	0.0030949	16	9	-0.0188186	-0.0382171
16	10	-0.0127558	0.0083994	16	11	0.0183569	-0.0043302	16	12	0.0200031	0.0053417
16	13	0.0134693	0.0011027	16	14	-0.0194970	-0.0386309	16	15	-0.0161367	-0.0310450
16	16	-0.0341988	-0.0064019								
17	1	-0.0286816	-0.0293496	17	2	-0.0042782	0.0141925	17	3	0.0119428	0.0093266
17	4	0.0116340	0.0224278	17	5	-0.0147210	-0.0050012	17	6	0.0050910	-0.0177731
17	7	0.0190439	-0.0103587	17	8	0.0393184	0.0073649	17	9	-0.0011019	-0.0347984
17	10	-0.0052074	0.0155743	17	11	-0.0123774	0.0154974	17	12	0.0296813	0.0129861
17	13	0.0170527	0.0208044	17	14	-0.0131460	0.0114902	17	15	0.0052124	0.0054143
17	16	-0.0315737	0.0022165	17	17	-0.0366559	-0.0215735				
18	1	0.0020036	-0.0353441	18	2	0.0019658	0.0217675	18	3	-0.0026138	-0.0050753
18	4	0.0485785	0.0015282	18	5	0.0049920	0.0224950	18	6	0.0250848	-0.0072579
18	7	-0.0025170	0.0086473	18	8	0.0375154	-0.0047905	18	9	-0.0150018	0.0304651
18	10	0.0020478	-0.0109039	18	11	-0.0093050	0.0031534	18	12	-0.0271222	-0.0186725
18	13	-0.0063145	-0.0350284	18	14	-0.0089800	-0.0124657	18	15	-0.0417201	-0.0181628
18	16	0.0082039	0.0032907	18	17	0.0048942	0.0043880	18	18	-0.0003413	-0.0084223
19	1	-0.0132130	0.0009653	19	2	0.0072922	-0.0039028	19	3	-0.0027786	0.0121573
19	4	0.0047233	0.0075195	19	5	-0.0021981	0.0316768	19	6	-0.0069907	0.0066877
19	7	0.0032117	0.0075083	19	8	0.0266181	-0.0142467	19	9	0.0034732	0.0167274
19	10	-0.0364663	-0.0085933	19	11	0.0203631	0.0120152	19	12	-0.0024038	-0.0006441
19	13	-0.0060661	-0.0282432	19	14	-0.0045298	-0.0130308	19	15	-0.0172043	-0.0127545
19	16	-0.0219716	-0.0091235	19	17	0.0296710	-0.0134720	19	18	0.0301456	-0.0071739
19	19	0.0061595	0.0018905								

Table 5.1

GEM-T2 NORMALIZED COEFFICIENTS (continued)

UNITS OF 10^{-6}

SECTORIALS AND TESSERALS

INDEX N	INDEX M	VALUE C	VALUE S	INDEX N	INDEX M	VALUE C	VALUE S	INDEX N	INDEX M	VALUE C	VALUE S
20	1	0.0157399	-0.0100026	20	2	0.0187443	0.0073043	20	3	0.0060908	0.0173144
20	4	0.0030529	-0.0036520	20	5	-0.0108465	0.0030199	20	6	0.0079275	0.0061471
20	7	-0.0118532	-0.0003759	20	8	-0.0056161	0.0006536	20	9	0.0237362	0.0108475
20	10	-0.0282901	-0.0114400	20	11	0.0155253	-0.0213370	20	12	-0.0061237	0.0157824
20	13	0.0276079	0.0059426	20	14	0.0110712	-0.0137433	20	15	-0.0267134	0.0015518
20	16	-0.0153321	-0.0020238	20	17	0.0067026	-0.0133355	20	18	0.0127771	-0.0002315
20	19	-0.0122968	0.0094362	20	20	0.0065287	-0.0031206				
21	1	-0.0129057	0.0405056	21	2	0.0046612	0.0044867	21	3	0.0022573	0.0228423
21	4	-0.0044913	0.0116340	21	5	0.0118863	-0.0035430	21	6	-0.0072367	0.0019953
21	7	-0.0123222	0.0001135	21	8	-0.0149498	0.0041740	21	9	0.0213432	-0.0017646
21	10	-0.0070501	-0.0018894	21	11	0.0139045	-0.0350282	21	12	-0.0027053	0.0113223
21	13	-0.0174796	0.0131394	21	14	0.0196161	0.0094325	21	15	0.0178718	0.0136236
21	16	0.0080497	-0.0076515	21	17	-0.0069162	-0.0022420	21	18	0.0232517	-0.0088069
21	19	-0.0238225	0.0135908	21	20	-0.0200855	0.0198500	21	21	0.0075325	-0.0082327
22	1	0.0099264	-0.0007388	22	2	-0.0200252	0.0082418	22	3	0.0071928	-0.0058210
22	4	-0.0101392	0.0105595	22	5	0.0035063	0.0014637	22	6	0.0091120	0.0066547
22	7	0.0101694	-0.0002510	22	8	-0.0095379	-0.0090097	22	9	0.0166858	-0.0077710
22	10	0.0022397	0.0178636	22	11	-0.0050223	-0.0130492	22	12	0.0067411	-0.0107053
22	13	-0.0168282	0.0196012	22	14	0.0094908	0.0081424	22	15	0.0250399	0.0060758
22	16	-0.0030291	-0.0080446	22	17	0.0115363	-0.0156888	22	18	0.0069583	-0.0123205
22	19	0.0066686	-0.0055346	22	20	-0.0160290	0.0213725	22	21	-0.0180893	0.0189315
22	22	-0.0029881	0.0063133								
23	1	0.0037148	0.0123740	23	2	-0.0031104	0.0012627	23	3	-0.0101724	-0.0062826
23	4	-0.0155617	0.0035853	23	5	-0.0052477	-0.0015027	23	6	0.0015575	0.0139561
23	7	-0.0031648	-0.0021497	23	8	0.0039870	-0.0038722	23	9	-0.0047139	-0.0049946
23	10	0.0145802	-0.0073488	23	11	0.0107774	0.0175629	23	12	0.0171677	-0.0235240
23	13	-0.0107830	-0.0055874	23	14	0.0049840	-0.0041804	23	15	0.0178661	-0.0024984
23	16	0.0077297	0.0116023	23	17	-0.0047031	-0.0093385	23	18	0.0038581	-0.0130571
23	19	-0.0071011	0.0098609	23	20	0.0133809	-0.0056003	23	21	0.0125823	0.0095773
23	22	-0.0071855	-0.0041004	23	23	-0.0052198	-0.0055011				

Table 5.1

GEM-T2 NORMALIZED COEFFICIENTS (continued)

UNITS OF 10^{-6}

SECTORIALS AND TESSERALS

INDEX N	INDEX M	VALUE C	VALUE S	INDEX N	INDEX M	VALUE C	VALUE S	INDEX N	INDEX M	VALUE C	VALUE S
24	1	0.0051628	-0.0180893	24	2	-0.0090488	0.0104115	24	3	0.0109703	-0.0134462
24	4	0.0061443	0.0128870	24	5	-0.0036825	-0.0103708	24	6	-0.0044245	-0.0008275
24	7	-0.0066587	0.0008340	24	8	0.0036226	-0.0004805	24	9	0.0003555	0.0008362
24	10	0.0149022	0.0090421	24	11	0.0166042	0.0178060	24	12	0.0131551	-0.0098125
24	13	-0.0026082	0.0020559	24	14	-0.0184135	0.0001713	24	15	0.0068975	-0.0134144
24	16	0.0000656	0.0060941	24	17	-0.0094173	-0.0061764	24	18	-0.0009003	-0.0087192
24	19	-0.0064920	-0.0160590	24	20	-0.0041907	0.0041638	24	21	0.0095449	0.0083697
24	22	0.0039264	0.0029011	24	23	-0.0039449	-0.0102118	24	24	0.0069433	-0.0058543
25	1	-0.0001213	0.0024822	25	2	0.0029768	0.0064225	25	3	-0.0076282	-0.0005357
25	4	0.0004873	0.0012827	25	5	0.0007279	-0.0010421	25	6	0.0097998	-0.0032113
25	7	-0.0030747	-0.0015639	25	8	0.0012752	-0.0060006	25	9	-0.0110394	0.0179832
25	10	0.0034928	-0.0046031	25	11	0.0113608	0.0011630	25	12	-0.0116149	0.0110666
25	13	0.0085694	-0.0133846	25	14	-0.0227691	0.0146888	25	15	-0.0022238	-0.0006265
25	16	0.0049545	-0.0129923	25	17	-0.0122607	-0.0022734	25	18	-0.0002533	-0.0152155
25	19	0.0057873	0.0067874	25	20	-0.0040459	-0.0044319	25	21	0.0079852	0.0050917
25	22	-0.0035323	-0.0004352	25	23	0.0046537	-0.0061790	25	24	0.0029133	-0.0107787
25	25	0.0060245	0.0071522								
26	1	-0.0028070	-0.0073703	26	2	-0.0056504	0.0097048	26	3	0.0040400	-0.0102009
26	4	0.0078713	-0.0000766	26	5	0.0094198	0.0069132	26	6	0.0050751	0.0059712
26	7	0.0049869	0.0005297	26	8	0.0093342	-0.0076946	26	9	0.0057272	-0.0029598
26	10	-0.0092304	0.0038226	26	11	0.0008841	0.0045249	26	12	-0.0212486	0.0049014
26	13	0.0010963	0.0032697	26	14	0.0057684	0.0047964	26	15	-0.0125965	0.0054078
26	16	0.0034254	-0.0083706	26	17	-0.0047597	0.0075931	26	18	-0.0137738	0.0106819
26	19	0.0006076	-0.0004177	26	20	0.0086624	-0.0128697	26	21	-0.0048840	-0.0030598
26	22	0.0159200	0.0069691	26	23	-0.0002731	0.0127468	26	24	-0.0007826	0.0148666
26	25	-0.0026733	0.0069748	26	26	0.0052708	-0.0000985				

Table 5.1

GEM-T2 NORMALIZED COEFFICIENTS (continued)

UNITS OF 10^{-6}

SECTORIALS AND TESSERALS

INDEX N	INDEX M	VALUE C	VALUE S	INDEX N	INDEX M	VALUE C	VALUE S	INDEX N	INDEX M	VALUE C	VALUE S
27	1	-0.0035303	0.0029610	27	2	0.0132584	-0.0027799	27	3	0.0010333	-0.0046858
27	4	-0.0041245	0.0009974	27	5	0.0054595	0.0011611	27	6	0.0112437	0.0032302
27	7	0.0003011	-0.0039260	27	8	-0.0029323	-0.0070659	27	9	-0.0007766	0.0068108
27	10	-0.0062129	0.0014086	27	11	0.0030759	-0.0026179	27	12	-0.0060021	-0.0082350
27	13	-0.0048427	-0.0044872	27	14	0.0117476	0.0039195	27	15	-0.0039800	0.0018040
27	16	0.0074675	-0.0024580	27	17	0.0008834	0.0015530	27	18	-0.0032588	0.0082895
27	19	0.0033212	-0.0064472	27	20	0.0036407	-0.0030400	27	21	0.0016848	-0.0095695
27	22	0.0025138	0.0072865	27	23	-0.0047462	-0.0019623	27	24	-0.0012730	-0.0011155
27	25	0.0146344	0.0043651	27	26	-0.0058949	0.0062190	27	27	0.0069877	0.0052110
28	1	0.0007985	-0.0001762	28	2	-0.0108103	-0.0035345	28	3	0.0032027	-0.0037991
28	4	0.0060301	-0.0043044	28	5	0.0032984	-0.0049939	28	6	-0.0121280	0.0047574
28	7	-0.0043293	0.0001170	28	8	0.0026980	-0.0036584	28	9	0.0055538	-0.0057419
28	10	-0.0045815	0.0020475	28	11	-0.0050948	0.0003167	28	12	0.0076502	0.0032069
28	13	0.0027151	0.0047829	28	14	-0.0026236	-0.0063300	28	15	-0.0086891	0.0048007
28	16	-0.0103802	-0.0091985	28	17	0.0108110	-0.0063308	28	18	-0.0002811	-0.0015230
28	19	0.0056672	0.0194739	28	20	-0.0033181	0.0058553	28	21	0.0052391	0.0009208
28	22	-0.0029075	-0.0024117	28	23	0.0024804	0.0085840	28	24	0.0038943	-0.0128299
28	25	0.0047364	-0.0081026	28	26	0.0066282	0.0051238	28	27	-0.0092538	0.0010361
28	28	0.0046014	0.0004890								
29	1	-0.0024216	-0.0014721	29	2	0.0110462	-0.0040312	29	3	0.0057915	-0.0033659
29	4	-0.0087806	0.0021315	29	5	0.0046600	-0.0010136	29	6	0.0059052	0.0016687
29	7	-0.0038113	-0.0058313	29	8	-0.0076311	0.0002931	29	9	0.0032289	0.0050537
29	10	0.0036451	0.0027217	29	11	-0.0059549	0.0040286	29	12	-0.0014434	-0.0070513
29	13	0.0011914	-0.0033654	29	14	-0.0061923	0.0031900	29	15	-0.0029390	0.0009774
29	16	0.0005211	-0.0086891	29	17	0.0001709	-0.0018082	29	18	0.0023891	-0.0025693
29	19	-0.0072184	0.0025870	29	20	-0.0062694	0.0048432	29	21	-0.0063263	-0.0057773
29	22	0.0170347	0.0034640	29	23	-0.0031176	0.0014578	29	24	-0.0024439	0.0015924
29	25	0.0100794	0.0066976	29	26	0.0073942	-0.0057924	29	27	-0.0076838	-0.0041547
29	28	0.0053740	-0.0049759	29	29	0.0042149	-0.0078064				

Table 5.1

GEM-T2 NORMALIZED COEFFICIENTS (continued)

UNITS OF 10^{-6}

SECTORIALS AND TESSERALS

INDEX N	INDEX M	VALUE C	VALUE S	INDEX N	INDEX M	VALUE C	VALUE S	INDEX N	INDEX M	VALUE C	VALUE S
30	1	-0.0028920	-0.0012918	30	2	-0.0099354	-0.0027621	30	3	0.0002142	-0.0008170
30	4	-0.0015860	-0.0038591	30	5	0.0022161	-0.0016302	30	6	-0.0044003	0.0072634
30	7	0.0007888	0.0042382	30	8	0.0043515	0.0003917	30	9	-0.0007850	-0.0052641
30	10	0.0050687	-0.0023911	30	11	-0.0064772	0.0046730	30	12	-0.0009621	-0.0025128
30	13	0.0139154	0.0021559	30	14	0.0023111	-0.0014279	30	15	0.0015724	-0.0094384
30	16	-0.0010943	0.0017714	30	17	0.0010171	0.0005329	30	18	-0.0007191	-0.0007617
30	19	-0.0056279	-0.0021906	30	20	-0.0041997	0.0055677	30	21	-0.0117710	-0.0059539
30	22	-0.0033343	-0.0028411	30	23	-0.0032034	-0.0012062	30	24	-0.0039237	-0.0004978
30	25	0.0054745	-0.0048253	30	26	-0.0035853	0.0091820	30	27	-0.0060251	0.0112707
30	28	-0.0012153	-0.0015664	30	29	0.0010564	0.0055391	30	30	0.0013675	0.0004697
31	1	0.0016404	-0.0018644	31	2	0.0048821	0.0017028	31	3	0.0026006	-0.0030161
31	4	-0.0027794	-0.0008999	31	5	-0.0029227	-0.0020585	31	6	-0.0002222	-0.0004138
31	7	-0.0013591	-0.0009187	31	8	-0.0018443	-0.0023340	31	9	0.0014198	-0.0018380
31	10	0.0036988	-0.0048314	31	11	0.0002831	0.0084056	31	12	0.0002142	0.0023222
31	13	0.0088911	0.0028272	31	14	-0.0115379	0.0025878	31	15	-0.0004972	-0.0036711
31	16	-0.0038187	0.0001522	31	17	-0.0082264	0.0061006	31	18	0.0005808	-0.0010290
31	19	0.0025791	0.0021631	31	20	-0.0002625	0.0026803	31	21	-0.0027361	0.0055945
31	22	-0.0072540	-0.0079895	31	23	0.0096422	0.0094387	31	24	-0.0038312	0.0014093
31	25	-0.0120197	-0.0031623	31	26	-0.0137464	-0.0039037	31	27	-0.0016461	0.0066680
31	28	0.0056474	0.0034777	31	29	-0.0027890	-0.0044736	31	30	0.0022103	0.0035575
31	31	-0.0033367	-0.0027473								
32	1	-0.0090314	-0.0012789	32	2	-0.0029573	0.0040291	32	3	0.0004785	0.0023346
32	4	0.0024110	-0.0040056	32	5	-0.0003123	-0.0031440	32	6	-0.0045793	0.0013563
32	7	-0.0025447	0.0043308	32	8	0.0013932	0.0028456	32	9	-0.0009975	0.0000644
32	10	0.0010293	-0.0031557	32	11	-0.0046493	-0.0024290	32	12	-0.0043837	0.0061778
32	13	0.0094405	0.0023561	32	14	0.0043713	0.0094320	32	15	0.0050396	-0.0040359
32	16	0.0046018	0.0036467	32	17	-0.0104291	0.0039702	32	18	0.0048077	-0.0018535
32	19	0.0051995	-0.0033663	32	20	0.0007365	-0.0003261	32	21	-0.0017672	0.0087413
32	22	-0.0032033	-0.0021634	32	23	0.0017026	-0.0002988	32	24	-0.0038090	0.0014151
32	25	-0.0151375	0.0049203	32	26	-0.0011721	-0.0024842	32	27	-0.0034562	-0.0045753
32	28	0.0061368	0.0013247	32	29	-0.0005561	0.0048120	32	30	0.0044686	-0.0009518
32	31	-0.0007472	0.0006465	32	32	0.0008406	-0.0009347				

Table 5.1

GEM-T2 NORMALIZED COEFFICIENTS (continued)

UNITS OF 10^{-6}

SECTORIALS AND TESSERALS

INDEX N	INDEX M	VALUE C	VALUE S	INDEX N	INDEX M	VALUE C	VALUE S	INDEX N	INDEX M	VALUE C	VALUE S
33	1	-0.0012150	0.0004394	33	2	-0.0047376	0.0025501	33	3	-0.0033879	-0.0008039
33	4	0.0025399	0.0003482	33	5	-0.0026538	0.0028221	33	6	-0.0002660	-0.0040242
33	7	-0.0010350	0.0001357	33	8	-0.0023213	0.0012362	33	9	-0.0000792	0.0019665
33	10	0.0000662	0.0000643	33	11	0.0038344	-0.0014331	33	12	0.0034476	0.0037405
33	13	0.0031547	0.0065764	33	14	0.0033425	0.0004678	33	15	-0.0035966	0.0020241
33	16	0.0014493	0.0012668	33	17	-0.0004057	0.0055681	33	18	-0.0047096	-0.0022672
33	19	0.0061747	-0.0005676	33	20	0.0021109	-0.0011467	33	21	0.0014493	0.0007041
33	22	-0.0118245	-0.0033280	33	23	0.0019181	-0.0033512	33	24	0.0061512	-0.0008436
33	25	0.0011943	-0.0109797	33	26	0.0092990	-0.0014860	33	27	-0.0027450	0.0021797
33	28	-0.0027311	0.0012973	33	29	-0.0157601	0.0030203	33	30	0.0049395	-0.0202818
33	31	0.0025623	-0.0004724	33	32	0.0042551	0.0041997	33	33	-0.0012969	-0.0010797
34	1	-0.0033414	0.0005675	34	2	0.0037065	0.0038544	34	3	-0.0013019	0.0035500
34	4	0.0042593	-0.0033683	34	5	-0.0006455	0.0017485	34	6	0.0002144	-0.0012583
34	7	0.0034243	0.0011937	34	8	0.0004447	-0.0007169	34	9	-0.0001090	0.0001286
34	10	-0.0040002	-0.0018078	34	11	0.0019073	-0.0029264	34	12	0.0006767	0.0046957
34	13	-0.0061986	0.0042770	34	14	-0.0035000	0.0025978	34	15	0.0036657	0.0020312
34	16	0.0053231	-0.0011762	34	17	-0.0036913	0.0053905	34	18	-0.0023261	-0.0021200
34	19	0.0021381	-0.0015244	34	20	0.0044075	-0.0023144	34	21	0.0026418	-0.0013922
34	22	0.0031804	0.0029675	34	23	-0.0014497	-0.0041274	34	24	0.0073031	0.0038280
34	25	0.0087043	-0.0046268	34	26	0.0010343	-0.0116631	34	27	0.0113708	-0.0023311
34	28	0.0026301	-0.0151921	34	29	0.0015415	-0.0050392	34	30	-0.0099883	-0.0022580
34	31	0.0024133	0.0011638	34	32	-0.0016885	-0.0015230	34	33	0.0031092	0.0031187
35	1	-0.0036385	0.0022889	35	2	-0.0037195	0.0018563	35	3	-0.0000686	0.0021050
35	4	0.0032155	0.0003722	35	5	0.0011993	-0.0004083	35	6	-0.0004934	-0.0018728
35	7	0.0003892	-0.0010328	35	8	-0.0003935	0.0002122	35	9	-0.0014617	-0.0022985
35	10	-0.0012014	0.0006867	35	11	-0.0013493	-0.0058743	35	12	0.0008706	-0.0036950
35	13	-0.0014377	0.0050514	35	14	-0.0067127	-0.0007107	35	15	-0.0024511	0.0053901
35	16	0.0021675	0.0022863	35	17	0.0064255	-0.0048059	35	18	0.0003659	-0.0020175
35	19	-0.0031481	0.0001443	35	20	-0.0005265	-0.0006631	35	21	0.0057826	0.0022281
35	22	0.0013102	0.0042641	35	23	-0.0052469	-0.0024676	35	24	0.0036355	0.0030476
35	25	0.0028269	0.0024095	35	26	-0.0059897	-0.0010138	35	27	0.0123398	-0.0119025
35	28	0.0026952	-0.0143957	35	29	0.0087215	0.0000144	35	30	-0.0010179	0.0007707
35	31	0.0031635	0.0058546	35	32	-0.0085880	-0.0066388	35	33	0.0035674	0.0074216
35	34	-0.0023873	-0.0020957	35	35	0.0004264	0.0002939				

Table 5.1

GEM-T2 NORMALIZED COEFFICIENTS (continued)

UNITS OF 10^{-6}

SECTORIALS AND TESSERALS

INDEX N	INDEX M	VALUE C	VALUE S	INDEX N	INDEX M	VALUE C	VALUE S	INDEX N	INDEX M	VALUE C	VALUE S
36	1	-0.0000994	0.0030539	36	2	0.0019970	-0.0005808	36	3	-0.0033624	0.0004424
36	4	0.0021730	-0.0005808	36	5	-0.0008162	0.0017294	36	6	-0.0005222	-0.0025178
36	7	0.0003130	-0.0007355	36	8	-0.0017377	0.0006080	36	9	-0.0002901	-0.0003904
36	10	-0.0016219	-0.0019382	36	11	0.0005904	0.0013284	36	12	-0.0012515	0.0002742
36	13	-0.0014463	0.0037768	36	14	-0.0034694	-0.0034283	36	15	0.0021795	-0.0013811
36	16	0.0017441	-0.0002383	36	17	0.0029224	-0.0013639	36	18	0.0000306	0.0001666
36	19	-0.0006995	0.0007721	36	20	-0.0019394	-0.0002075	36	21	0.0023106	-0.0043551
36	22	-0.0004554	0.0016395	36	23	-0.0020415	-0.0015928	36	24	0.0003477	-0.0029341
36	25	0.0009118	0.0090988	36	26	0.0030418	0.0064559	36	27	-0.0084166	0.0053537
36	28	0.0014083	-0.0017120	36	29	0.0013412	-0.0009171	36	30	-0.0064073	0.0012876
36	31	-0.0021614	-0.0008776	36	32	0.0001945	0.0028940	36	33	-0.0040937	-0.0058627
36	34	-0.0021684	0.0018189	36	35	0.0004685	-0.0022694	36	36	0.0003862	0.0003681
37	1	0.0012319	0.0001916	37	2	0.0004221	-0.0005978	37	11	0.0006510	0.0001766
37	12	-0.0056621	-0.0016479	37	13	-0.0027263	-0.0033993	37	14	-0.0060312	-0.0014478
37	15	0.0031061	0.0014075	37	23	-0.0006754	-0.0001414	37	24	-0.0031592	-0.0017562
37	25	0.0025593	0.0035134	37	26	0.0047325	0.0066686	37	27	-0.0020980	0.0036567
37	28	0.0087116	0.0065301	37	29	0.0098388	0.0025075	37	35	-0.0024592	-0.0013532
37	36	0.0001707	-0.0004965	37	37	0.0001206	0.0000323				
38	1	-0.0008977	0.0014341	38	2	-0.0001716	-0.0029714	38	11	-0.0002873	0.0015236
38	12	-0.0007471	-0.0015682	38	13	0.0007526	-0.0025080	38	14	-0.0017509	0.0011694
38	15	-0.0011212	-0.0012693	38	23	0.0005393	0.0042255	38	24	-0.0032644	-0.0014449
38	25	-0.0008437	-0.0054262	38	26	-0.0034160	0.0008996	38	27	-0.0018622	0.0017607
38	28	-0.0042911	-0.0023492	38	29	0.0033413	0.0002975	38	35	-0.0002156	0.0047209
38	36	-0.0023693	-0.0031212	38	37	0.0007651	-0.0010824	38	38	-0.0001299	-0.0007536
39	1	-0.0005408	-0.0010038	39	2	0.0010235	-0.0011502	39	11	0.0023327	0.0017152
39	12	-0.0003924	0.0027686	39	13	0.0000842	-0.0023104	39	14	-0.0015218	-0.0023118
39	15	0.0032395	-0.0041952	39	23	0.0001069	0.0004055	39	24	-0.0033169	-0.0011282
39	25	-0.0000773	-0.0007880	39	26	-0.0047950	0.0051451	39	27	-0.0061557	-0.0016127
39	28	-0.0046927	-0.0068865	39	29	-0.0054089	-0.0035670	39	35	0.0025554	0.0010262
39	36	0.0004012	0.0014546	39	37	-0.0005434	0.0012182	39	38	-0.0000242	-0.0002651
39	39	-0.0004411	-0.0007030								

Table 5.1

GEM-T2 NORMALIZED COEFFICIENTS (continued)

UNITS OF 10^{-6}

SECTORIALS AND TESSERALS

INDEX N	INDEX M	VALUE C	VALUE S	INDEX N	INDEX M	VALUE C	VALUE S	INDEX N	INDEX M	VALUE C	VALUE S
40	1	0.0003977	0.0011647	40	2	-0.0003638	-0.0015783	40	11	0.0006976	-0.0006294
40	12	0.0002103	0.0002648	40	13	-0.0023484	-0.0033431	40	14	0.0000423	0.0010452
40	15	0.0001404	0.0025006	40	23	0.0011245	-0.0014907	40	24	0.0004783	0.0018836
40	25	-0.0007236	-0.0024068	40	26	0.0050145	0.0015346	40	27	-0.0009711	-0.0002623
40	28	0.0017698	0.0040420	40	29	0.0010936	0.0002024	40	35	0.0009078	-0.0027760
40	36	0.0013914	0.0029042	40	37	-0.0016385	0.0016023	40	38	-0.0002456	0.0009014
40	39	0.0004278	-0.0008566	40	40	-0.0007832	0.0004286				
41	1	-0.0012735	-0.0002474	41	2	-0.0003915	-0.0001628	41	11	0.0001253	0.0008125
41	12	0.0027148	0.0011758	41	13	0.0016950	0.0037141	41	14	0.0011678	0.0033150
41	15	0.0001752	-0.0021864	41	23	0.0001894	0.0006816	41	24	0.0017087	-0.0000413
41	25	-0.0018848	0.0011051	41	26	0.0047837	-0.0080686	41	27	-0.0011405	0.0014509
41	28	-0.0042768	-0.0009932	41	29	0.0002297	0.0023047	41	35	0.0005460	0.0004614
41	36	-0.0011322	-0.0010519	41	37	0.0005529	-0.0017954	41	38	-0.0000004	0.0010341
41	39	-0.0003088	-0.0005950	41	40	0.0004386	-0.0004779	41	41	0.0003718	0.0000932
42	1	0.0005314	-0.0005602	42	2	0.0006463	-0.0005361	42	11	0.0012176	-0.0003672
42	12	0.0014837	-0.0010948	42	13	-0.0001945	-0.0001583	42	14	-0.0004083	-0.0016310
42	15	-0.0014494	0.0009136	42	23	0.0003650	-0.0014766	42	24	0.0011082	-0.0002960
42	25	0.0007718	0.0029789	42	26	-0.0043012	-0.0032607	42	27	0.0026574	-0.0013152
42	28	-0.0001477	0.0038958	42	29	-0.0038343	0.0007940	42	35	-0.0011902	0.0002851
42	36	0.0020302	0.0001011	42	37	0.0000419	-0.0010701	42	38	0.0008246	-0.0013107
42	39	-0.0004072	0.0018459	42	40	0.0014332	-0.0007298	42	41	-0.0007583	0.0011773
42	42	-0.0003950	0.0006384								
43	1	-0.0000801	0.0006980	43	2	-0.0009052	0.0002684	43	11	-0.0012732	-0.0003219
43	12	0.0006744	-0.0008274	43	13	0.0021243	0.0006238	43	14	-0.0015029	0.0027864
43	15	-0.0011884	0.0003396	43	23	0.0004332	-0.0001977	43	24	0.0009323	0.0010513
43	25	-0.0000106	-0.0000279	43	26	-0.0038657	0.0002359	43	27	0.0064481	0.0040941
43	28	-0.0009041	0.0088787	43	29	-0.0030416	-0.0001038	43	35	-0.0014784	-0.0008165
43	36	0.0009173	-0.0010471	43	37	0.0004137	0.0004758	43	38	0.0005844	-0.0007628
43	39	0.0000636	0.0009355	43	40	0.0006770	-0.0018402	43	41	0.0003727	0.0006843
43	42	-0.0000040	0.0014679	43	43	0.0005206	-0.0003446				

Table 5.1

GEM-T2 NORMALIZED COEFFICIENTS (continued)

UNITS OF 10^{-6}

SECTORIALS AND TESSERALS

INDEX N	INDEX M	VALUE C	VALUE S	INDEX N	INDEX M	VALUE C	VALUE S	INDEX N	INDEX M	VALUE C	VALUE S
44	1	0.0003607	-0.0013679	44	2	0.0003827	0.0002025	44	11	-0.0004076	0.0001039
44	12	0.0002370	-0.0006809	44	13	0.0022158	0.0012390	44	14	0.0000781	-0.0014568
44	15	0.0002006	-0.0002003	44	23	-0.0005775	0.0013145	44	24	-0.0000937	-0.0006180
44	25	-0.0009530	0.0003498	44	26	0.0006944	0.0002133	44	27	0.0023722	-0.0010719
44	28	-0.0006070	0.0006113	44	29	-0.0010401	0.0010422	44	35	0.0004452	-0.0008040
44	36	-0.0014576	-0.0008633	44	37	0.0014011	0.0005423	44	38	-0.0007831	0.0000100
44	39	0.0005722	-0.0004058	44	40	-0.0025763	0.0021954	44	41	0.0008232	-0.0033431
44	42	-0.0007761	-0.0017942	44	43	0.0033228	-0.0031176				
45	1	0.0005985	0.0004237	45	2	0.0004368	-0.0000209	45	11	0.0001412	0.0000590
45	12	-0.0008687	-0.0006642	45	13	-0.0001789	-0.0015556	45	14	0.0001497	-0.0011032
45	15	0.0000472	0.0014005	45	23	0.0001626	-0.0003155	45	24	-0.0004551	0.0003981
45	25	0.0003315	-0.0000499	45	26	-0.0001672	0.0014993	45	27	-0.0035157	-0.0031132
45	28	0.0041335	0.0015628	45	29	-0.0015676	-0.0014500	45	35	-0.0006418	0.0005526
45	36	-0.0004240	0.0015014	45	37	-0.0009526	0.0004916	45	38	-0.0012071	-0.0003560
45	39	-0.0002498	-0.0012155	45	40	0.0000759	0.0001791	45	41	-0.0002698	-0.0022017
45	42	0.0003088	-0.0022125	45	43	-0.0014341	0.0007685				
46	1	0.0001015	-0.0003826	46	2	-0.0004226	0.0003950	46	11	-0.0006195	0.0003284
46	12	-0.0007867	-0.0001659	46	13	-0.0001781	-0.0002787	46	14	-0.0004805	0.0005088
46	15	-0.0008514	-0.0007146	46	23	-0.0001955	0.0003558	46	24	-0.0004017	0.0002148
46	25	0.0001034	-0.0011842	46	26	0.0009290	0.0019075	46	27	-0.0027679	0.0010807
46	28	-0.0001444	-0.0051128	46	29	0.0012952	-0.0004013	46	35	0.0000787	0.0009159
46	36	-0.0007748	-0.0002935	46	37	-0.0009421	-0.0005581	46	38	0.0002615	0.0007468
46	39	0.0001432	-0.0007604	46	40	0.0015445	-0.0022705	46	41	0.0010908	0.0027997
46	42	0.0025786	0.0003211	46	43	-0.0049981	0.0067415				
47	1	0.0002578	-0.0004162	47	2	0.0003201	-0.0000655	47	11	0.0001376	-0.0000463
47	12	0.0000610	-0.0000789	47	13	-0.0005166	-0.0004930	47	14	0.0008991	-0.0015224
47	15	-0.0004991	-0.0003982	47	23	-0.0003664	0.0002947	47	24	-0.0002185	-0.0004732
47	25	0.0000520	-0.0005149	47	26	0.0025919	-0.0008137	47	27	0.0001144	-0.0002077
47	28	-0.0012427	-0.0061424	47	29	0.0026123	-0.0001748	47	35	0.0007548	-0.0003826
47	36	0.0004963	-0.0004788	47	37	0.0005910	0.0005039	47	38	0.0006871	0.0001658
47	39	0.0001867	0.0007972	47	40	-0.0002424	0.0008652	47	41	-0.0012101	0.0049201
47	42	0.0001616	-0.0002018	47	43	-0.0002763	0.0014006				

Table 5.1

GEM-T2 NORMALIZED COEFFICIENTS (continued)

UNITS OF 10^{-6}

SECTORIALS AND TESSERALS

INDEX N	INDEX M	VALUE C	VALUE S	INDEX N	INDEX M	VALUE C	VALUE S	INDEX N	INDEX M	VALUE C	VALUE S
48	1	0.0003046	-0.0000520	48	2	-0.0001156	0.0000266	48	11	-0.0000840	-0.0002836
48	12	-0.0003423	0.0008075	48	13	-0.0006091	0.0000016	48	14	0.0006563	-0.0000642
48	15	0.0013529	0.0004300	48	23	0.0000714	-0.0006788	48	24	-0.0001353	0.0001288
48	25	0.0004989	-0.0001313	48	26	-0.0005574	-0.0007245	48	27	-0.0015614	0.0018315
48	28	0.0010872	-0.0003583	48	29	0.0010901	-0.0008134	48	35	-0.0001013	-0.0000840
48	36	-0.0000500	-0.0002415	48	37	0.0005848	0.0002152	48	38	-0.0000023	0.0001246
48	39	0.0000298	0.0002324	48	40	-0.0005143	0.0000675	48	41	-0.0023096	-0.0012475
48	42	-0.0017835	0.0022795	48	43	0.0006515	-0.0031204				
49	1	-0.0001271	-0.0000742	49	2	-0.0001821	0.0001924	49	11	-0.0001688	-0.0000892
49	12	0.0001294	-0.0002083	49	13	-0.0008453	0.0006552	49	14	0.0009397	0.0004278
49	15	0.0001999	0.0003013	49	23	-0.0000603	0.0000869	49	24	0.0001393	-0.0001039
49	25	-0.0001050	-0.0003731	49	26	-0.0010793	0.0004647	49	27	0.0008298	-0.0001865
49	28	-0.0010886	-0.0039837	49	29	0.0009901	0.0006039	49	35	0.0003440	0.0000990
49	36	-0.0001666	0.0002194	49	37	-0.0003462	-0.0007660	49	38	0.0000034	0.0007022
49	39	0.0004688	-0.0002714	49	40	0.0001510	-0.0010102	49	41	0.0036592	-0.0090655
49	42	-0.0013530	0.0032350	49	43	0.0053307	-0.0042881				
50	1	0.0001087	-0.0002989	50	2	0.0000871	-0.0000100	50	11	0.0001134	0.0000712
50	12	0.0001734	0.0002233	50	13	0.0003917	0.0005087	50	14	-0.0000748	-0.0001355
50	15	-0.0005822	-0.0005293	50	23	-0.0001094	-0.0000953	50	24	0.0001688	-0.0000813
50	25	-0.0001091	0.0007127	50	26	0.0000998	-0.0002666	50	27	0.0020302	-0.0006323
50	28	-0.0007618	0.0019200	50	29	0.0005131	-0.0004751	50	35	-0.0000060	0.0001081
50	36	0.0005849	0.0005168	50	37	-0.0006281	0.0000720	50	38	0.0001051	-0.0003868
50	39	-0.0002382	0.0005366	50	40	0.0008509	0.0019168	50	41	0.0014055	0.0029946
50	42	0.0014752	-0.0002408	50	43	-0.0021834	-0.0030942				

wavenumbers of interest for orbital computations than are the ocean tidal terms at the same wavenumbers.

However, one must exercise caution when comparing dynamic satellite solutions for ocean tidal terms with those obtained oceanographically. Firstly, oceanographic measurements are relative to a land or sea-bottom reference while the effects sensed by satellite data are geocentrically referenced. More importantly, the satellite experiences a changing gravitational attraction which results from all mass redistribution within the Earth/ocean/atmospheric system. Within the semi-diurnal and diurnal bands, clearly tidal effects are dominant and a comparison between ocean models and satellite solutions is reasonably straightforward under the assumption that the solid Earth tides have been well modeled. However, at monthly, semi-annual, annual and longer periods, there are important climatological effects (e.g. Gutierrez and Wilson, 1988), changes in the hydrosphere pertaining to ground water retention cycles and the volume of water stored in continental aquifers (e.g. Chao, 1988), in snow cover (e.g. Chao and O'Connor, 1988) and other sources of mass redistribution which are not "tidal" in origin, and certainly not isolated to changes in the ocean surface at these periodicities. We believe that the large value we obtained for the Sa tide at third degree represents north to south hemispheric mass transport effects with an annual cycle which is not of a tidal origin. This coefficient is large, but at the same time, it seems well determined within our analysis. However, radial non-conservative force modeling errors may be accomodated by an adjustment of this term.

Although admitting to these limitations, we have in the past compared our tidal solutions with both ocean models and other satellite solutions. These comparisons are found in Christodoulidis et al., (1988). While these comparisons will not be repeated herein, it is fair to say that GEM-T2 compares equally well with the results given for GEM-T1 within this reference.

Table 5.2 presents the GEM-T2 tidal solution. It has been compared with the solution developed in GEM-T1 (given in Marsh et al., 1988) and overall, the agreement is very good. Principally, in GEM-T2 we were able to extend the solution for the m=0 long period tidal band to include a third degree coefficient for the Sa, Ssa, Mf and Mm lines. In the diurnal band (m=1), the solution for O1, P1, and K1 has been extended to include the adjustment of terms of degree 5. Further, within the semi-diurnal band, where m=2, a solution containing terms of degree 6 has been performed for K2, S2, M2, N2, and T2 tide lines. In each case, an additional degree above GEM-T1's cutoff was accomplished with 90 adjusting coefficients in the GEM-T2 solution.

Table 5.2
GEM-T2 Dynamic Ocean Tidal Model

Darwinian Name/ Constituent			Values		Uncertainties	
Tide	Degree	Order	Amplitude (cm)	Phase (deg)	Amplitude (cm)	Phase (deg)
-- Long Period Band * --						
Mm	2	0	0.740	256.318	0.317	23.973
Mm	3	0	0.814	16.653	0.673	46.210
Sa	2	0	3.033	28.771	0.404	8.034
Sa	3	0	6.472	320.140	0.574	5.210
Mf	2	0	2.069	237.076	0.312	8.662
Mf	3	0	1.032	354.630	0.827	42.651
Ssa	2	0	1.276	249.472	0.415	17.933
Ssa	3	0	0.866	89.398	0.560	36.494
-- Diurnal Band --						
K1	2	1	2.845	325.513	0.165	3.349
K1	3	1	0.903	14.513	0.109	7.145
K1	4	1	2.487	258.163	0.208	4.895
K1	5	1	2.184	106.526	0.215	5.676
O1	2	1	2.717	315.443	0.128	2.688
O1	3	1	1.390	83.019	0.151	6.271
O1	4	1	1.904	279.743	0.210	6.197
O1	5	1	1.520	118.638	0.210	7.830
P1	2	1	1.105	313.188	0.167	8.650
P1	3	1	0.344	359.467	0.109	18.970
P1	4	1	0.837	262.941	0.212	14.419
P1	5	1	0.442	148.854	0.216	27.769
-- Semi-Diurnal Band --						
K2	2	2	0.319	313.503	0.043	7.775
K2	3	2	0.231	189.952	0.040	7.468
K2	4	2	0.169	112.652	0.043	14.517
K2	5	2	0.079	96.276	0.034	23.516
K2	6	2	0.043	203.524	0.045	59.854
M2	2	2	3.320	321.257	0.047	0.814
M2	3	2	0.304	156.469	0.056	10.574
M2	4	2	0.994	127.174	0.046	2.669
M2	5	2	0.290	8.059	0.036	6.943
M2	6	2	0.403	320.819	0.049	6.946

* symmetries exist in the harmonic expansion of the m=0 tides so that the values represent the sums of the C^+ and C^- (prograde and retrograde) terms (see Christodoulidis et al., 1988: Appendix A).

-- Semi-Diurnal Band (continued) --

S2	2	2	0.831	300.412	0.044	3.017
S2	3	2	0.328	221.479	0.034	6.079
S2	4	2	0.333	87.229	0.042	7.639
S2	5	2	0.136	9.561	0.032	15.998
S2	6	2	0.215	284.419	0.044	12.013
N2	2	2	0.678	334.416	0.061	5.171
N2	3	2	0.088	155.802	0.060	39.477
N2	4	2	0.250	139.018	0.049	11.169
N2	5	2	0.094	341.627	0.037	22.892
N2	6	2	0.059	3.215	0.054	52.701
T2	2	2	0.046	273.217	0.044	55.890
T2	3	2	0.005	119.652	0.034	420.136
T2	4	2	0.036	242.628	0.045	72.181
T2	5	2	0.088	70.699	0.033	21.134
T2	6	2	0.042	221.127	0.047	63.835

5.3 Tidal Braking in the Earth/Moon/Sun System Using Dynamic Tide Model of GEM-T2

Modern satellite tracking systems allow us to monitor the orbital motion of near-Earth satellites to unprecedented levels of accuracy. The GEM-T2 geopotential is a model which uses these observations to deduce both the static and tidal potential fields. The complete GEM-T2 tidal model containing both the adjusted and unadjusted terms has been used to estimate the effects of the Earth's tides on the Earth/Moon/Sun system. The solid Earth tidal model which is used has no phase angle (Wahr, 1981) so it is free of dissipation, but any residual phase due to anelastic properties of the solid Earth would be compensated for in the adjusting ocean tidal coefficient set of GEM-T2 for the twelve major tidal frequencies which are allowed to adjust. Therefore, this model should accurately reflect the external tidal potential sensed on Earth orbiting satellites and can be used directly to infer the tidal contribution to the exchange of angular momentum within the Earth/Moon and Earth/Sun systems.

Using the development given in Christodoulidis et al., (1988), we have calculated the secular change in the mean motion of the Moon and the tidal braking in the Earth's rotation rate using GEM-T2. Table 5.3 presents a comparison of the GEM-T1 and GEM-T2 tidal constituents when used to compute these two effects. The secular change in the lunar mean motion estimated from GEM-T2 is -26.6 ± .5 arcsec century^{-2} which can be compared with GEM-T1's implied value of -25.3 ± .6. The major difference in the models is the change in the second degree value for the Mf tide (both in amplitude and phase) and a small change in second degree M2 which increased slightly in amplitude. These changes combine to move the GEM-T2 value for the calculated secular change in the lunar mean motion further away from the value being obtained from lunar laser ranging which is -24.9 ± 1.0 (Newhall et al., 1986).

The tidal braking of the rate of the Earth's rotation due to conservation of angular momentum in the Earth/Moon/Sun system yields a value of -6.31 ± .16 x 10^{-22} rad s^{-2}. GEM-T1 yielded a value of -5.98 ± .22. Taking into account the effect of the secular change in the second degree zonal harmonic as given by Yoder et al., (1983) of 1.29 ± 0.28 when mapped into the braking of the Earth's rotation rate (see Christodoulidis et al., 1988 and Bursa, 1986), artificial satellites give a combined value of 5.02 ± 0.32 and 4.69 ± 0.36 x 10^{-22} rad s^{-2} for GEM-T2 and GEM-T1 respectively. These values are consistent with recent astronomic studies (e.g. Stephenson and Morrison, 1984) who find a value of 2.4 ms/century for eclipse records prior to 1620 and 1.4 ms/century for telescopic data since 1620. The GEM-T2 and GEM-T1 values correspond to 1.88 and 1.76 ms/century.

5.4 The GEM-T2 Earth Rotation and Polar Motion Series

The GEM-T2 solution is based on tracking data spanning the period from mid-1960 to mid-1987. The quality of the data is not uniform at all; it has therefore been decided that the reference frame be adjusted only during the years when the data contains robust subsets of high quality laser tracking on such satellites as Lageos, Starlette and Ajisai. This translates to the period from 1980 onward.

The definition of the adopted reference system and its realization has been discussed extensively in Marsh et al., (1988). The most important features which we will need for the present are the fact that the apriori series is based on a combination of BIH and Lageos SL6-derived values. The series have been compared over a 6-year overlapping period and the resulting transformation applied to the BIH segment to put it in the SL6 frame. Finally, the average of the pole coordinates over the 6 years 1979-84 has been subtracted to create the apriori series in a coordinate system with an origin that is nearly coincident with the center of the wobble. This results in a systematic offset of the TOPEX/Poseidon solution reference frame to that of IERS(BIH) or SL7.1 of some 38 mas in the x component, and 280 mas in the y component.

Table 5.3 Comparison of GEM-T1 and GEM-T2 Dynamic Tide Models for Secular Change in the Mean Motion of the Moon ($\dot{n}$) and in the Rotational Velocity of the Earth ($\dot{\Omega}$)

Tide	GEM-T1		GEM-T2	
	$\dot{n}$	$\sigma_{\dot{n}}$	$\dot{n}$	$\sigma_{\dot{n}}$
	units: arcsec century^{-2}			
056.554 Sa	0.00	0.00	0.00	0.00
057.555 Ssa	-0.00	0.00	-0.00	0.00
058.554	0.00	0.00	0.00	0.00
065.455 Mm	-0.03	0.31	-0.13	0.12
075.555 Mf	-0.56	0.18	-1.18	0.16
075.565	-0.10	0.06	-0.10	0.06
135.655 Q1	-0.18	0.04	-0.18	0.04
145.545 O1f	-0.10	0.02	-0.10	0.02
145.555 O1	-2.92	0.25	-3.12	0.21
155.455 M1f	0.00	0.00	0.00	0.00
155.655 M1	0.01	0.00	0.01	0.00
162.556 π1	-0.00	0.00	-0.00	0.00
163.555 P1	-0.00	0.00	-0.00	0.00
164.556 S1	0.00	0.00	0.00	0.00
165.545 K1f	----	----	----	----
165.555 K1 moon	----	----	----	----
165.555 K1 sun	----	----	----	----
165.565 K1s	----	----	----	----
166.554 Ψ1	0.00	0.00	0.00	0.00
167.555 ϕ1	0.00	0.00	0.00	0.00
175.455 J1	0.01	0.00	0.01	0.00
185.555 OO1	-0.00	0.00	-0.00	0.00
245.655 N2	-1.43	0.16	-1.39	0.14
255.545 M2s	0.02	0.01	0.02	0.01
255.555 M2	-20.00	0.40	-20.44	0.39
265.455 L2	0.01	0.00	0.01	0.00
271.557	0.00	0.00	0.00	0.00
272.556 T2	-0.00	0.00	-0.00	0.00
273.555 S2	-0.00	0.00	-0.00	0.00
274.554 R2	0.00	0.00	0.00	0.00
275.555 K2 moon	----	----	----	----
275.555 K2 sun	----	----	----	----
285.455	0.00	0.00	0.00	0.00
295.555	0.00	0.00	0.00	0.00
total	-25.27	0.61	-26.61	0.51

	$\dot{\Omega}$	σ_{Ω}	$\dot{\Omega}$	σ_{Ω}
		units: 10^{-22} rad s^{-2}		
056.554 Sa	0.00	0.00	0.00	0.00
057.555 Ssa	-0.04	0.03	-0.08	0.07
058.554	-0.00	0.00	-0.00	0.00
065.455 Mm	-0.00	0.12	-0.00	0.05
075.555 Mf	-0.12	0.07	-0.26	0.06
075.565	-0.01	0.02	-0.01	0.02
135.655 Q1	-0.03	0.01	-0.03	0.01
145.545 O1f	-0.01	0.01	-0.01	0.01
145.555 O1	-0.65	0.07	-0.69	0.06
155.455 M1f	0.00	0.00	0.00	0.00
155.655 M1	0.00	0.00	0.00	0.00
162.556 π1	-0.00	0.00	-0.00	0.00
163.555 P1	-0.12	0.10	-0.14	0.04
164.556 S1	0.00	0.00	0.00	0.00
165.545 K1f	0.00	0.00	0.00	0.00
165.555 K1 moon	----	----	----	----
165.555 K1 sun	----	----	----	----
165.565 K1s	0.01	0.00	0.01	0.00
166.554 ψ1	0.00	0.00	0.00	0.00
167.555 ϕ1	0.00	0.00	0.00	0.00
175.455 J1	0.00	0.00	0.00	0.00
185.555 OO1	-0.00	0.00	-0.00	0.00
245.655 N2	-0.21	0.04	-0.21	0.04
255.545 M2s	0.00	0.00	0.00	0.00
255.555 M2	-4.45	0.09	-4.55	0.09
265.455 L2	0.00	0.00	0.00	0.00
271.557	-0.00	0.00	-0.00	0.00
272.556 T2	-0.00	0.05	-0.00	0.04
273.555 S2	-0.35	0.04	-0.34	0.03
274.554 R2	0.00	0.00	0.00	0.00
275.555 K2 moon	----	----	----	----
275.555 K2 sun	----	----	----	----
285.455	0.00	0.00	0.00	0.00
295.555	0.00	0.00	0.00	0.00
total	-5.98	0.22	-6.31	0.16

The estimated Earth Orientation Parameter (EOP) series are displayed in Figures 5.1 through 5.4, their formal (unscaled) accuracies are shown in Figures 5.5, 5.6, and 5.7. The differences of the estimated coordinates of the pole from the apriori values are plotted in Figures 5.8, 5.9 and 5.10. The results are remarkably close, within 0.5 mas, to those obtained with the GEM-T1 solution. The systematic bias of some 17 mas in the y component is now well understood and its source is an erroneous transformation of part of the apriori series. Because the adjustment in the pole is free, the error only affects the display. The RMS about the mean for these corrections to the apriori are 4.2 mas for the x component and 3.5 mas for the y component. These values are nearly identical to those within the GEM-T1 solution.

To further evaluate the solved EOPs we compared the common part of our solution to that of the VLBI-based IRIS series. The overlapping period is 84/01/05 to 87/02/18. Transformation parameters estimated from this comparison are given in Table 5.4. Our origin is very consistent with that of IRIS once we have accounted for all the systematic differences between frames. Of more interest, however is the agreement between the series when the systematics are eliminated. The RMS differences in x and y are 2.2 mas and 2.5 mas respectively, and 0.4 msec and 0.16 msec for Earth rotation (A.1-UT1R) and length of day (LODR) correspondingly. If we assume that the errors between the two series are random and uncorrelated, which is realistic since they come from independent techniques and data sets, then the above RMSs can be multiplied by 0.707 to give the individual series uncertainties. This results in realistic error estimates for polar motion at about 1.5 mas and length of day variations at 0.1 msec.

5.5 GEOSAT TRANET Station Coordinates

In general, the station positions were held fixed in our GEM-T2 solution as was done for GEM-T1. These apriori station coordinates were predominantly based on the ultra-precise geodetic positioning available from LAGEOS laser ranging analyses. Available geodetic survey ties were extensively used enabling older systems to be tied into the laser-described geocentric network. Other methods were required to secure good coordinates for all of the different historical tracking systems; this included using network analyses which were used to relate previous Unified S-Band and TRANET Doppler station solutions into the TOPEX/Poseidon reference system.

For our GEOSAT analyses however, we only had DMA TRANET II positions available for GEM-T2. These stations required positioning within the TOPEX/Poseidon reference frame, but lacked suitable common stations with earlier solutions to effect these ties. This was not a problem encountered with our TRANET analyses performed using SEASAT data because laser tracking was also available on SEASAT and the Doppler positions were derived from the satellite positioning solutions directly. Even though approximately ten of the same geographic locations commonly were occupied between the GEOSAT timeframe and that of SEASAT, the local station eccentricity data linking the electronic centers of the instruments to their corresponding survey markers was not available. Instrument maintenance and system upgrades had occurred at all sites since the SEASAT era which precluded simple transformations to obtain appropriate GEOSAT tracking station coordinates. Consequently, we elected to adjust the GEOSAT TRANET II stations within GEM-T2.

Our 80-day set of GEOSAT tracking data starting at the beginning of the ERM repeat mission was utilized for this coordinate determination. This data set had representation from the complete TRANET Network of nearly 50 stations. These solved-for coordinates are available from the authors upon request.

Table 5.5 compares our adjusted GEOSAT station coordinates with the WGS-84 positions available from DMA. The RMS of fit in the intercomparison is better than 0.5 m in each coordinate after removal of a seven-parameter Wolf-Bursa transformation. Considering the Doppler coordinates are not likely to be derivable from this type of tracking data to better than about 30 cm in each coordinate, this level of agreement is considered quite good. The

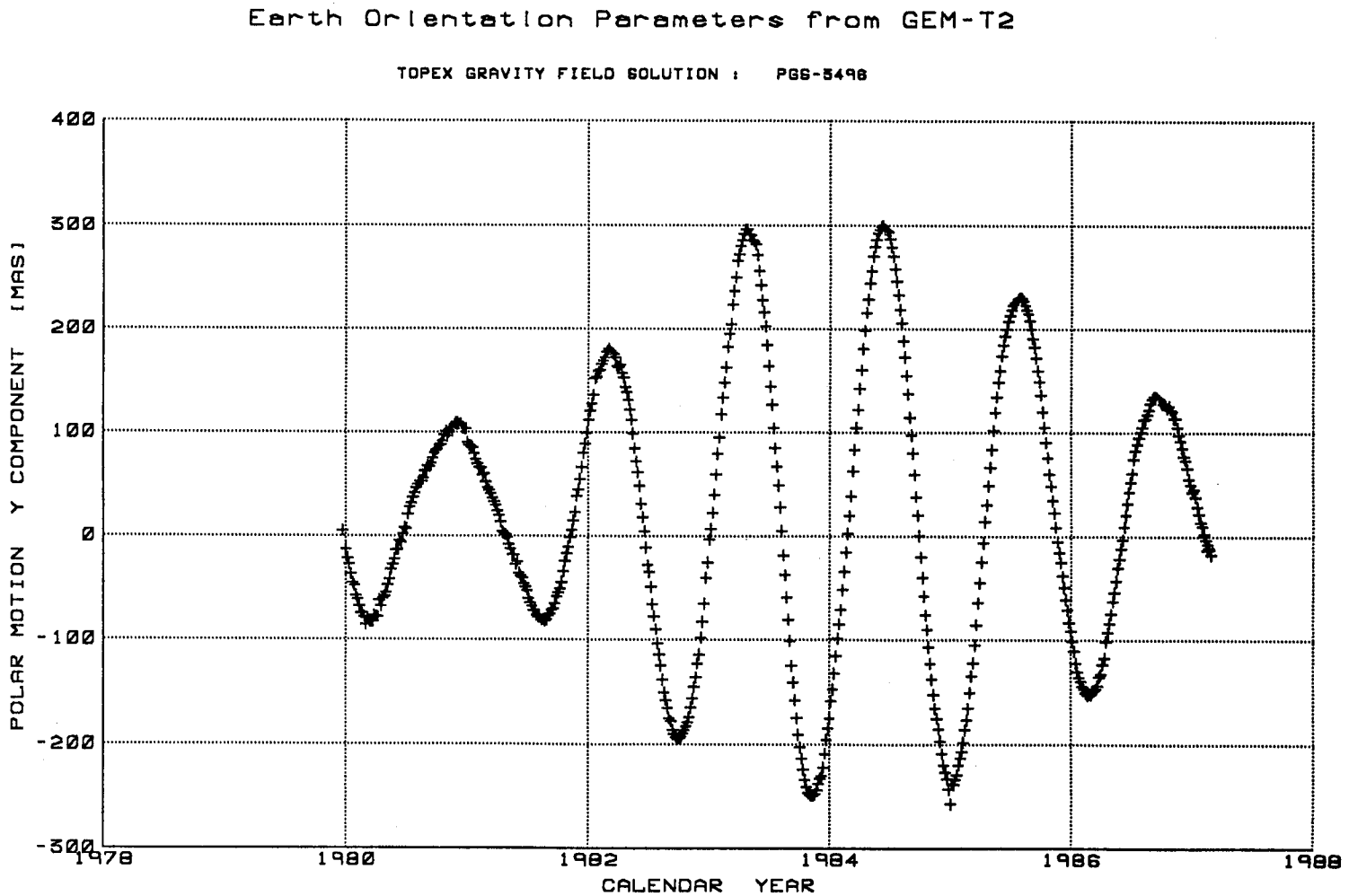
Earth Orientation Parameters from GEM-T2
TOPEX GRAVITY FIELD SOLUTION : PGS-5498
POLAR MOTION Y COMPONENT [MAS]
400
300
200
100
0
-100
-200
-300
1978
1980
1982
1984
1986
1988
CALENDAR YEAR

Figure 5.2

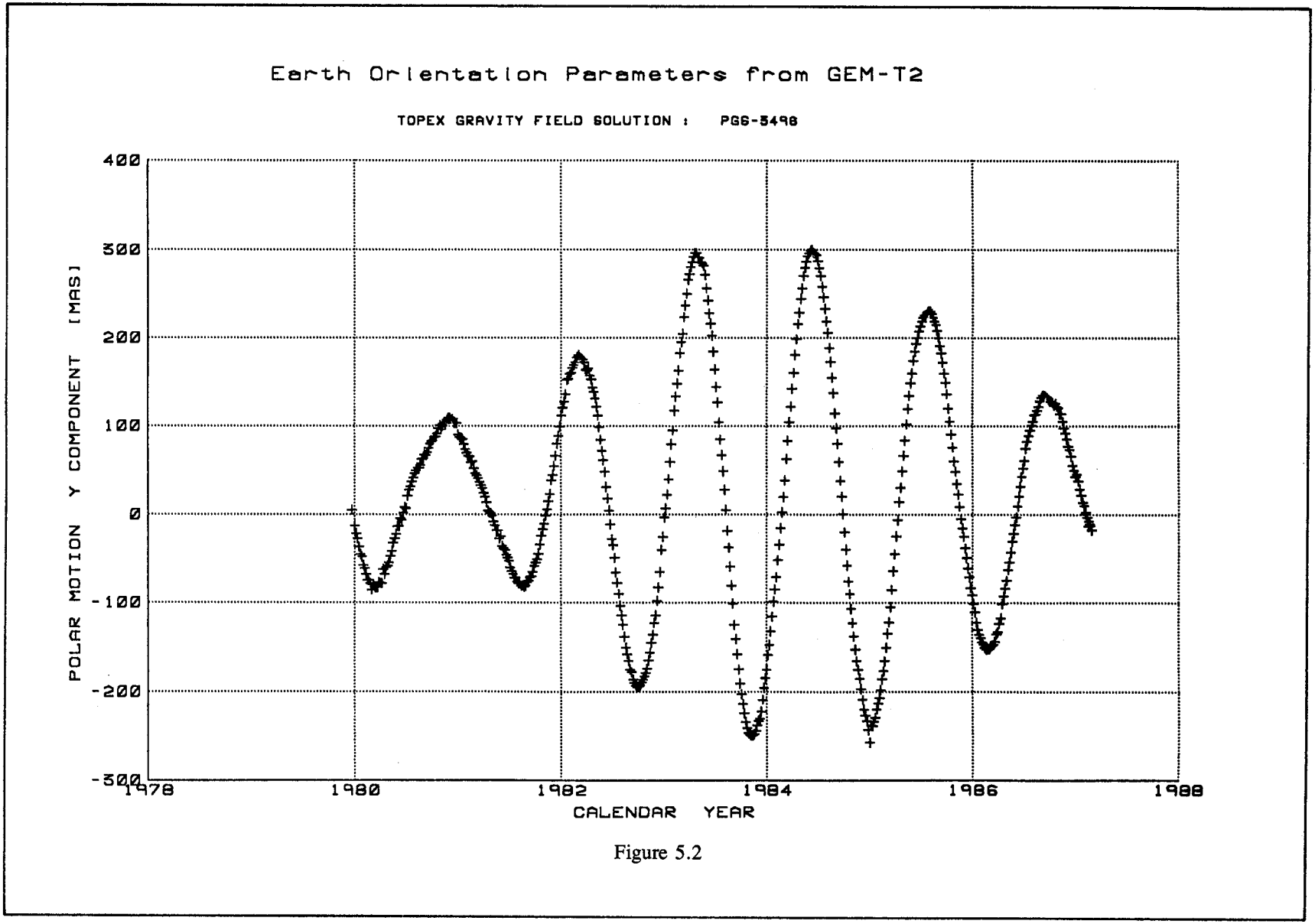
Earth Orientation Parameters from GEM-T2
TOPEX GRAVITY FIELD SOLUTION : PGS-5498
POLAR MOTION Y COMPONENT [MAS]
400
300
200
100
0
-100
-200
-300
1978
1980
1982
1984
1986
1988
CALENDAR YEAR

Figure 5.2

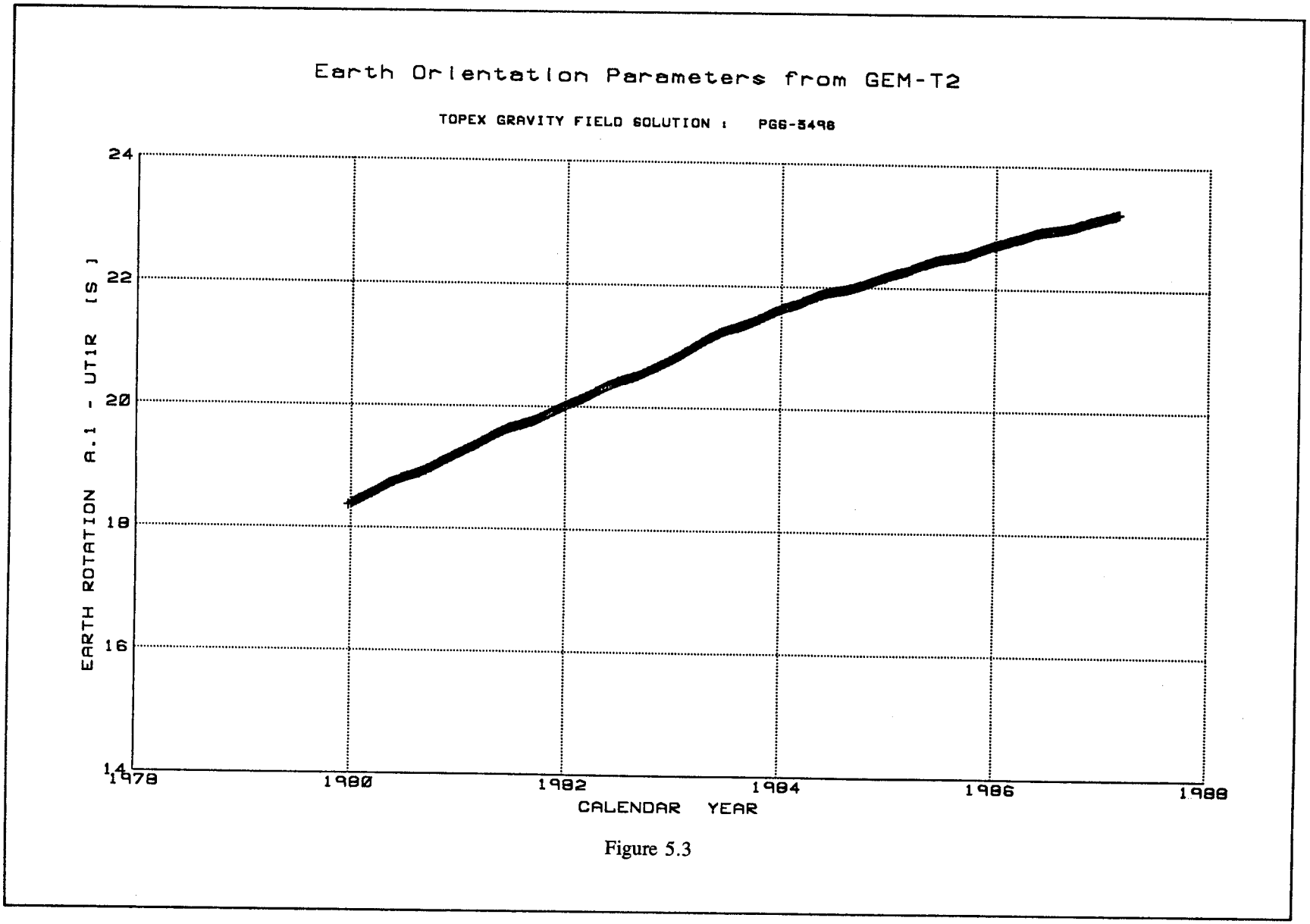
Earth Orientation Parameters from GEM-T2
TOPEX GRAVITY FIELD SOLUTION : PGS-5498
EARTH ROTATION A.1 - UT1R (S)
24
22
20
18
16
14
1978
1980
1982
1984
1986
1988
CALENDAR YEAR

Figure 5.3

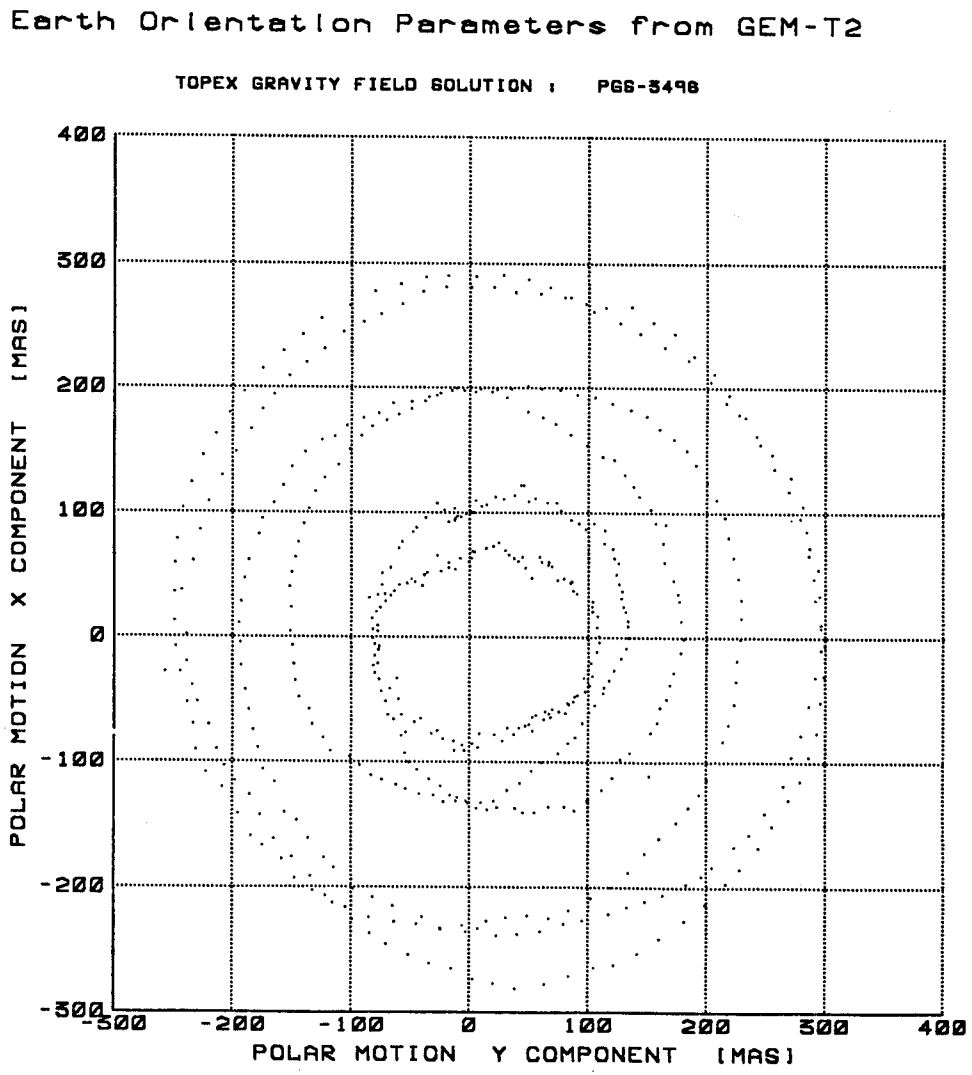
Earth Orientation Parameters from GEM-T2
TOPEX GRAVITY FIELD SOLUTION : PGS-3498
POLAR MOTION X COMPONENT [MAS]
400
300
200
100
0
-100
-200
-300
-500
-200
-100
0
100
200
300
400
POLAR MOTION Y COMPONENT [MAS]

Figure 5.4

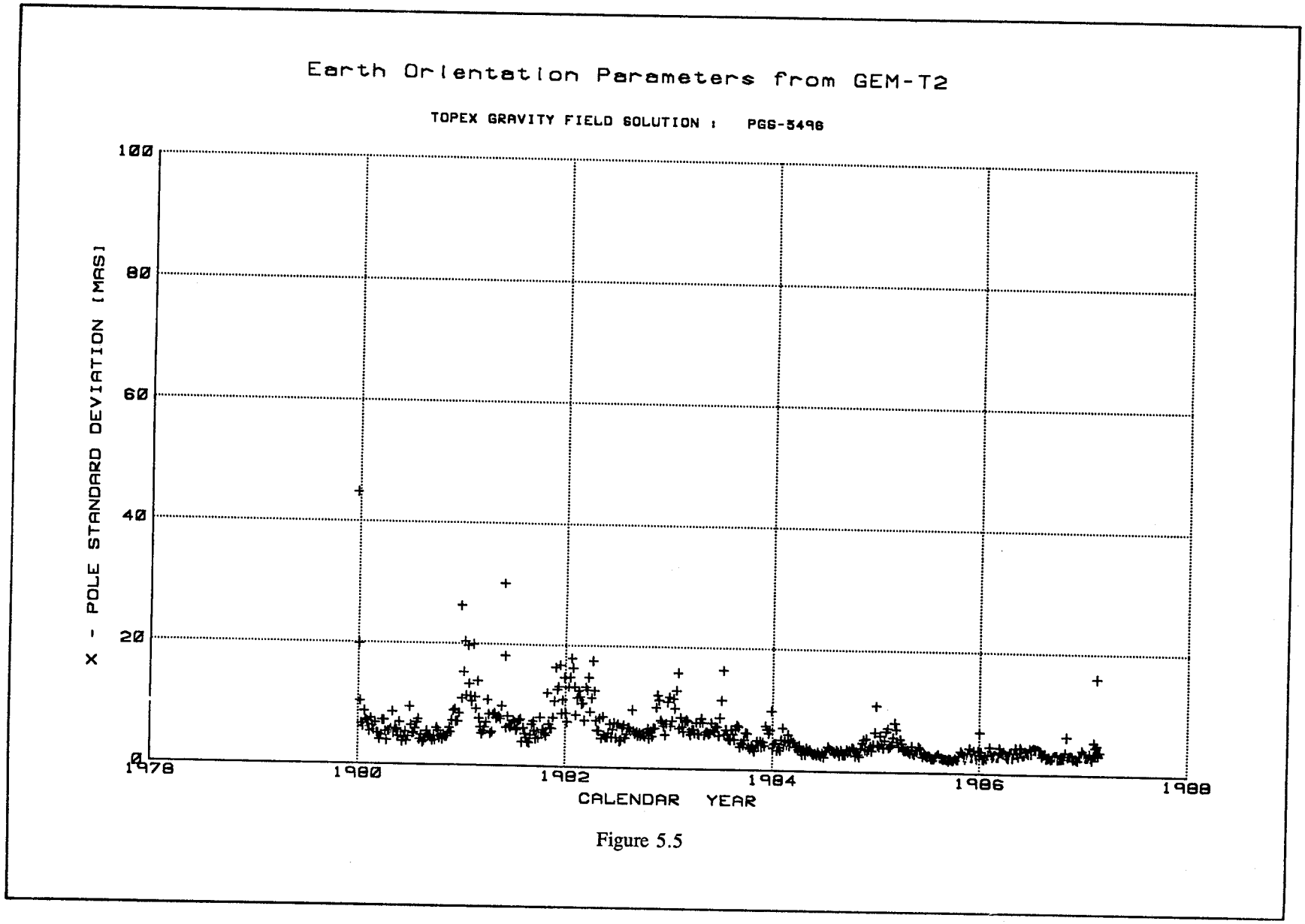
Earth Orientation Parameters from GEM-T2
TOPEX GRAVITY FIELD SOLUTION : PGS-5498
X - POLE STANDARD DEVIATION (MAS)
100
80
60
40
20
0
1978
1980
1982
1984
1986
1988
CALENDAR YEAR

Figure 5.5

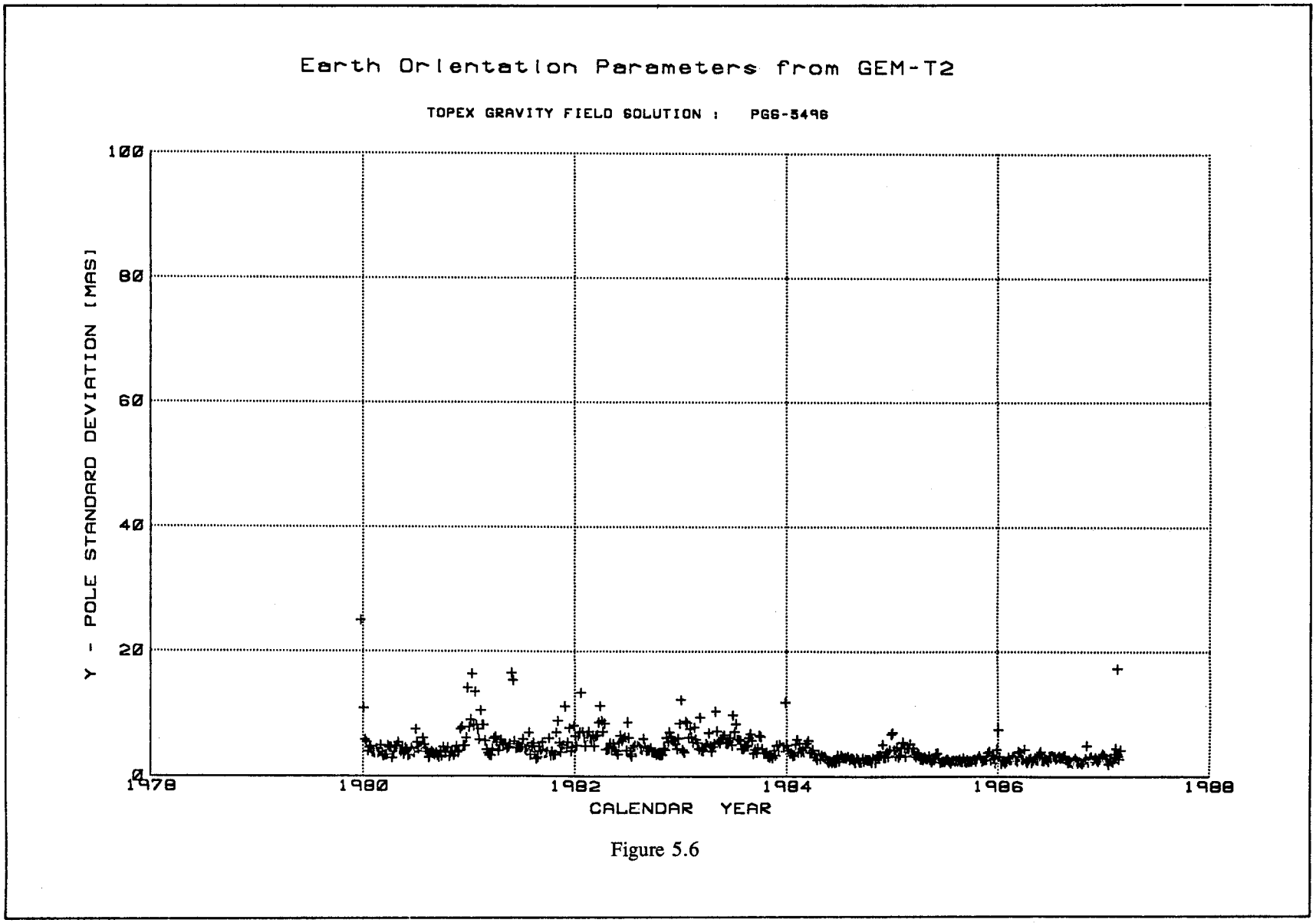
Earth Orientation Parameters from GEM-T2
TOPEX GRAVITY FIELD SOLUTION : PGS-5496
Y - POLE STANDARD DEVIATION [MAS]
100
80
60
40
20
0
1978
1980
1982
1984
1986
1988
CALENDAR YEAR

Figure 5.6

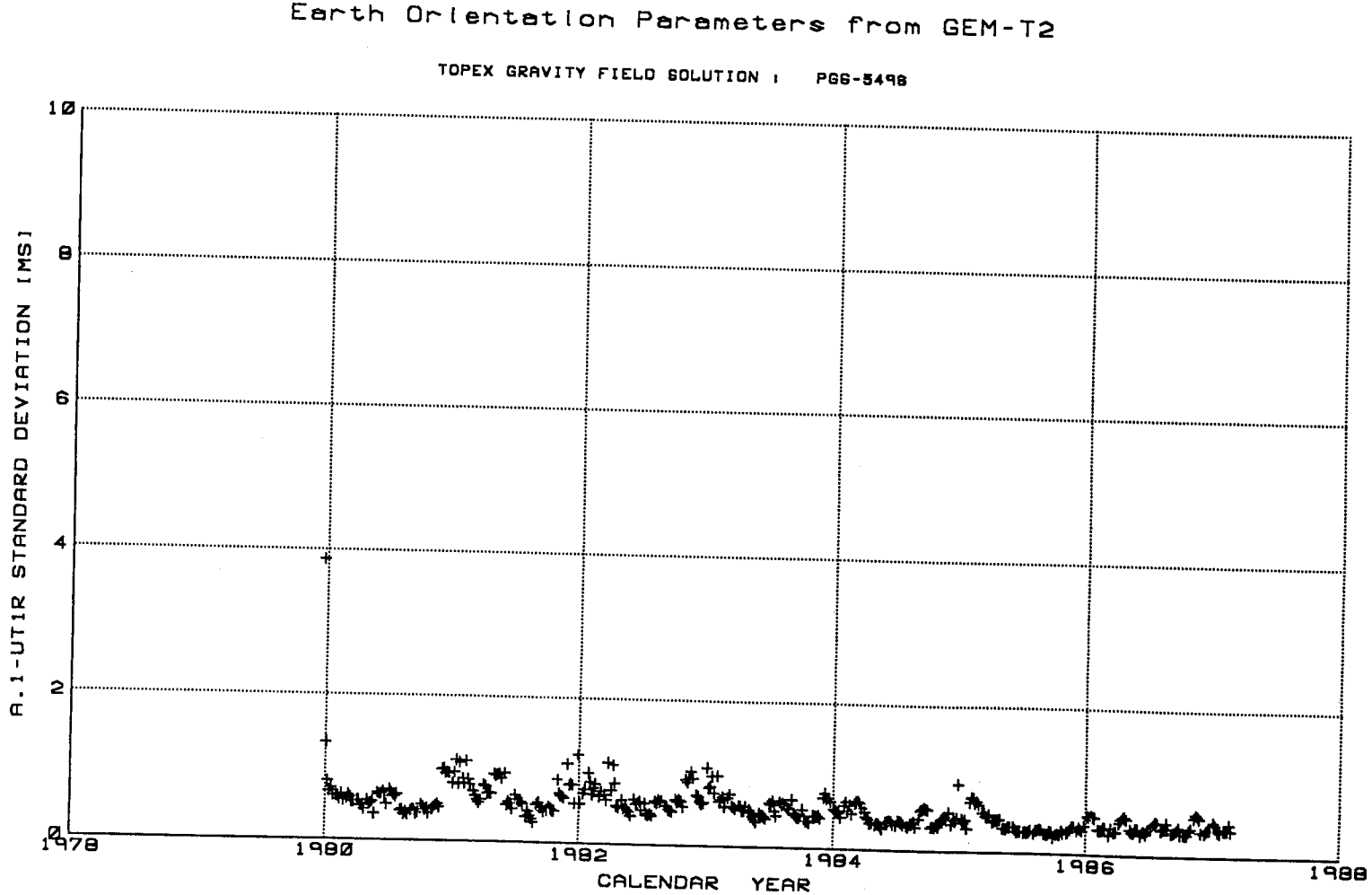
Earth Orientation Parameters from GEM-T2
TOPEX GRAVITY FIELD SOLUTION : PGS-5498
A.1-UT1R STANDARD DEVIATION [MS]
10
8
6
4
2
0
1978
1980
1982
1984
1986
1988
CALENDAR YEAR

Figure 5.7

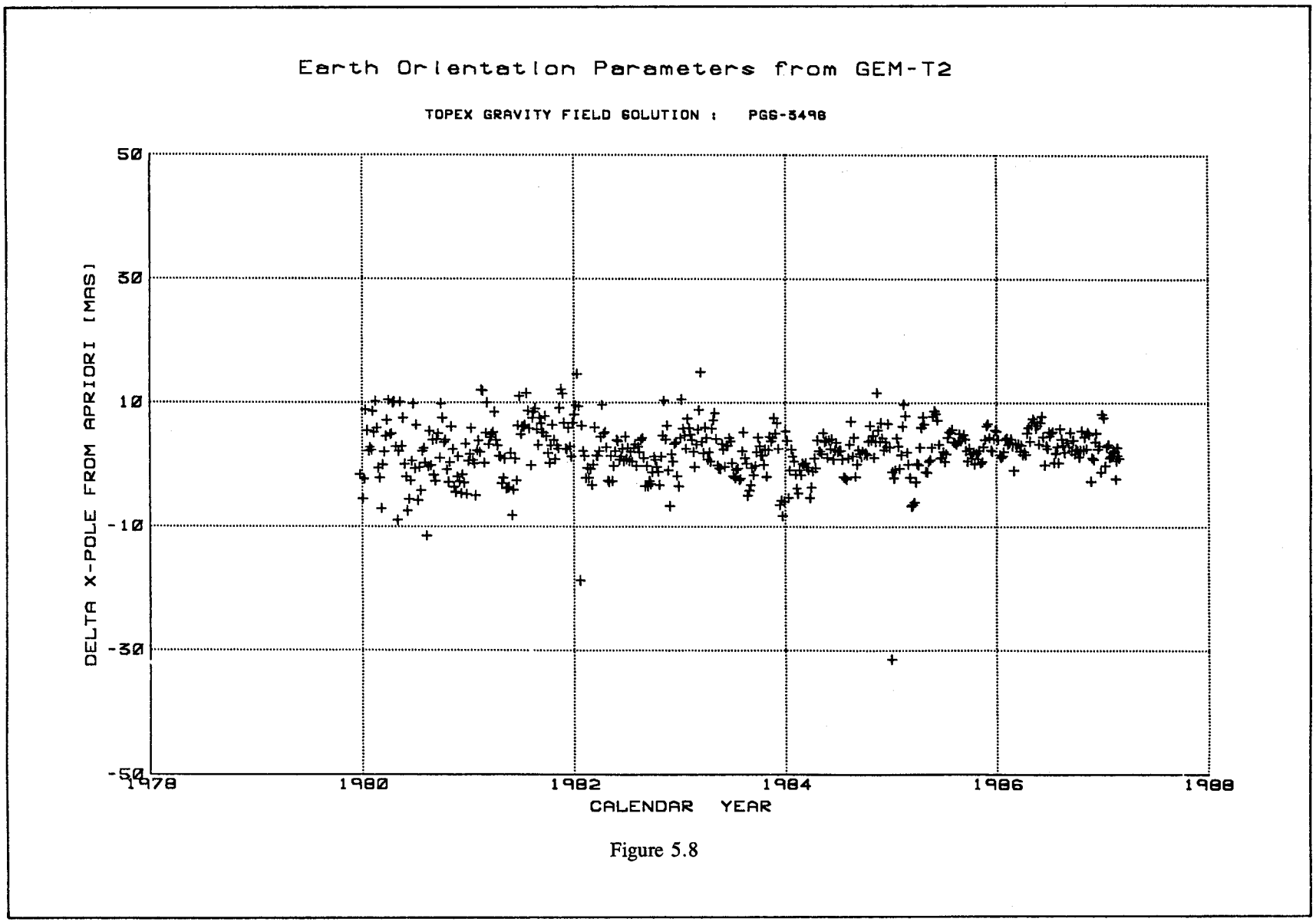
Earth Orientation Parameters from GEM-T2
TOPEX GRAVITY FIELD SOLUTION : PGS-5498
DELTA X-POLE FROM APRIORI [MAS]
50
30
10
-10
-30
-50
1978
1980
1982
1984
1986
1988
CALENDAR YEAR

Figure 5.8

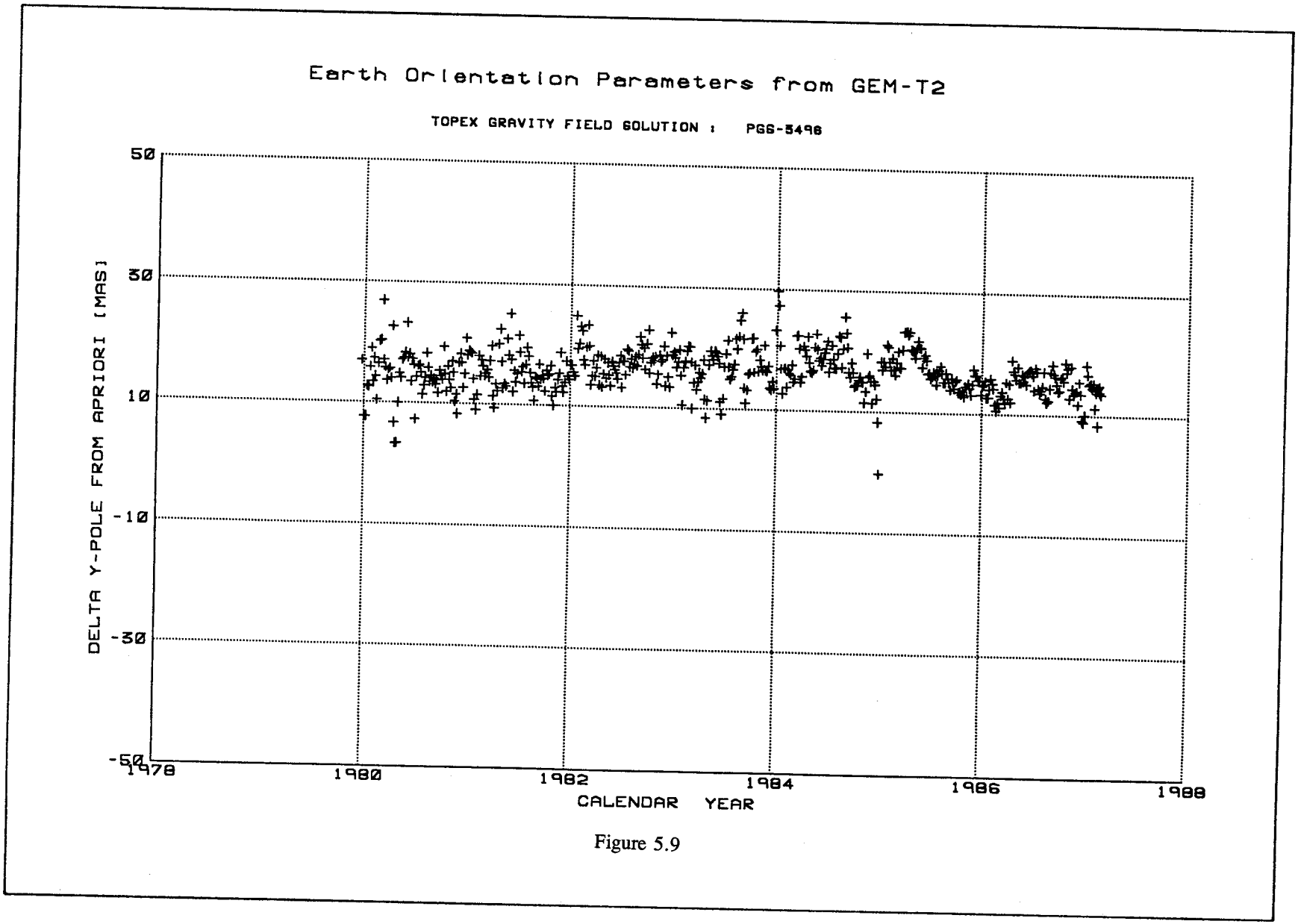
Earth Orientation Parameters from GEM-T2
TOPEX GRAVITY FIELD SOLUTION : PGS-5498
DELTA Y-POLE FROM APRIORI (MAS)
50
30
10
-10
-30
-50
1978
1980
1982
1984
1986
1988
CALENDAR YEAR

Figure 5.9

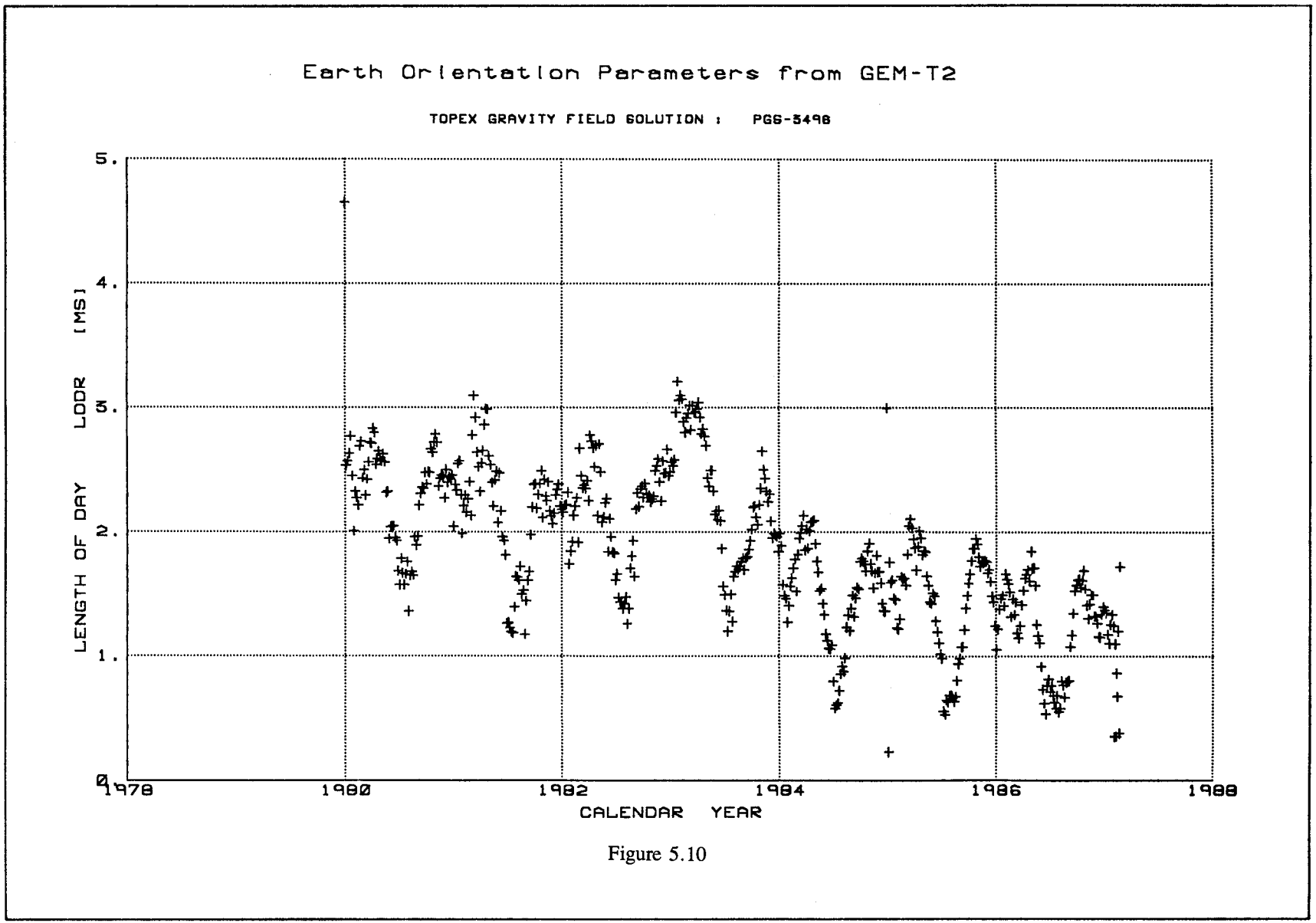
Earth Orientation Parameters from GEM-T2
TOPEX GRAVITY FIELD SOLUTION : PGS-3498
LENGTH OF DAY LODR [MS]
5.
4.
3.
2.
1.
0
1978
1980
1982
1984
1986
1988
CALENDAR YEAR

Figure 5.10

Table 5.4

O R T H O G O N A L A F F I N E
==========

T R A N S F O R M A T I O N
==========

R(NGS)8711 ===> PGS-3496

Xmean	-41.35	RMSx	41.40	S.D.Xmn	2.12
Ymean	-261.06	RMSy	261.07	S.D.Ymn	2.61
Umean	0.75	RMSu	0.85	S.D.Umn	0.40
Lmean	-0.03	RMSl	0.17	S.D.Lmn	0.17

Transformation Parameters
==========

-B2	-A1	A2
-41.3550	-0.0297	-0.4011
-261.0445	0.0297	-0.4011
-B1	A1	A2

mas		mas/d
X0 = -4.135E+01	X1 =	2.453E-04
Y0 = -2.611E+02	Y1 =	-4.887E-03
U0 = 1.127E+01	U1 =	-4.481E-03

msec		msec/d
L0 = -2.570E-02	L1 =	-1.251E-04

X Offset (B2)	41.35503	±	0.16
Y Offset (B1)	261.04448	±	0.16
Cosine Term A1	0.02971	±	0.16
Sine Term A2	-0.40111	±	0.16

Degrees of Freedom 454
Unit Weight Std.Err. 2.37

Correlation - Std. Deviation Matrix
==========

0.1570			
-0.0340	0.1570		
-0.0243	0.0000	0.1570	
0.0000	-0.0243	0.0340	0.1570

RMS(x) =	2.19	RMS(y) =	2.53
RMS(u) =	0.39	RMS(l) =	0.16

transformation parameters indicated that there is no significant center of mass disagreement between these two modern reference frames; the orientation parameters which were estimated are as expected from the difference in polar motion and UT1 origins between TOPEX/Poseidon "zero-mean" and BIH terrestrial origins. The center of mass offset in both x and y are significantly different from zero, being around 30 cm. It should be noted that the geocentricity of the Doppler Network is not guaranteed to correspond to that of the lasers; the lack of survey ties preclude direct intercomparison. For example, any systematic effect on the network determination due to higher order ionospheric effects could manifest itself in the same way in both WGS-84 and the GEM-T2 adjustments. However, we believe that these discrepancies are probably at the sub-meter level. Also of note, the earlier problems we have observed with DMA coordinates in the Z direction have greatly diminished with these recent solutions.

Table 5.5
COMPARISON OF GEOSAT GEM-T2 TRANET DOPPLER COORDINATES
WITH DMA/HTC SMTP WGS-84 COORDINATES

RMS OF FIT FOR 47 MATCHING STATIONS

Earth Fixed:		Geodetic Coordinates	
X	46 cm	Geodetic Latitude	0.014 arcsec
Y	42 cm	Longitude	0.021 arcsec
Z	41 cm	Spheroid Height	39 cm

TRANSFORMATION PARAMETERS

Center of Mass		Rotation about Axis*		Scale
X	30 ± 8 cm	X	0.266 ± 0.03 arcsec	0 ± 12 parts per billion
Y	-25 ± 8 cm	Y	0.046 ± 0.03 arcsec	
Z	-5 ± 8 cm	Z	0.039 ± 0.03 arcsec	

* Expected Rotations from origin differences:

about X 0.280 arcsec

about Y 0.038 arcsec

SECTION 6. THE DETERMINATION OF OPTIMAL DATA WEIGHTS AND THE CALIBRATED ACCURACY OF GEM-T2

Determining optimum data weights and producing a reliable error model are now part of an automated iterative procedure which has been employed in GEM-T2's development for the first time. This approach, as described in Lerch (1989), allows a new ease in the determination of data weights and provides a calibrated error model as an integral part of the method. Prior to the introduction of this approach, optimal data weighting was obtained from experimental solutions which were tested against orbital tracking data and independent gravity anomaly blocks until no further improvement was seen in model tests. The top rated model was adopted and its uncertainty was then calibrated after the fact to assure its reliability. Our experience has shown that these models both performed well and were well calibrated although the method was arduous. Calibration of model errors has historically been a complicated and time consuming undertaking. The techniques which were used to verify the models and calibrate their uncertainties have evolved. The most recent attempts directly laid the foundation for the development of our new automated procedure. In general, they consisted of three types of tests which are reviewed here since method (a) is associated with the development of the optimal weighting algorithm presented in Section 4. The gravitational field calibrations which have been used are:

(a) Calibration tests which compare the differences in the coefficients between two solutions with the expected value of these differences using the solution error covariances. This method has been extensively utilized with GEM-T1 in comparison with versions of this model lacking specific data subsets.

(b) Calibration tests which compare the eigenvectors of these subset solutions in a fashion which parallels that used in method (a) but which is extended to include the off-diagonal contributions in the error covariances.

(c) The oldest method (which has been used for over 15 years) is to compare the harmonic gravitational models with independent gravity information. Since GEM-T1 and GEM-T2 are "satellite-only" models, their results can be compared to the gravitational signal directly measured by surface gravimetry or the gravity anomalies inferred from satellite altimetry. In the past, other tests using satellite deep resonance passages, the longitudinal acceleration of synchronous satellites, and tests on new sets of tracking data have provided the basis for these tests.

In method (a) the calibration test is essentially given in equation (4.14). This method has been refined to separately test the spectral components of the gravitational models by segregating the results into constituents of a given degree, $k_t(l)$, and order, $k_t(m)$. Balanced solutions with proper data weights were found to calibrate well in general for any degree or order. Method (b) has not been employed as yet on GEM-T2 although it was found to give comparable results to method (a) for GEM-T1 (Lerch et al., 1988). Results for GEM-T2 are also given later in this section for method (c). Method (c) confirms that the calibrated error estimates of GEM-T2 as obtained from our optimum weighting algorithm are highly reliable as demonstrated with tests against independent altimeter-derived gravity anomaly blocks.

6.1 Computations of Optimum Weights for GEM-T2

Using the weighting algorithm of Section 4.1 we show in Table 6.1 the preliminary subset and complete solution calibrations based on the factors, k_t, and weights[1], W_t obtained over successive iterations. The subset solutions are obtained by deleting each of the major data sets listed in the first column of this table from the complete solution. The first solution, Preliminary Geopotential Solution (PGS)-3429 used initial data weights which were obtained in two ways. The apriori weights for PGS-3429 were based on the weights obtained in GEM-T1 as shown in Table 4.1a. For the data sets not included in GEM-T1 (Table 4.1b), initial weights were obtained by testing a solution which combined GEM-T1 with each of these new data sets individually against GEM-T1 itself, where in this case, GEM-T1 is the subset solution. We then applied the weighting algorithm from equations (4.14) and (4.15) to converge on a set of weights for all of the data which was previously not part of GEM-T1. This approach produced a set of apriori weights for all of the major data sets of GEM-T2. This is the set of PGS-3429 data weights presented in the third column of Table 6.1.

A set of subset solutions was computed for PGS-3429 where each of the major data sets was individually omitted from this preliminary version of GEM-T2. A set of calibration factors, K_t, were obtained which are listed in the second column of Table 6.1. The initial calibration factors indicated that these preliminary weights were quite reasonable. In Table 6.1 the calibration factor (K_t) scales the errors of the gravity parameters instead of the variances of these errors as given by k_t, hence the values shown are:

$$K_t = k_t^{1/2}$$

for the calibration factors in the table. The K_t calibration factor is more appropriate for examining the convergence since its stability and sensitivity directly reflect the errors instead of their variances.

The weights on the data were then adjusted using equation (4.15) for the data sets where K_t significantly differed from unity (shown as the underlined values) producing the values for the next iteration of GEM-T2 which was PGS-3454. The procedure of computing subset solutions was repeated and a new set of calibration factors was obtained. These are shown in the fifth column of Table 6.1 and they are noticeably closer to unity as compared to the factors obtained with PGS-3429. The process was again iterated, where new data weights were again computed and PGS-3480 was solved using these values. The process of computing subset solutions was again repeated and new calibration factors were derived. These are shown in the sixth column of Table 6.1. Based on the calibration factors of PGS-3480, a new set of data weights for select data sets was determined which produced the GEM-T2 model. These W_t values are shown in the eighth column of this table. Subset solutions for GEM-T2 were computed and yielded the final set of calibration factors presented in the final column of Table 6.1. All of these values are acceptably close to unity and the optimal weighting method has converged. It is desirable that K_t converge to values slightly less than one in order to be conservative in the error estimation of the geopotential field. For the case of the GEOS-3/ATS-6 data, the data weight was reduced giving a value of K_t which was deliberately held at a conservative value because this data degraded the model's performance when tested against independent data.

[1] The σ's of unit weight are: 1 meter for range data, 1 cm/s for range-rate data and 2 seconds of arc for camera data.

Table 6.1

DATA WEIGHTS AND CALIBRATION OF GEM-T2

SUBSET SOLUTION DATASET	PGS3429 CALIBRATION FACTORS	PGS3429 WEIGHTS	PGS3454 WEIGHTS	PGS3454 CALIBRATION FACTORS	PGS3480 WEIGHTS	PGS3480 CALIBRATION FACTORS	GEM-T2 WEIGHTS	GEM-T2 [2] CALIBRATION FACTORS
AJISAI	1.28	.4	.3 [1]	1.21	.2	1.29	.1	.79
LAGEOS	1.29	.8	.8	1.00	.8	1.11	.8	.87
STARLETTE	1.04	.2,.2,.04	.2,.2,.04	1.01	.2,.2,.04	.96	.2,.2,.04	.96
4-LASER*	1.02	.015	.015	1.00	.015	.96	.015	1.01
GEOSAT	.59	.01	.015	.66	.035	.75	.05	.81
GEOS-3:ATS LASER,SST	.68	.015,.1,.02	.015,.05,.02	.73	.015,.1,.02	.66	.015,.1,.02	.66 [3]
NOVA	.82	.07	.075	.83	.1	.83	.15	.90
LANDSAT	.90	.0075	.0075	.90	.009	.92	.009	.92
1980 GEOS-3 LASER	.86	.1	.15	.91	.2	.97	.2	.96
1980 GEOS-1 LASER	.87	.1	.15	.97	.15	.99	.15	1.05
OPTICAL*	.95	.05,.06	.05,.06	.95	.05,.06	.94	.05,.06	.92
SEASAT		.02	.02	1.02	.02	.97	.02	.94
OSCAR		.015	.015	1.47	.007	.95	.007	1.13
3-LASER*		.015	.015	.82	.015	.83	.02	.87

1. UNDERLINED WEIGHTS ARE THE ADJUSTED ONES IN THE ITERATED SOLUTIONS
2. CALIBRATION FACTORS ARE CONSERVATIVE BUT SUFFICIENTLY CONVERGED
3. ATS SST WEIGHT DELIBERATELY UNDERWEIGHTED BASED UPON COMPARISON WITH SEASAT ALTIMETER ANOMALIES

* 4-LASER: Laser data from GEOS-1, GEOS-2, GEOS-3 and BEC satellites
3-LASER: Laser data from DI-C, DI-D and PEOLE satellites
OPTICAL: Camera data from 20 satellites

In general, the weights have converged for GEM-T2. One interesting fact about its subset solutions is their good overall level of performance when tested against surface gravity anomalies and test satellite orbital arcs. Unlike GEM-T1, we find that the subset solutions for GEM-T2 all perform nearly as well as the complete model itself on these independent tests. This is also true for the prediction of TOPEX/Poseidon's radial orbital accuracy. Hence this indicates that no individual data set dominates the GEM-T2 solution which was not found to be the case to the same degree in GEM-T1.

This method assures a self-consistent set of data weights. This means that the model changes predictably based on the solution error covariances given these weights when data is removed from the solution. If this is so, then we are properly characterizing the data contribution to the solution's accuracy and the resulting error covariance should be calibrated and contain a realistic estimate of solution uncertainty. This is tested in the next section where GEM-T2 is calibrated with the independent global gravity information provided by altimeter-derived gravity anomaly blocks.

In practice, the gravitational models are also subjected to other tests using independent data (method (c)). Weights on certain data sets may again be adjusted if a specific data set seems to produce results which conflict with independent data. In such a case, a data set may be down weighted. As noted above, this was found to be the case and was used to downweight the contribution of the ATS-6/GEOS-3 SST observations in GEM-T2. These observations were found to degrade the testing of the model against independently measured altimeter-deduced gravity anomalies. This calibration is discussed in the next subsection.

6.3 Calibration of GEM-T2 with 5° x 5° Mean Gravity Anomalies from Altimetry

Altimeter-derived gravity anomalies were also used to calibrate GEM-T2. Since the previous methods indirectly test a field by comparing it internally to its data contributions, a possible concern is that both the full and subset solutions share a common systematic error which would be untested using this method. The direct calibration of the model with independent and globally distributed altimeter gravity anomalies was undertaken to avoid this problem.

Mean 5° x 5° gravity anomalies are somewhat commensurate in field resolution with the harmonic model of GEM-T2. The values we are using here were computed from the 1° x 1° values developed from the SEASAT and GEOS-3 Missions which were kindly provided to us by Rapp (1986). The gravity anomaly calibration was performed using the method given in Lerch et al., (1988) for GEM-T1. Herein, we also corrected the altimeter anomalies using the high degree and order gravitational field of Rapp and Cruz (1986) to remove contributions to the Δg values for all terms extending to degree 300 which are neglected from the GEM-T2 solution. The calibration factor obtained from this comparison is given as:

$$k = \left(\frac{\Sigma\, k_l^2}{1066} \right)^{1/2} \qquad (6.1)$$

where k_l is an individual calibration factor computed for each of the 1066 5° blocks as:

$$k_l = \frac{| \Delta g - \Delta g_c |_l}{[\, \sigma^2(\Delta g) + \sigma^2(\Delta g_c)\,]^{1/2}} \qquad (6.2)$$

and Δg and Δg_c are the observed and GEM-T2 -computed gravity anomalies. When computing the gravity anomalies from GEM-T2 we used the spectral smoothing operator of Pellinen (Jekeli and Rapp, 1980). The gravity anomaly uncertainties are obtained from the altimeter analysis of Rapp (1986) and GEM-T2 models respectively. The typical accuracy estimate for a 5° block predicted from GEM-T2 is 3.5 mgals whereas those obtained from altimetry have accuracies in the 0.5 to 1 mgal range. Therefore, one can (in the extreme) assume that the altimeter anomalies are perfect, with little resulting change in the computed calibration factor for the tested gravity field. As a consequence, this test is especially strong for it is insensitive to the accuracy assessment for the independent data so long as $\sigma(\Delta g) << \sigma(\Delta g_c)$. The global calibration factor obtained for GEM-T2 from this analysis is:

$$k = 0.98$$

which indicated a high level of calibration consistency and gives an independent demonstration of the values of the semiautomated calibration/data weighting approach.

Table 6.2 summarizes the GEM-T2 calibrations and demonstrates the performance of the subset solutions when tested against these altimeter anomalies. Therein, one sees the RMS Δg residual between the gravitational field and the altimeter anomalies. Also shown is the covariance prediction of global geoid error and the final calibration factors for the data subsets in GEM-T2. Quite encouragingly, each data subset made a positive contribution towards better resolving the geoid through a statistical prediction (which is expected) as well as improving the agreement of the model when tested against altimetry.

Table 6.2

Summary of Calibration Factors for GEM-T2 Using Subset Solutions and Other Measures of Subset Field Performance

Data Subset Omitted from GEM-T2	K_t (Overall Calib.) Factor	Estimated Geoid Ht. Error (m)	Comparison with Altim Grav. Anom. (mgals**2)
none	----	140.5	12.5
Ajisai	0.79	141.3	12.6
GEOSAT	0.81	145.8	12.9
NOVA-1	0.90	146.2	12.9
Peole, D1D, D1C	0.87	159.0	12.8
Lageos	0.87	141.4	12.6
pre-1980 GEOS 1,2,3, BEC	1.01	146.2	13.6
Oscar	1.13	141.1	12.6
Starlette	0.96	150.2	14.1
SEASAT	0.94	141.1	12.7
Landsat	0.92	142.8	12.7
1980 GEOS-1	1.05	141.3	12.5
1980 GEOS-3	0.96	143.2	12.6
Optical Data	0.92	147.1	13.5
GEOS-3/ATS-6 SST	0.66	140.7	12.5

6.4 The Calibrated Accuracy of GEM-T2

Based on the calibrations described in the previous subsections, Figure 6.1 presents the estimated uncertainty in the coefficients for GEM-T2. This figure is also useful as a means for seeing which orders within the model were solved out to degree 50. For comparison purposes, PGS-3218 was a test model which used the GEM-T1 observation set but was solved to the complete size of GEM-T2 (recall GEM-T1 as published was truncated beyond degree 36). Figure 6.2 shows the RMS coefficient uncertainty by degree for GEM-T2 and PGS-3218, and compares both to the expected power in the gravity field as deduced from a well-known scaled version of "Kaula's rule". Our use of a least squares constraint method has permitted us to recover a model which at highest degree and order is nearly 100% in error. Without the use of this constraint, a model so recovered would be more than an order of magnitude less certain at high degree and order. Our methodology causes the errors to be bound by 100% while at the same time giving near zero for the adjusted values of coefficients which approach this level of uncertainty. This is sensible, for a zero value of a coefficient is no more than 100% in error, while a free adjustment would produce erroneously large coefficients which could be orders of magnitude in error.

The geoid commission uncertainty for GEM-T2 is estimated to be 141 cm. For the part of the model complete to degree and order 36, the commission error in GEM-T2 is estimated to be 105 cm globally which can be compared with the GEM-T1 estimate of 155 cm. Taking the GEM-T2 covariance, the 36 x 36 portion of the model has a geographical geoid error distribution as indicated in Figure 6.3. The dearth of low inclination satellites in GEM-T2 is evident by examining Figure 6.3, where there is a clear bulge in the geoid uncertainty in the equatorial region. However, this model remains a major improvement over the gravity modeling accuracy achieved within GEM-T1.

Figure 6.4 shows a comparison between the satellite-only GEM-T1 and GEM-T2 fields at different levels of model truncation in their ability to predict the values of the 5° x 5° gravity anomaly blocks obtained from SEASAT/GEOS-3 altimetry. Again, GEM-T2 outperforms GEM-T1. However, we are concerned that the portion of the model (albeit incomplete) above degree 36 seems to degrade the comparison. When investigating this problem, we believe that the complete model should have been adjusted to C,S(50,43) as opposed to the selected orders solved for in GEM-T2. However, we do not have these additional parameters available within our existing satellite tracking normal equations, but will provide for them when the GEM-T2 model is iterated prior to the launch of TOPEX/Poseidon.

Figure 6.1 Estimated Errors for GEM-T2 Coefficients

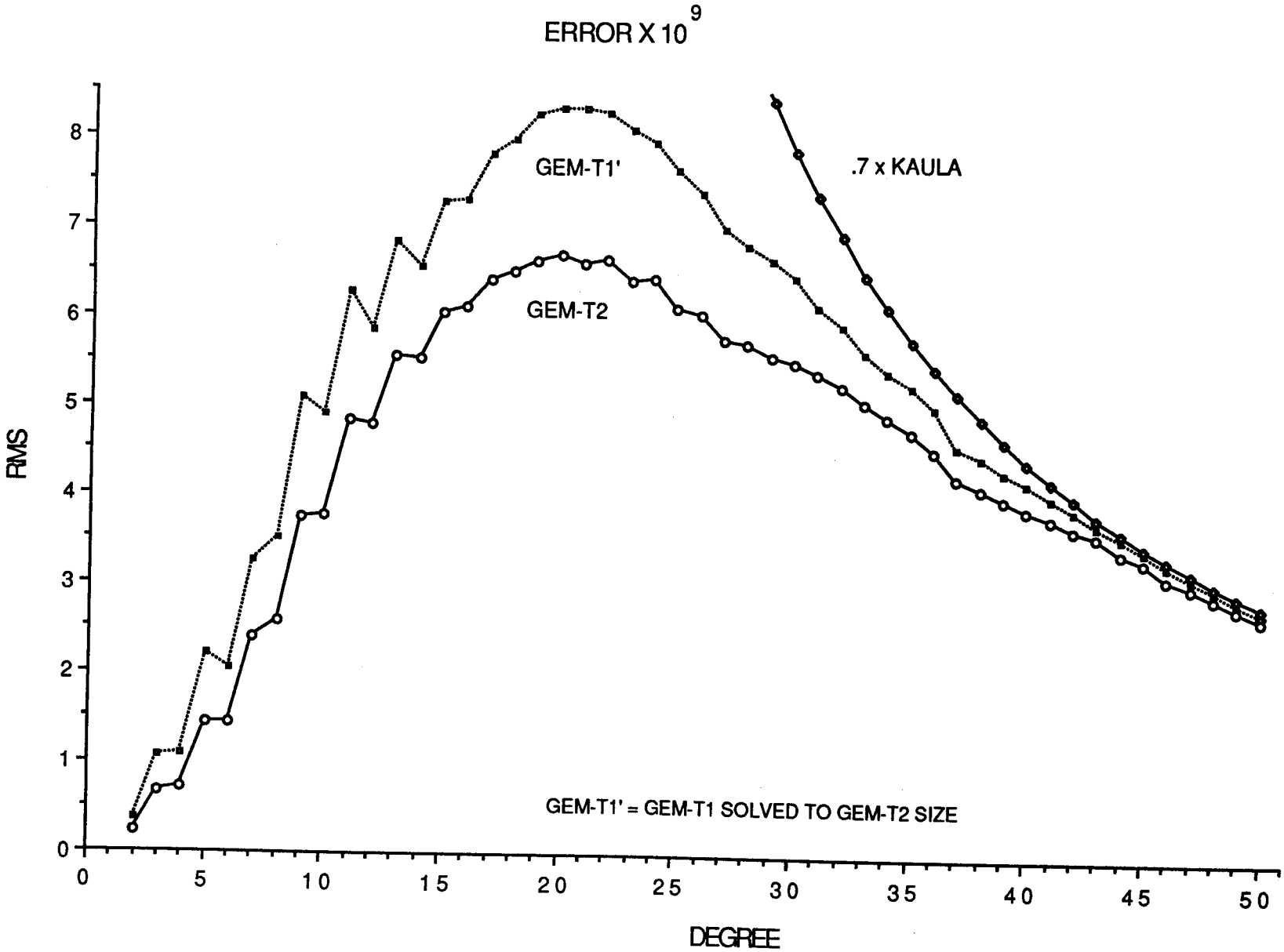

Figure 6.2 RMS of Coefficient Errors Per Degree

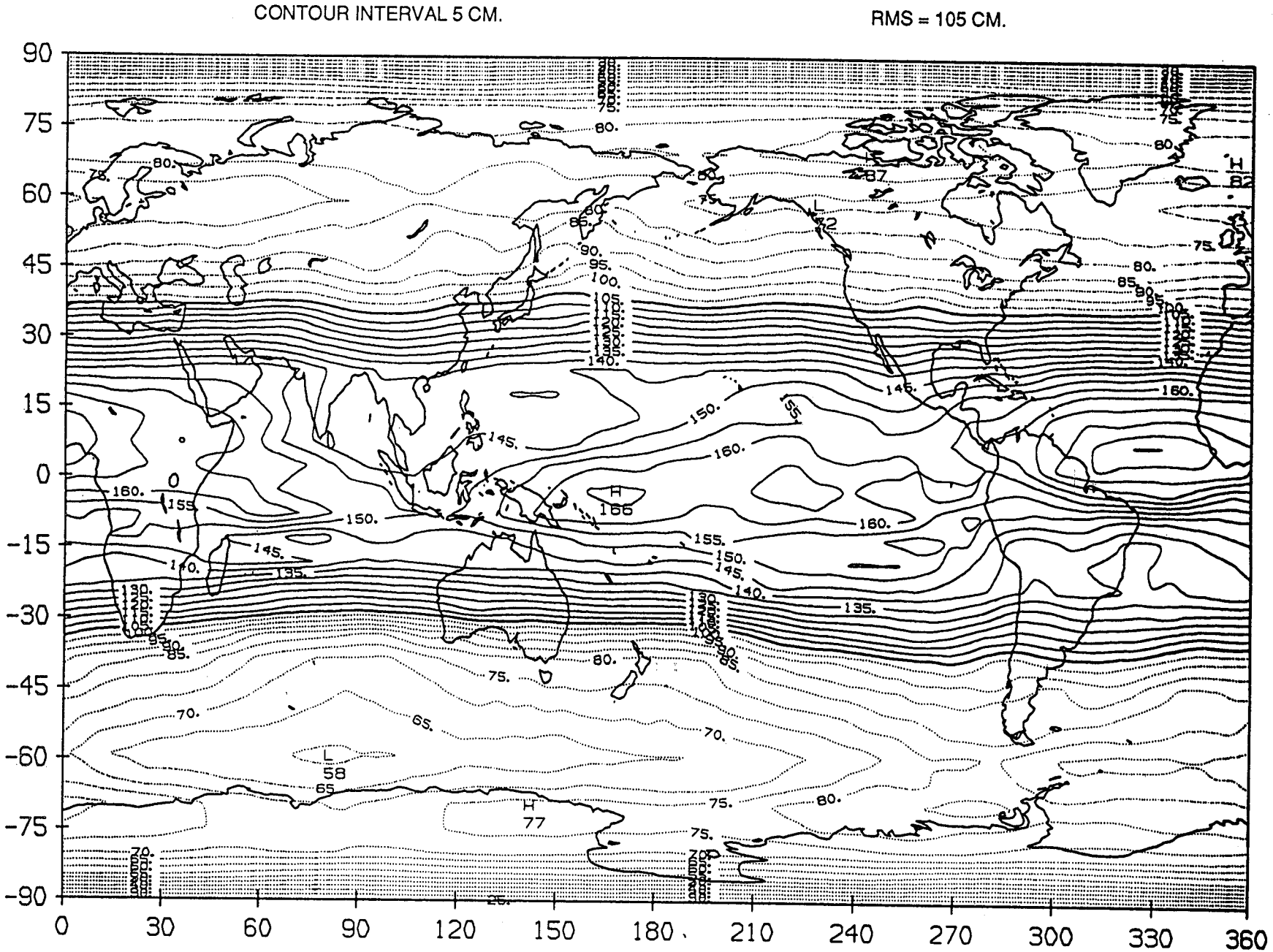

Figure 6.3 Geoid Height Standard Deviations Using GEM-T2 Covariances to 36 × 36

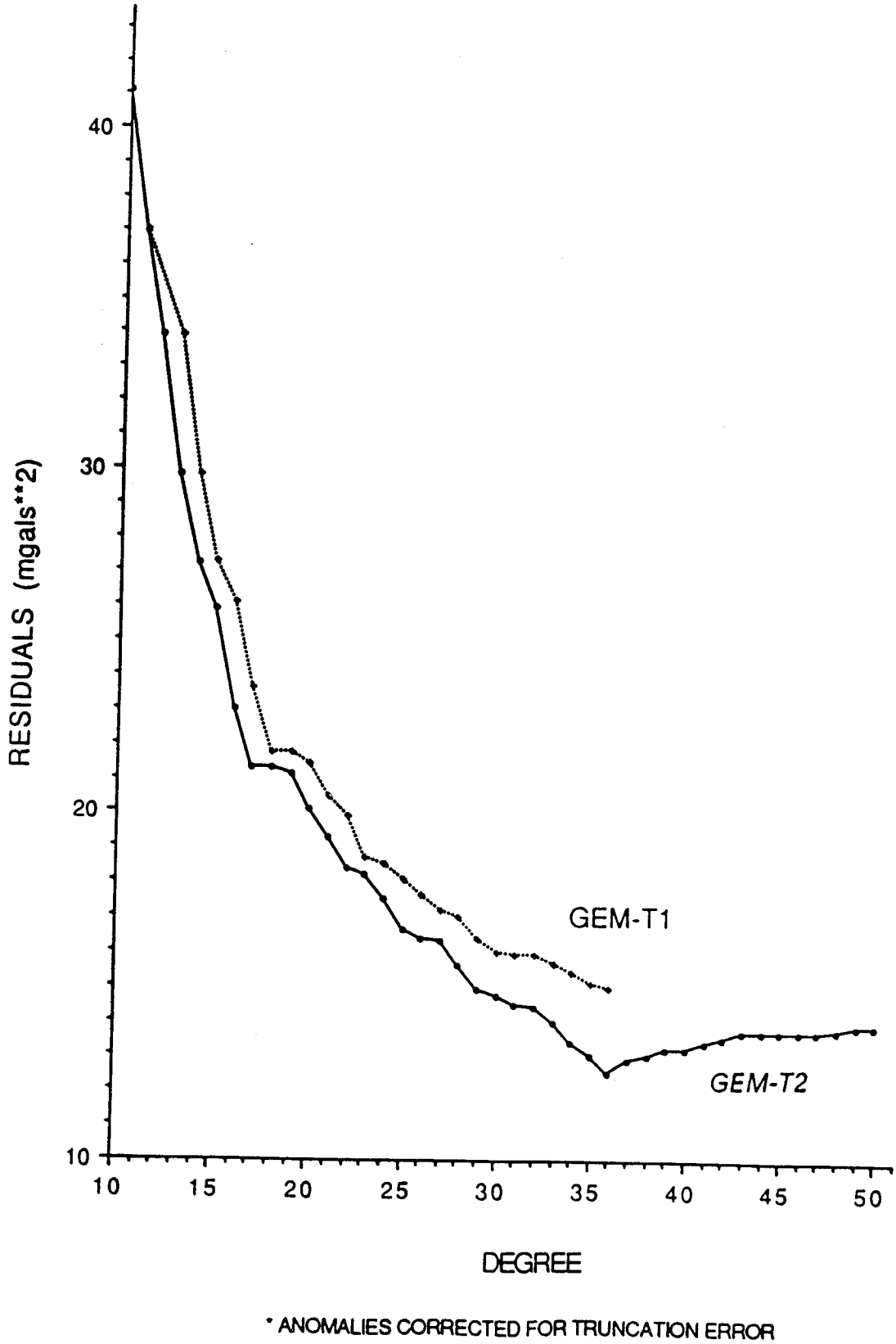

Figure 6.4 Gravity Model Comparison with 1071 5° × 5° SEASAT Altimeter Gravity Anomalies*

SECTION 7. ORBIT ACCURACIES FOR GEM-T2

One of the principal demands made of terrestrial gravitational models is to accurately represent the conservative forces acting on Earth-orbiting satellites. The requirements for precise orbit modeling are an important element in the success of many geodetic missions. This includes satellites designed to monitor the Earth's tectonic motions like LAGEOS and those requiring accurate radial positioning of an altimeter bearing satellite to locate the ocean surface in a geocentric reference frame like SEASAT and TOPEX/Poseidon. GEM-T2 has been tested with satellite tracking data acquired on a number of missions to assess its overall performance and to compare it with other contemporary models.

7.1 Gravity Model Tests Using Tracking Observations

Table 7.1 displays a series of test orbital arcs spanning all of the satellites available for our analysis which have modern precise laser and Doppler tracking. Compared therein, is the RMS of fit obtained on these test orbits for all of the recent "satellite-only" Goddard Earth Models produced over the last decade. Two important points are evident in these results. First, there has been enormous progress in the accuracy by which we are able to model the conservative forces arising from the static and tidal geopotential acting on near-Earth satellites, with GEM-T2 continuing this tradition. Second, there remains a significant gap in the accuracy by which we are able to compute and thereby reconstruct an orbital history as compared to the inherent accuracy of the data themselves. These test arcs were 5 to 6 days in length containing globally distributed observations for all satellites with the exception of LAGEOS, where 30-day orbital arc lengths were used.

Very significant improvement is seen in the modeling performance of Starlette and GEOS-3 with GEM-T2. There are two factors which have contributed to these results. By extending the GEM-T2 model to include coefficients of 41st, 42nd and 43rd orders, GEM-T2 now models higher order resonance effects which are especially significant on these two satellites. The general overall improvement obtained with GEM-T2 is an additional contributing factor which is seen in the overall orbit modeling improvement across these tests.

7.2 Radial Orbit Accuracy on SEASAT

The altimeter data taken by SEASAT enables us to isolate the radial modeling performance of different gravitational fields on its orbit. This is possible by evaluating the difference in the altimeter measured sea surface height at groundtrack crossover locations. Since the sea surface height is approximately static given its conformance to the geoid (with small effects due to mesoscale sea surface variability and mis-modeled tides being present), the value of the sea surface height can be considered time-invariant. When the height of the sea surface above the reference ellipsoid at the same geographical point on the Earth's surface is measured by crossing altimeter passes, the difference in the heights is a reasonably strong measure of the non-geographically correlated radial orbit error. This assessment of the radial error is not complete, for part of the gravity error contribution is geographically dependent yet it subtracts when forming the crossover difference. Nevertheless, there remains the time-dependent radial error which is well sensed by this method, although other errors can contribute to this difference at the 5- to 20-cm level (i.e., mismodelled tidal and atmospheric refraction corrections, and mesoscale oceanographic effects).

Table 7.2 shows a comparison on six test SEASAT arcs, three of which were taken when SEASAT was in a 17-day repeating groundtrack configuration, the others when SEASAT was in a 3-day repeat. TRANET Doppler data from a global network of stations was the only data used in the orbit adjustment process. These orbits were then passed through the independent altimetry and an assessment of the crossover misclosure was obtained. Four fields are compared within Table 7.2:

Table 7.1

Orbit Accuracy Assessments of Satellite Fields Using Test Arcs
(rms of fit)

Gravity Field	LAGEOS (m)	AJISAI (m)	STRLT (m)	BE-C (m)	GEOS1 (m)	GEOS2 (m)	GEOS3 (m)	NOVA (cm/s)
GEM-9 (1979)	.333	.951	1.16	.873	1.26	1.18	1.72	0.95
GEM-L2 (1981)	.199	.797	1.00	.893	1.07	1.09	1.87	0.79
GEM-T1 (1987)	.069	.181	.172	.396	.387	.655	.693	0.44
GEM-T2 (1989)	.066	.151*	.102	.334	.316	.667	.249	0.37*
NOISE FLOOR	.038	.038	.040	.102	.206	.343	.101	.335

* Satellite now in model

(a) PGS-S4 (Lerch et al., 1982a) was a "tailored" gravity model which used SEASAT laser, S-Band range-rate and altimeter data which for its time, was the state-of-the-art for SEASAT precise orbit determination. This gravity field was used for the Geophysical Data Records to produce the orbital information for the distributed data. By using SEASAT altimetry, this model would be expected to perform quite well on SEASAT, and did reduce the radial modeling inaccuracies on this trajectory from the 2-4 meter level to that of ± 75-cm.

(b) GEM-T1 (Marsh et al., 1988) was a "satellite-only" model which utilized SEASAT TRANET and laser observations. It contained no altimetry, but does contain the considerable improvement which was accrued in our efforts to improve the models for TOPEX/Poseidon.

(c) GEM-T2 is the new GSFC "satellite-only" model described in this report which contained the same SEASAT observation set as that of GEM-T1. Any improvement in the SEASAT performance is therefore, a direct result of improving the general gravitational field.

(d) PGS-3337 (Marsh et al., 1989) is a preliminary combination model complete to degree and order 50 which utilizes GEM-T1's tracking data with surface gravimetry and SEASAT altimetry. Unlike PGS-S4, this model now simultaneously solves for a harmonic model of the dynamic sea surface height which causes the sea surface to depart from the geoid at the 60-70-cm level.

Table 7.2 shows excellent results for GEM-T2 which exceed those found in GEM-T1 by a considerable amount. These models are certainly superior to that achieved with PGS-S4 although this latter model used the SEASAT altimeter data directly. As a point of interest, the GEM-T2 error covariance matrix predicts 19 cm for the radial accuracy one should obtain from this field. The prediction for GEM-T1 is 44 cm.

7.3 Projected Orbit Errors Due to Static Gravitational Modeling Uncertainties

The error covariance matrix can be used to project the gravitational modeling error onto any orbital configuration. This projection uses the first-order analytical perturbation theory developed by Kaula (1966) and gives a harmonic estimate of modeling error. This estimate does not take into account the distribution of tracking data nor does it consider the additional error arising from the erroneous estimation of the orbital state (epoch) position which propagates with the well-known "once-per-revolution" orbit errors commonly seen in data analyses. However, with the distribution of modern tracking networks and the typical performance of these tracking systems in their support of numerous missions, we have found through comparisons with numerical tests and data simulations, that these first-order projections are quite reliable in mapping a given gravity error into orbit error overall.

For these projections, we have developed an additional preliminary gravitational field. PGS-3520 (Marsh et al., 1989) is a combination model which is similar in design to that of PGS-3337. It is a model complete to degree and order 50 which utilizes tracking observations, surface gravimetry and SEASAT altimetry. Unlike PGS-3337 which relied on the tracking data used in forming GEM-T1, PGS-3520 is based on GEM-T2. Unlike GEM-T1 and GEM-T2, this combination model has not been extensively calibrated, and it is only introduced herein to give some indication of what a GEM-T3 model is likely to do in gravity modeling performance. GEM-T3 will use nearly all of the data available for gravity modeling improvement, and therefore PGS-3520 can give at least a preliminary estimate of what the total yield from historical data is likely to be.

Table 7.3 presents the projected orbit uncertainties in the radial, along-track and cross-track (normal) ballistic components for many existing and to-be-launched satellites. It compares the projected performance of GEM-T1, GEM-T2 and PGS-3520. For the TOPEX/Poseidon orbit in specific, these estimates indicate that we are approaching the level of modeling required to support this mission's radial error budget. Figure 7.1 presents a radial orbit uncertainty projection for a satellite at the nominal altitude of TOPEX/Poseidon (1341 km) using the GEM-T2 covariances for different orbital inclinations. For comparison purposes, also shown are the

Table 7.2
SEASAT Altimeter Crossover Results for 6-Day Arcs
TRANET Range-Rate Observations Only

Epoch	Number of	RMS of Crossovers (m) PGS-S4[1]	GEM-T1	GEM-T2	PGS-3337[2]
			17 Day Repeating Grouundtrack		
7/27/78	1234	0.623	0.933	0.683	0.691
8/02/78	1299	0.868	0.688	0.510	0.439
8/08/78	1407	1.316	0.695	0.620	0.422
			3 Day Repeating Groundtrack		
9/17/78	1472	1.249	0.632	0.534	0.368
9/23/78	1539	1.215	0.675	0.579	0.399
9/29/78	1498	0.922	0.710	0.651	0.536
average/(2)$^{1/2}$		0.72	0.51	0.42	0.34

1 PGS-S4 was a SEASAT "tailored" model developed by Lerch et al., (1982a).

2 PGS-3337 is a combination model combining GEM-T1 with surface gravimetry and SEASAT altimetry. It was solved complete to degree and order 50 (Marsh et al., 1989).

Table 7.3
Projected Orbit Errors Due to Commission Errors in the Static Gravitational Field
-- Errors in cm for a 10-Day Arc --

	Radial			Along Track		
Satellite	GEM-T1	GEM-T2	PGS-3520	GEM-T1	GEM-T2	PGS-3520
SPOT	268	120	65	3590	1940	1120
AJISAI	14	6	4	66	27	21
GEOSAT	44	20	10	272	98	73
LAGEOS	1	1	1	5	3	3
STARLETTE	27	12	8	83	37	24
GEOS-3	66	22	13	488	146	116
PEOLE	494	447	107	1670	1510	390
BE-C	33	25	14	160	136	101
GEOS-1	15	6	4	187	101	84
GEOS-2	28	17	11	438	286	229
DI-D	50	42	21	189	185	102
DI-D	36	29	15	213	196	149
SEASAT	44	19	10	263	94	71
OSCAR	72	41	24	294	149	96
NOVA	68	29	18	1380	570	453
TOPEX	24	9	6	187	91	71

	Cross Track			Total		
Satellite	GEM-T1	GEM-T2	PGS-3520	GEM-T1	GEM-T2	PGS-3520
SPOT	218	130	68	3610	1950	1120
AJISAI	18	8	5	70	29	22
GEOSAT	75	43	29	286	109	79
LAGEOS	2	1	1	6	3	3
STARLETTE	36	18	10	94	43	27
GEOS-3	65	27	16	497	150	117
PEOLE	560	512	118	1827	1654	421
BE-C	41	31	16	169	142	103
GEOS-1	18	8	6	189	102	85
GEOS-2	36	20	14	441	288	230
DI-D	61	50	23	205	196	107
DI-D	38	31	16	220	201	150
SEASAT	74	36	23	277	103	75
OSCAR	108	60	34	322	166	104
NOVA	117	57	34	1384	574	454
TOPEX	29	13	9	191	93	72

projections for GEM-T1 and PGS-3520. The large improvement seen at 65.5° inclination between GEM-T1 and GEM-T2 is largely a result of the additional high-precision GEOS-3 observations added to GEM-T2 which are at this inclination. The satellite-only solutions are highly dependent on the inclination distribution of the data which is used to compute the model. Weak low inclination data sets result in poor projected field performance for a satellite orbiting at an inclination of less than 35° (or greater than 145°) when either GEM-T1 or GEM-T2 are used. The sensitivity of the model uncertainties to orbital inclination are significantly reduced with the introduction of altimeter and surface gravimetry into combination models. PGS-3520 shows significantly flatter uncertainties than either of the satellite models. Figures 7.2 and 7.3 show the gravitational modeling uncertainty of GEM-T1 and GEM-T2 projected on the radial component of the TOPEX/Poseidon orbit for terms grouped by degree and order respectively. Both of these figures indicate a broad general improvement in GEM-T2 which is found across the perturbation spectrum of TOPEX/Poseidon's orbit. Of special interest is the improved modeling of the resonance and m=1 orders found with GEM-T2.

7.4 Discussion of the SEASAT Altimeter Crossover Results

An explanation is warranted to reconcile our prediction of GEM-T2's SEASAT radial orbit error shown in Table 7.3 and the 59-cm ($= 42 \times 2^{1/2}$) RMS altimeter misclosure error shown in Table 7.2. The first topic to address is the relationship of the 19-cm estimate to the crossover measurement. It is well known that altimeter crossover tests only detect part of the radial orbit error--that part which is time varying and not the geographically correlated error. The 19-cm estimate in Table 7.3 is a combined value containing the total radial error. It has also been found that the error is approximately equally distributed between the geographically correlated error and the time varying error globally. Therefore, one would expect only 14 cm coming from the contribution of each arc to the crossover discrepancy. We have performed a numerical simulation on SEASAT using GEM-T2 and a gravitational field ("clone") which is one standard deviation away from GEM-T2. This experiment showed a 19.4 cm RMS radial orbit difference (which agrees very well with our analytical prediction of 19 cm) in the orbits predicted by the two models; moreover it was found that 14 cm was the time varying error which would be sensed in the crossover results, with the geographically correlated error contributing 14 cm. Rosborough (1986) has shown that the time varying radial error maps by a factor of 2 into the crossover residuals given the changing sign of the geopotential error propagation into the ascending vs. descending track. Therefore, one would expect a 28 cm contribution from GEM-T2's errors in the crossover misclosure. There are numerous other errors which enter into the crossover computation which are described in Table 7.4. The total contribution from these errors accounts for an additional 24 cm in the crossover RMS. What remains to explain the 59-cm value obtained experimentally from the real data are other sources of orbit error including the modeling of atmospheric drag, solar pressure, Earth albedo and the contribution of data systematics arising from the TRANET II tracking systems used to compute these orbits. Our analyses show that drag and solar radiation pressure errors on SEASAT are typically 15 cm over a 6-day arc. Therefore, solving the following equation and ignoring the small contribution from Earth albedo, we get:

$$59^2 = 28^2 + 24^2 + (15x2^{1/2})^2 + X^2$$

where X = 41 cm and it represents the error in the orbit due to TRANET II being the only tracking data used in the orbit's determination. The question which remains: Is this value reasonable? Confirmation of this estimate can be found in Marsh et al., (1989a; Table 9) where the crossover RMS for PGS-3337 using Doppler data alone was 47 cm and 31 cm when altimetry treated as tracking data was added to the solution. $(47^2 - 31^2)^{1/2} = 35$ cm which shows the improvement obtained with the introduction of altimeter data. It is also clear to us that the use of altimetry has not eliminated all of the systematic errors (e.g., neglect of third-order ionospheric refraction modeling, oscillator errors, station position errors, etc.) introduced in the orbit computation from the TRANET data, for these data are still being used. Also, the introduction of altimetry has its own error sources. Furthermore, from Table 4.1 it is shown that the "true" value of the TRANET II observations in the gravitational field determination is represented by a noise estimate of 7cm/s as obtained in our optimal data weighting method. If one were to take the noise-only uncertainty for the SEASAT orbit's radial component assuming 7cm/s Doppler data

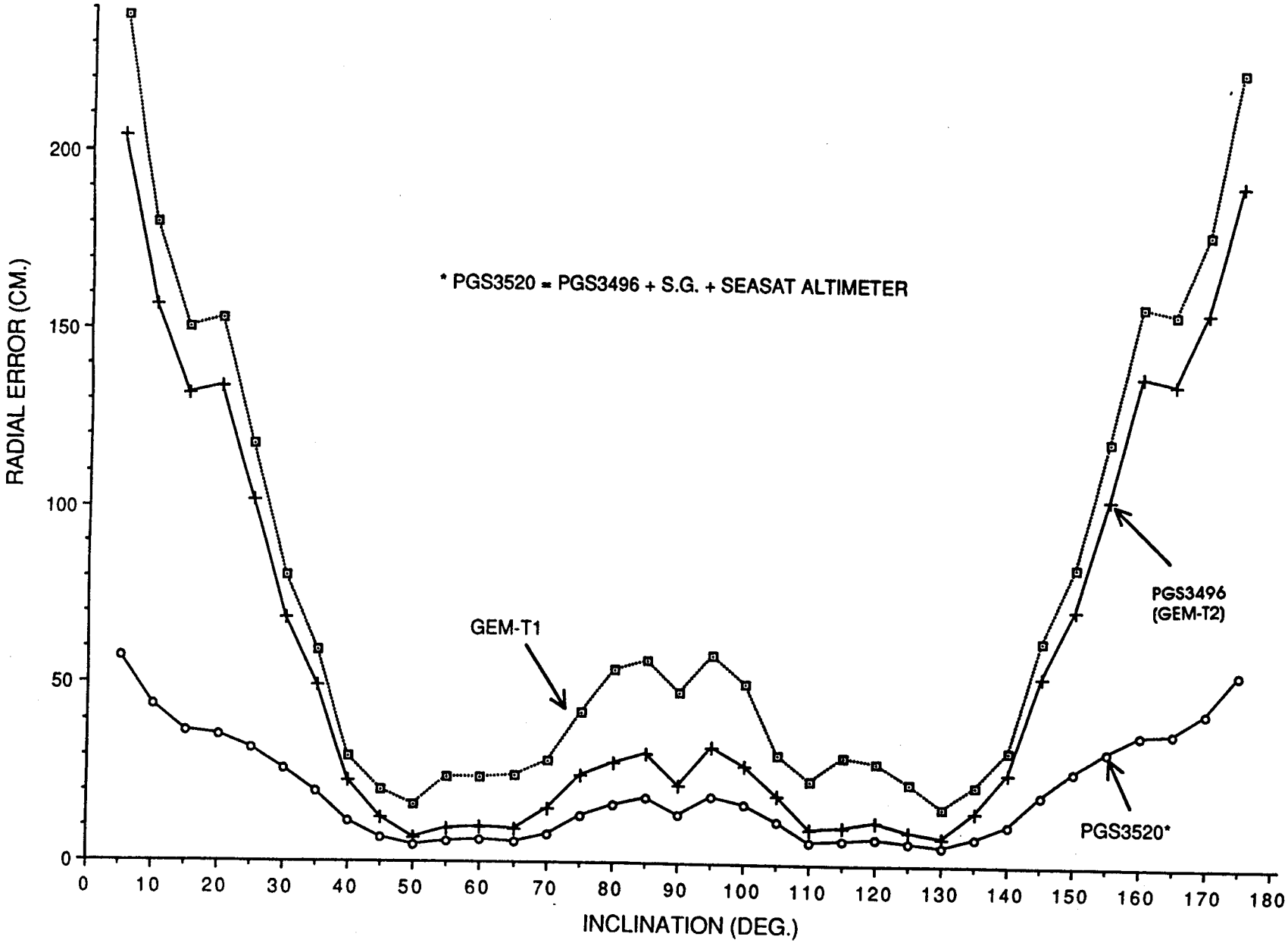

Figure 7.1 Predicted Radial Error From Gravity Covariances 1341 Km. Altitude

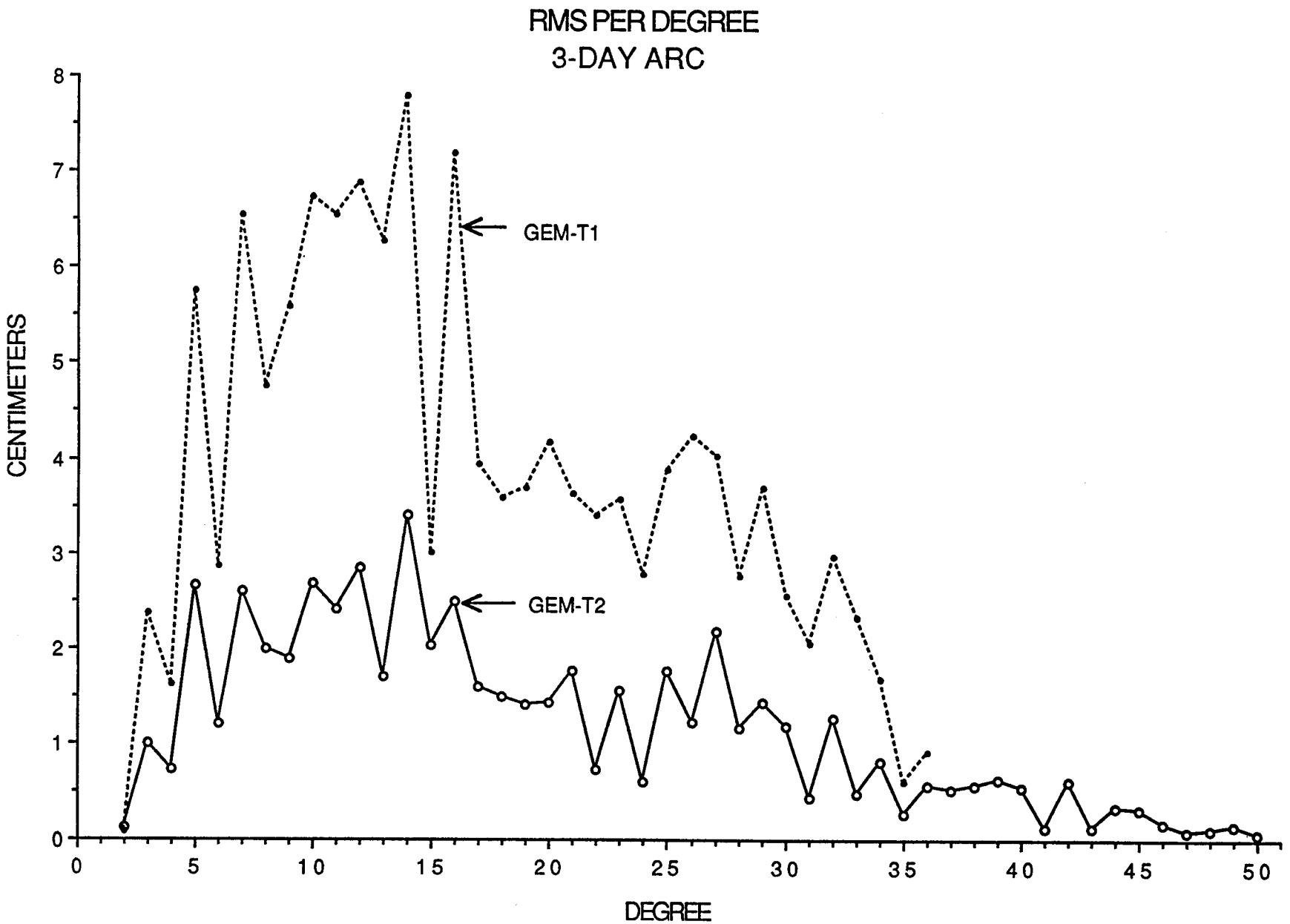

Figure 7.2 TOPEX Projected Radial Error

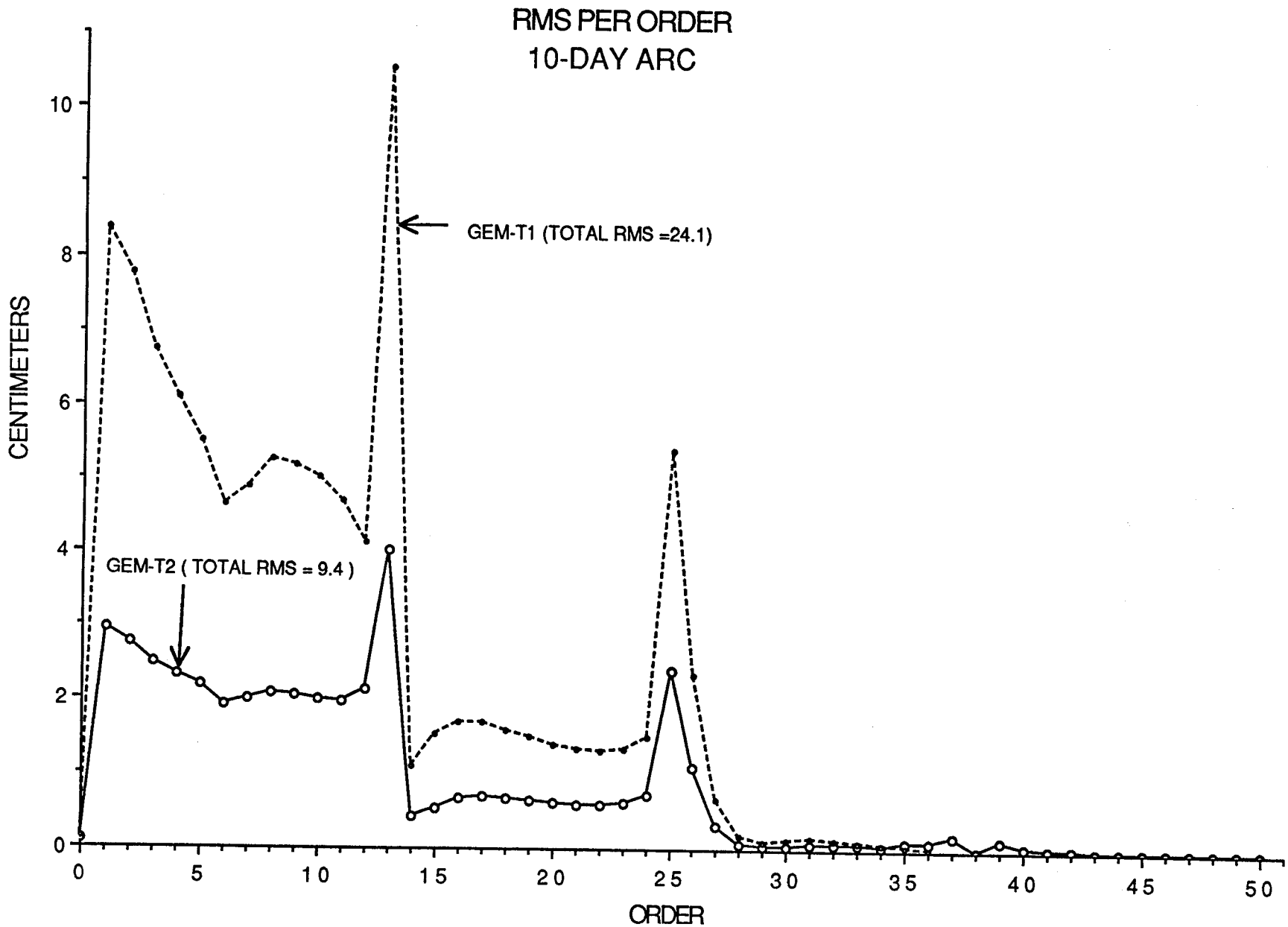

Figure 7.3 TOPEX Projected Radial Error

noise, the noise contribution would exceed 45 cm for each of the tested arcs.

Nevertheless, the original estimate for GEM-T2's performance on SEASAT shown in Table 7.3 assumed perfect orbit tracking information in all components; in this experiment with PGS-3337, a 35-cm improvement is obtained through the introduction of restricted high-quality orbital radial information over the oceans. Our estimate of 35 to 40 cm is a realistic assessment of the radial orbit error contribution coming from the exclusive use of Doppler tracking to produce the results in Table 7.2. Therefore, we conclude that our overall error estimate for the gravitational field's contribution to SEASAT shown in Table 7.3 is confirmed to be realistic and consistent with other contributing error sources.

Table 7.4
Error Sources Contributing to Altimeter Crossover Misclosures on SEASAT

Error Source	Approximate Magnitude (cm)
Ocean/solid Earth tides	10
EM Bias	5
Data Noise (altimeter)	10
Media	5
Spatial Interpolation	2
Altimeter pointing/timing	2
Root Sum of Squares:	16
TOTAL: Two observations involved in crossover computation	24[1]

[1] Obtained by: $16 \times 2^{1/2}$

SECTION 8.
SUMMARY

High precision ground based tracking of artificial satellites has provided an observational data set which has formed the basis for improving existing models of the long-wavelength gravitational field. These data have been used at GSFC to produce a new "satellite-only" model. GEM-T2 is an improved gravitational field which has a twofold increase in the amount of data previously analyzed to form GEM-T1 (Marsh et al., 1987; 1988). Data acquired on 31 different satellites are now utilized. The model is based on modern geodetic reference parameters, supercomputer capabilities and a new technique of optimum data weighting with automatic error calibration. The GEM-T2 solution is the largest exclusively-satellite model ever published by GSFC. It contains more than 600 coefficients above degree and order 36, which was the truncation limit of GEM-T1. These additional coefficients enable GEM-T2 to better define the satellite zonal, low-order, and resonance effects needed in the precision computation of near-Earth satellite motion. The solution, like GEM-T1, simultaneously estimates a model of the temporal changes in the geopotential at the major astronomic frequencies to provide improved modeling of the dynamic tides sensed by satellite motion. GEM-T2 extends this adjustment to include 90 parameters distributed over 12 major tidal lines.

GEM-T2 is an advancement in the geoid modeling obtainable from an analysis of satellite tracking observations. The commission error for the 36x36 (complete) portion of the field has been reduced to 102-cm global RMS uncertainty. GEM-T2 has directly benefitted from an optimum data weighting technique with automatic error calibration (Lerch, 1989). This procedure, used for the first time in the development of a GEM model, has produced a well-calibrated solution. The calibration has been verified using independent satellite altimeter-derived gravity anomalies.

This model has also increased our ability to accurately model the gravitational accelerations experienced by near-Earth satellites. For TOPEX/Poseidon applications, which are of direct importance in this model undertaking, projections indicate that we are close to meeting the project's specified requirement of reducing the gravitational modeling errors to be no more than 10-cm RMS. Harmonic analyses using the error covariance of the GEM-T2 model which has been extensively calibrated, indicates that we are on the threshold of achieving these goals.

ACKNOWLEDGEMENTS

The authors would like to acknowledge the TOPEX/Poseidon Project at JPL for its support of our gravity modeling improvement activity. We also are thankful for the support this work is receiving from NASA's Geodynamics Program.

Many individuals have provided valuable information and help in the development of GEM-T2. Richard Rapp and Nick Pavlis of Ohio State University are to be thanked for their analysis and evaluation of the surface gravimetry. George Born and George Rosborough of the University of Colorado have assisted us in improving our methods for calibrating the model. The University of Texas' Center for Space Research under the direction of Byron Tapley has also played an important role as a sounding board for our activities.

REFERENCES

Anderle, R.J., "Doppler Satellite Data Characteristics," Naval Surface Weapons Center Document TR 83-353, October 1983.

Bursa, M., "Geodynamcis Due to the Varying Second Zonal Geopotential Harmonic," paper presented at the 26th COSPAR Conference, Toulouse, France, 1986.

Chao, B.F., W.P. O'Connor, A.T. Chang, D.K. Hall, and J.L. Foster, "Snow Load Effect on the Earth's Rotation and Gravitational Field, 1979-1985," J. Geophys. Res., 92, B9, pp. 9415-9422, 1987.

Chao, B.F. and W.P. O'Connor, "Global Surface-Water-Induced Seasonal Variations in the Earth's Rotation and Gravitational Field," Geophys. J., 94, pp. 263-270, 1988.

Chao, B.F., "Excitation of the Earth's Polar Motion due to Mass Variations in Major Hydrological Reservoirs," J. Geophys. Res., 93, B11, pp. 13811-13819, 1988.

Christodoulidis, D.C., R.G. Williamson, D. Chinn, and R. Estes, " On the Prediction of Ocean Tides for Minor Constituents," Proceedings of the 10th International Symposium on Earth Tides, edited by R. Vieira, pp. 659-678, Conseja Superior de Investigaciones, Madrid, Spain, 1986.

Christodoulidis, D.C., D.E. Smith, R.G. Williamson, and S.M. Klosko, "Observed Tidal Braking in the Earth/Moon/Sun System," J. Geophys. Res., 93, B6, pp. 6216-6236, 1988.

Figgatte, C. and A. Polesco, "Laser Preprocessor Program User's Guide," Contract Report 5-24300, Task 769, Computer Science Corporation, June, 1982.

Goad, C., "A Modified Hopfield Tropospheric Refraction Correction Model," paper presented at the Fall Meeting of the American Geophysical Union, December 1974.

Gross, J.E., "Preprocessing Electronic Satellite Observations," Ohio State Contractor's Report, NASA CR 1183, November 1968.

Gutierrez, R. and C.R. Wilson, "Seasonal Air and Water Mass Redistribution Effects on LAGEOS and Starlette," paper in press, 1988.

Hedin, A.E., "High Altitude Atmospheric Modeling," NASA Tech. Memo. 100707, Greenbelt, MD, October 1988.

Hotter, F., "Preprocessing Optical Satellite Observations," Ohio State Report 82, Columbus, OH, May 1968.

Jacchia, L.G., "Revised Static Model of the Thermosphere and Exosphere with Empirical Temperature Profiles," Special Report 332, Smithsonian Astrophysical Observ., Cambridge, MA, 1971.

Jekeli, C. and R.H. Rapp, "Accuracy of the Determination of Mean Anomalies and Mean Geoid Undulations from a Satellite Gravity Field Mapping Mission," Report No. 307, Department of Geodetic Science, Ohio State University, Columbus, Ohio, August, 1980.

Kahn, W.D., S.M. Klosko, W.T. Wells, "Mean Gravity Anomalies from a Combination of Apollo/ATS 6 and GEOS-3/ATS 6 SST Tracking Campaigns," J. Geophys. Res., 87, B4, pp. 2904-2918, 1982.

Kaula, W.M., Theory of Satellite Geodesy, Blaisdell, Waltham, MA, 1966.

Lerch, F.J., S.M. Klosko, R.E. Laubscher, C.A. Wagner, "Gravity Model Improvement Using GEOS-3 (GEM-9 and 10)," J. Geophys. Res., 84, 3897-3915, 1979.

Lerch, F.J., J.G. Marsh, S.M. Klosko, and R.G. Williamson, "Gravity Model Improvement for SEASAT," J. Geophys. Res., 87, C5, pp. 3281-3296, 1982a.

Lerch, F.J., S.M. Klosko, G.B. Patel, "Gravity Model Development from LAGEOS," Geophys. Res. Letters, 9, pp. 1263-1266, 1982b.

Lerch, F.J., "Error Spectrum of Goddard Satellite Models for the Gravity Field," Geodynamics Branch Annual Report-1984, NASA Tech. Memo. 86223, Greenbelt, MD, August 1985.

Lerch, F.J., J.G. Marsh, S.M. Klosko, E.C. Pavlis, G.B. Patel, D.S. Chinn, and C.A. Wagner, "An Improved Error Assessment for the GEM-T1 Gravitational Model," NASA Tech. Memo 100713, Greenbelt, MD, November 1988.

Lerch, F.J., "Optimum Data Weighting and Error Calibration for Estimation of Gravitational Parameters," to be published in Manuscpt. Geodetica, 1989.

Lieske, J.H., "Precessional Matrix Based on IAU(1976) System of Astronomical Constants, Astron. Astrophys., 73, 282, 1976.

Marini, J.W. and C.W. Murray, "Correction of Laser Range Tracking Data for Atmospheric Refraction at Elevations Above 10 Degrees," GSFC Report X-591-73-351, Greenbelt, MD, November 1973.

Marsh, J.G., F.J. Lerch, B.H. Putney, D.C. Christodoulidis, D.E. Smith, T.L. Felsentreger, B.V. Sanchez, S. M. Klosko, E.C. Pavlis, T.V. Martin, J.W. Robbins, R.G. Williamson, O.L. Colombo, D.D. Rowlands, W.F. Eddy, N.L. Chandler, K.E. Rachlin, G.B. Patel, S. Bhati, and D.S. Chinn, "An Improved Model of the Earth's Gravitational Field," NASA Tech. Memo. 4019, Greenbelt, MD, July 1987.

Marsh, J.G., F.J. Lerch, B.H. Putney, D.C. Christodoulidis, D.E. Smith, T.L. Felsentreger, B.V. Sanchez, S. M. Klosko, E.C. Pavlis, T.V. Martin, J.W. Robbins, R.G. Williamson, O.L. Colombo, D.D. Rowlands, W.F. Eddy, N.L. Chandler, K.E. Rachlin, G.B. Patel, S. Bhati, and D.S. Chinn, "A New Gravitational Model for the Earth from Satellite Tracking Data: GEM-T1," J. Geophys. Res., 93, B6, pp. 6169-6215, 1988.

Marsh, J.G., F.J. Lerch, C.J. Koblinsky, S.M. Klosko, J.W. Robbins, R.G. Williamson, G.B. Patel, "Dynamic Sea Surface Topography, Gravity, and Improved Orbit Accuracies from the Direct Evaluation of SEASAT Altimeter Data," NASA TM in press, Greenbelt, Md, 1989.

Marsh, J.G., F.J. Lerch and the GSFC Gravity Modeling Team, "Earth Gravity Model Computation at Goddard Space Flight Center," paper presented at the Spring Meeting of the American Geophysical Union, Baltimore, MD, 1989.

Martin, T.V., W.F. Eddy, D.D. Rowlands, and D.E. Pavlis, "GEODYN II System Description," Vol. 1 through 5, EG&G Contractor Report, Lanham, MD, 1987.

Melbourne, W. et al., "Project MERIT Standards," Circ. 167, U.S. Naval Observatory, Washington, D.C., 1983.

Moritz, H., Advanced Physical Geodesy, Abacus, Tunbridge Wells Kent, Kent, England, 1980.

Newhall, X.X., J.G. Williams, and J.O. Dickey, "Earth Rotation From Lunar Laser Ranging," JPL Geod. Geophys. Preprint 153, Jet. Prolpul. Lab., Dec. 1986.

O'Toole, J., "CELEST Computer Program for Computing Satellite Orbits," Naval Surface Weapons Center/DL TR-3565, October 1976.

Rapp, R.H. and J.Y. Cruz, "Spherical Harmonic Expansion of the Earth's Gravitational Potential to Degree 360 Using 30' Mean Anomalies," The Ohio State University Department of Geodetic Science Report No. 376, Columbus, OH, 1986.

Rapp, R.H., "Gravity Anomalies and Sea Surface Heights Derived from a Combined GEOS-3/SEASAT Altimeter Data Set," J. Geophys. Res., 91, E5, pp. 4867-4876, 1986.

Rosborough, G.W., "Satellite Orbit Perturbations Due to the Geopotential," University of Texas, Center for Space Research Report CSR-86-1, January, 1986.

Stephenson, F.R. and L.V. Morrison, "Long-Term Changes in the Rotation of the Earth: 700 B.C. to A.D. 1980," Philos. Trans. R. Soc. London, Ser. A., 313, 47, 1984.

Tepper, W.D., "Orbit Analysis of a Drag Compensated Satellite Using Doppler Data," Center for Space Research Report TM-87-02, Univ. of Texas, Austin, TX, October, 1987.

Yoder, C.F., J.G. Williams, M.E. Parke, "Tidal Variations of Earth Rotation," J. Geophys. Res., 86, B2, pp. 881-891, 1981.

Yoder, C.F. et al., "Secular Variation of the Earth's Gravitational Harmonic J2 Coefficient from LAGEOS and Nontidal Acceleration of the Earth Rotation," Nature, 303, p. 757, 1983.

VonBun, F.O., W.D. Kahn, W.T. Wells, and T.D. Conrad, "Determination of 5 x 5 Degree Gravity Anomalies Using Satellite-to-Satellite Tracking Between ATS-6 and Apollo," Geophys. J. R. Astron. Soc., 61, pp. 645-658, 1980.

Wahr, J.M., "The Tidal Motions of a Rotating, Elliptical, Elastic and Oceanless Earth," PhD Thesis, Univ. Of Colorado, Boulder, 1979.

Wahr, J.M., "Body Tides on an Elliptical Rotating, Elastic and Oceanless Earth," Geophys. J. R. Astron. Soc., 64,677, 1981.

NASA National Aeronautics and Space Administration

Report Documentation Page

1. Report No.	2. Government Accession No.	3. Recipient's Catalog No.
NASA TM-100746		

4. Title and Subtitle

The GEM-T2 Gravitational Model

5. Report Date

October 1989

6. Performing Organization Code

626.0

7. Author(s)

J.G. Marsh, F.J. Lerch, B.H. Putney, T.L. Felsentreger, B.V. Sanchez, S.M. Klosko, G.B. Patel J.W. Robbins, R.G. Williamson, T.E. Engelis, W.F. Eddy, N.L. Chandler, D.S. Chinn, S. Kapoor, K.E. Rachlin, L.E. Braatz, and E.C. Pavlis

8. Performing Organization Report No.

89B00244

10. Work Unit No.

626-414-70-75-25

9. Performing Organization Name and Address

Goddard Space Flight Center
Greenbelt, Maryland 20771, and
ST Systems Corporation
Lanham, Maryland 20706

11. Contract or Grant No.

13. Type of Report and Period Covered

Technical Memorandum

12. Sponsoring Agency Name and Address

National Aeronautics and Space Administration
Washington, D.C. 20546-0001

14. Sponsoring Agency Code

15. Supplementary Notes

Authors Marsh through Sanchez are affiliated with the Space Geodesy Branch, NASA-Goddard Space Flight Center, Greenbelt, Maryland;
Authors Klosko through Braatz are affiliated with ST Systems Corporation, Lanham, Maryland.

16. Abstract GEM-T2 is the latest in a series of Goddard Earth Models of the terrestrial field. It was designed to bring modeling capabilities one step closer towards ultimately determining the TOPEX/Poseidon satellite's radial position to an accuracy of 10-cm RMS. It also improves our models of the long wavelength geoid to support many oceanographic and geophysical applications. GEM-T2 extends the spherical harmonic field to include more then 600 coefficients above degree 36 (which was the limit for its predecessor, GEM-T1). Like GEM-T1, it was produced entirely from satellite tracking data, but it now uses nearly twice as many satellites (31 vs. 17), contains four times the number of observations (2.4 million), has twice the number of data arcs (1132), and utilizes precise laser tracking from 11 satellites. The estimation technique for the solution has been augmented to include an optimum data weighting procedure with automatic error calibration for the gravitational parameters. Results for the GEM-T2 error calibration indicate significant improvement over previous satellite-only models. The error of commission in determining the geoid has been reduced from 155 cm in GEM-T1 to 105 cm for GEM-T2 for the 36 x 36 portion of the field, and 141 cm for the entire model. The orbital accuracies achieved using GEM-T2 are likewise improved. Also, the projected radial error on the TOPEX satellite orbit indicates 9.4 cm RMS for GEM-T2, compared to 24.1 cm for GEM-T1.

17. Key Words (Suggested by Author(s))	18. Distribution Statement
Gravitational Models, Geopotential, Satellite Geodesy, Satellite Data Analysis, Satellite Laser Ranging	Unclassified - Unlimited Subject Category 46

19. Security Classif. (of this report)	20. Security Classif. (of this page)	21. No. of pages	22. Price
Unclassified	Unclassified		